Regulation of Nucleosome Dynamics

by

Thuy Thi Minh Ngo

Dissertation

Submitted in partial fulfillment of the requirements
for the degree of Doctor of Philosophy in Biophysics and Computational Biology
in the Graduate College of the
University of Illinois at Urbana-Champaign, 2014

Urbana, Illinois

Doctoral Committee:

Professor Taekjip Ha, Director of Research, Chair
Professor Andrew S. Belmont
Associate Professor Yann Chemla
Associate Professor Aleksei Aksimentiev

Abstract

In eukaryotic cells, the genome is packed into fundamental units called nucleosomes, where 147 base pairs of DNA are wrapped around a protein core. Stable packing of DNA in nucleosomes imposes a barrier for accessibility of genetic code on DNA for replication, transcription, and repair. The dynamics of nucleosomal DNA provide a mean for gene regulation by genomic sequence and epigenetic modifications. Understanding the physical basis of how sequence and epigenetic modifications of DNA affect nucleosome dynamics and nucleosomal DNA exposure will help elucidate how genomic and epigenetic modifications regulate cellular functions, cell differentiation and cancer development.

This motivated us to investigate local conformational dynamics of the nucleosome under tension or in the relaxed state and its modulation by DNA sequence and modifications. We achieved the goals by utilizing single-molecule force fluorescence spectroscopy, which allows monitoring dynamics of nucleosome at a define locality, and single-molecule DNA cyclization measurements, which enables determining of correlation of nucleosome dynamics with DNA flexibility. Chapter 2 shows details of sample preparation and methods used in studies of this dissertation.

We made three profound discoveries: (1) the nucleosome unwraps directionally under force; (2) DNA flexibility is the basic physical property that controls nucleosome stability and nucleosomal DNA accessibility; and (3) two nucleosomal DNA ends are orchestrated such that the opening of one end helps stabilize the other end, providing a mechanism to amplify even a small difference in flexibility to a large mechanical asymmetry. These results are presented in Chapter 3.

In Chapter 4 and 5, we present results to further demonstrate the correlation between DNA flexibility and unwrapping force by varying DNA modifications such as DNA mismatches, 5-methylcytosine and 5-formylcytosine. DNA methylation (5-methylcytosine) decreases DNA flexibility and reduces nucleosome mechanical stability while DNA mismatches and 5-formylcytosine have opposite effects. Our results suggest a completely new mechanism through which DNA sequence and epigenetic marks on DNA may be utilized to regulate gene expression by controlling nucleosome accessibility for replication, transcription, repair and remodeling.

Finally, we identified slow spontaneous local gaping of nucleosomes under physiological conditions. Gaping modes switch along the direction normal to the DNA plane at minutes (1-10 minutes) time scale. The existence of nucleosome in different gaping modes may underlie the heterogeneous enzymatic reactions on chromatin substrates and the formation of multiple compression forms of chromatin fibers. These results are detailed in Chapter 6.

Acknowledgements

Foremost, I would like to thank my advisor, Professor Taekjip Ha, for financial support, guidance and, more motivation. TJ gave me enough support and freedom to go as far as possible in my research projects. I was extremely lucky to learn from an advisor who is driven by curiousty and excited by every piece of finding I made.

I am grateful to members of Ha lab, Matt, Sinan, Mike, Sultan, Kyung Suk, Salman, Reza, Kaushik, Prakit, Ruobo, Ankur, James, Felix, Qiucen, Hajin, I-ren, Xinghua, Gwangrog, Seung-Jae, Paul, Jaya, Ben, Farhan, Jingyi, Kyu Young, Hye Ran, Isaac, Christopher, Xuefeng, Liz, Chang-Ting, Digvijay, Vasudha, Boyang, Jaba, Anustup, Seongjin, Medhi, Jichuan and Betty for being great mentors, colleagues and friends. Everyone was not only helpful in troubleshooting and discussion, but also a model in many different ways for me learn about doing science and enjoying life. Specifically, I would like to thank Dr. Jaya Yodh and Dr. Ruobo Zhou for training me from the first steps when I joined the lab. Especially, I cannot be luckier than being a friend with Qiucen who is always my priceless support in any situation. Thanks Qiucen for sharing with me your way of living a meaningful/beautiful life.

I would like to thank my collaborators Dr. Christopher Maffeo, Dr. Jejoong Yoo, Professor Aleksei Aksimentiev, Dr. Qing Dai, Professor Chuan He, Dr. Miroslav Hejna, Dr. Tomas Rube, and Professor Jun Song. I would not be able to finish my PhD projects without their great support. I would like to thank Cindy and the late Professor Bob Clegg who helped make the Biophysics program a family.

I would like to thank my friends with whom I shared experiences in life. I was not alone in graduate school since I was shared by my classmates, Kiran, Marco, Piyush, Bo, Ken, David, Pengfei, Charles, Amanda, Mark, Tao. My life was full of joy thanks to the

Vietnamese community in Champaign-Urbana. Thanks anh chi Thang Cac, Minh My, Phong Quyen, Ha Huy, Vuong Ngan, Hoa Luyen, anh Giang, anh Nam, cac ban Huong Cuong, Thinh Chi, and others who brought me “home” every weekend.

My life cannot be more beautiful than seeing “happy” An, my daughter, enjoying every moment with her dad. Thanks to my husband for being my daughter’s first love.

Last but not least, I am grateful to my family, my parents, my sisters, my daughter and my husband for always being with me and loving me. I know I am living a meaningful life since my joy is their happiness. My dissertation is dedicated to them.

Table of Contents

List of Tables

List of Figures

Chapter 1

Introduction

1.1. Packaging of the genome into nucleosomes

In eukaryotes, DNA is packaged into a basic unit, the nucleosome [1]. Nucleosomes are regularly arranged at approximately every 200 base pairs (bp) along the DNA like "beads on a string", separated by short DNA linker [2]. Each nucleosome consists of 147 bps of DNA wrapped around histone octamer core composed of two copies each of the histones H2A, H2B, H3 and H4 [3] as depicted in Figure 1.1. DNA is stably packed on histone surface by electrostatic interactions and hydrogen bonds between DNA and the protein core [3].

Stable packing of DNA in nucleosomes imposes a barrier for accessibility of genetic code of DNA for replication, transcription, and repair [4-7]. The accessibility of nucleosomal DNA is made by partial unwrapping of DNA from the histone protein core either passively due to spontaneous fluctuations [4, 8-10] or actively by forces generated by polymerases and chromatin remodelers [11, 12]. Therefore, the dynamics of nucleosomal DNA provide a means for gene regulation by genomic sequence and epigenetic modifications.

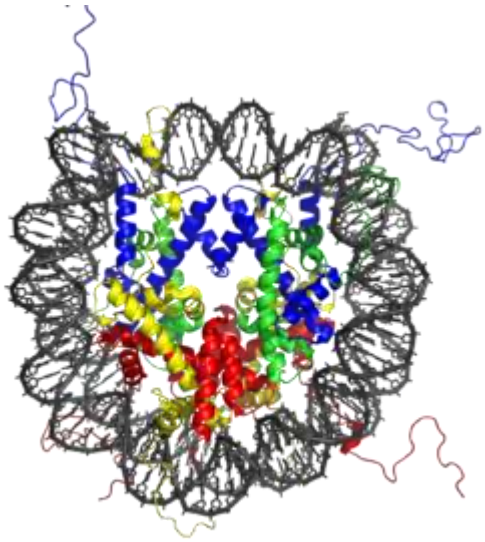

Figure 1.1: The crystal structure of the nucleosome core particle [3]

The nucleosome is the basic unit of DNA packaging in the eukaryotic nucleus. It consists of 147 bp dsDNA wrapped 1.7 turns around histone octamer which consists of two copies each of H2A (yellow), H2B (red), H3 (blue) and H4 (green).

1.2. Spontaneous nucleosome dynamics characterized by FRET

Nucleosomes are highly dynamic and differ from the canonical nucleosome crystal structure by spontaneous nucleosomal DNA breathing [8, 9] which was identified using FRET (Forster Resonance Energy Transfer). The FRET method is based on the energy transfer between two fluorophores which depends on the distance between them [13]. A donor and an acceptor fluorophore are attached to designed locations on nucleosomal DNA, thus allowing us to follow conformational changes in the donor-acceptor coordinate. The emission signal from donor and acceptor are recorded in separate emission channels splitting based on their wavelength. FRET efficiency is calculated as the ratio of acceptor intensity to the total intensity. As depicted in Figure 1.2, FRET efficiency is a function of distance between donor and acceptor dyes. If the two dyes are close, efficiency of energy transfer is high and the efficiency decreases with increasing

distance. FRET is sensitive for the donor - acceptor distance range of 3 nm – 8 nm. In single-molecule FRET (smFRET), we can follow individual molecule dynamics over time. Both bulk FRET and smFRET have been widely used to investigate conformational dynamics of bio-molecules in general and specifically for nucleosomes [8, 10, 14-17].

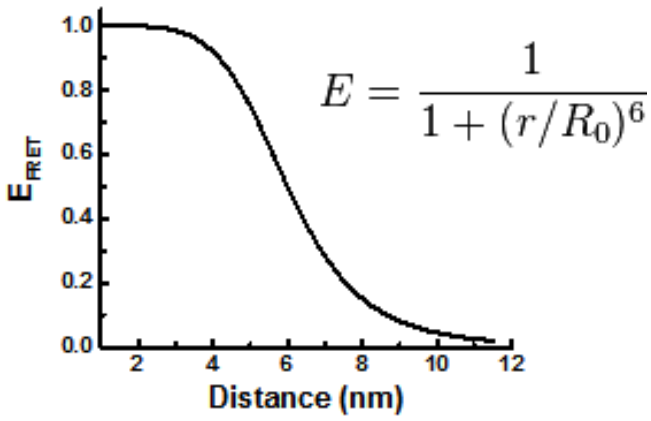

Figure 1.2: FRET (Förster Resonance Energy Transfer) as a function of distance

Energy transfer between a donor and an acceptor is the result of dipole coupling between them. We record emission signal from donor and acceptor which are separated by their wavelength, then calculate FRET as the ratio of acceptor intensity to the total intensity. FRET is a function of distance between donor and acceptor: If the two dyes are close, there is high efficiency and the efficiency decreases with increasing distance. We chose Cy3 as a donor and Cy5 as an acceptor. This pair has characteristic length R_0 = 6 nm. As a result, at 6 nm distance energy transfer efficiency is 50% and FRET is sensitive for the distance range of 3 nm – 8 nm.

Widom and colleagues identified and characterized nucleosome breathing in which nucleosomal DNA ends undergo partial, rapid unwrapping from the histone core in a reversible manner [8, 9]. Spontaneous unwrapping of nucleosomal DNA ends allow the accessibility to DNA binding factors to chromatin [4, 9]. Nucleosome unwrapping was identified to happen spontaneously in solution at physiological conditions [8, 10, 18]. Using stop-flow FRET and single-molecule FRET, unwrapping kinetics of nucleosomes were determined to take place on the millisecond time scale.

1.3. Nucleosome dynamics under tension characterized by optical tweezers

Many DNA enzymes such as polymerases and chromatin remodelers generate force to access nucleosomes. In addition, highly dynamic chromatin anchored to various subcellular structures is likely to experience tension. Therefore, it is important to understand the dynamics of nucleosomes under mechanical constraints. For the last two decades, nucleosome dynamics under tension was characterized using optical tweezers technique.

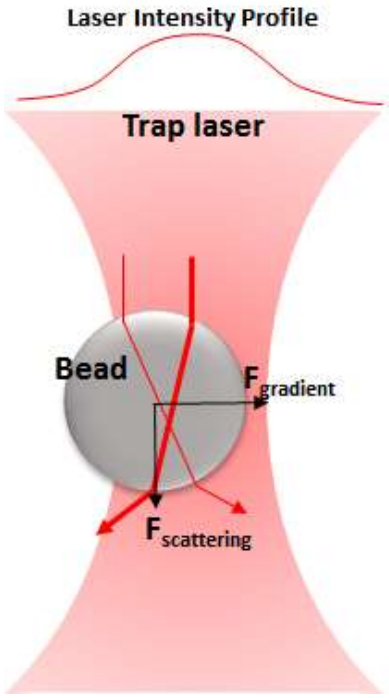

Figure 1.3: Principles of the optical trap

A laser beam is focused on a spot by a high NA objective. A micron-size polystyrene bead which is placed in the focus region bends optical rays passing through it due to the difference of the refractive index of the particle with that of the surrounding medium. The change in the radiation momentum due to the bending of light results in a force acting on the sphere. This force consists of gradient and scattering components. The gradient force tends to trap the particle at the middle of the focus plane where the light intensity is maximum.

Optical tweezers is a method to trap a micrometer scale object using radiation pressure. This technique has been widely used in single-molecule biophysics and polymer physics because an optical trap can generate forces in the pN range and measure displacements on the subnanometer scale. Typically, in a biophysics experiment, a DNA tether is used to link a bio-complex of interest to a polystyrene microsphere for measuring force generated by the complex, measuring dynamics via changes in tether extension or for manipulation. An optical trap is based on transferring radiation momentum to a micro-particle due to the bending of light when it strikes on the particle. Figure 1.3 illustrates that an optical trap is formed by focusing a laser beam by a high numerical aperture (NA) objective to a spot in the specimen plane. This spot creates an "optical trap" which is able to hold a small particle at its center. A particle which is placed in the focus region bends optical rays passing through it due to the difference of the refractive index of the particle with that of the surrounding medium. The change in the radiation momentum due to the bending of light results in a force acting on the sphere. This force consists of gradient and scattering components. The gradient force tends to trap the particle at the middle of the focus plane where the light intensity is maximum.

Using the optical tweezers method, nucleosomal DNA under tension was revealed to unwrap in two major stages; the outer turn unwraps at low force followed by unwrapping of the inner turn at higher force [19-21]. However, previous mechanical studies relied on end-to-end distance detection of the DNA tethers, interpretation of which can be indirect, and is unable to report on local conformational changes of different parts of the nucleosome.

1.4. Aims of this thesis research: regulation of nucleosome dynamics by DNA sequence and DNA modifications

There are 2 main goals to this thesis project. First, we aim to monitor local dynamics of the nucleosome under constraints at various coordinates by utilizing cutting–edge single-molecule optomechanical technology which combines optical trapping with fluorescence detection (aka 'fleezers') [22]. With this new approach, we should be able to unambiguously probe the force-dependent dynamics of a single nucleosome at a defined locality. We hope our findings will serve as a platform for interpreting local interaction of enzymes, involving in transcription and DNA repair pathways, with chromatin substrates.

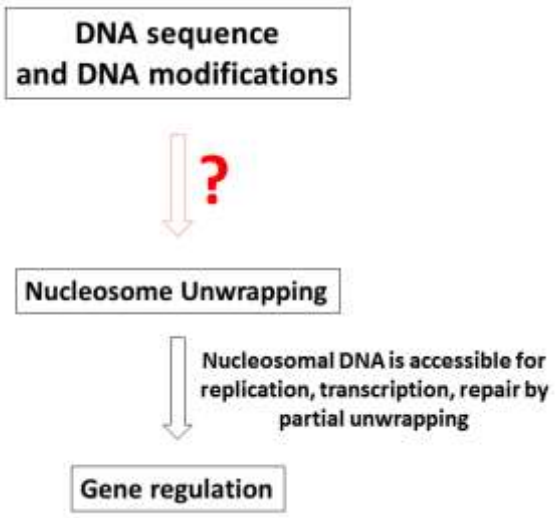

Figure 1.4: Target of the thesis

The final goal of this thesis is to find a basic physical principle of how DNA sequence and modifications affect nucleosome dynamics and nucleosomal DNA exposure which control nucleosomal accessibility for replication, transcription and repair.

Understanding the physical basis of how DNA sequence and modifications affect nucleosome dynamics will help elucidate how genomic and epigenetic modifications

regulate cellular functions (Figure 1.4). In the nucleosome, DNA of about one persistence length (147 bp) has to be bent and twisted to form ~1.7 turns around the histone octamer [3, 23, 24]. DNA sequence may affect the strength of DNA-histone interactions through formation of specific DNA-histone interactions or by affecting the static curvature, dynamic flexibility, permanent or local twist [25]. These mechanical properties of DNA are affected by sequence composition and a variety of modifications [25-30]. The DNA sequence and modifications has a profound effect on nucleosome positioning, structure and stability [23, 25, 31, 32], but how it affects nucleosome dynamics is poorly understood.

The second target of this thesis is to find a basic physical principle of how DNA sequence and modifications affect nucleosome dynamics and nucleosomal DNA exposure (Figure 1.4). We hope that this study will provide the missing link between DNA physics, nucleosome dynamics and nucleosomal DNA accessibility. We believe that by demonstrating the physical basis which controls nucleosome unwrapping, this dissertation will aid understanding parts of fundamental principles of how genomic and epigenetic modifications regulate gene expression in performing cellular functions, cell differentiation and cancer development.

Chapter 2

Methods

2.1. Combination of smFRET with optical tweezers

We are combining smFRET with optical tweezers (fleezers) to create a powerful tool for locally monitoring conformational changes of biomolecular complexes using fluorescence tags under mechanical manipulation. One reason we have developed this technology is that optical tweezers only provides end-to-end distance readout on the projection of the reaction coordinate. If the reaction coordinate is a poor coordinate then any changes in bio-complexes' conformation will be hidden. Using the hybrid instrument, in principle, we can attach fluorophores at arbitrary positions on the complexes for local probing. The second reason to adopt this technology is that optical tweezers can provide high resolution if the tether is held at high force. With fleezers, the molecular complexes can be held at low force but we still can achieve nm resolution by FRET. The difficulties in combining the two techniques are (i) overlapping of the high intensity trap laser with the fluorescence excitation laser will significantly reduce the lifetime of fluorophores due two-photon excitation of dyes or other destructive chemical pathways; (ii) the high intensity of trapping laser which will give significant high background in comparison with weak single molecule fluorescence signal. In our lab, we chose to separate trap laser from the molecular substrates by a long lambda DNA linker.

The technique was successfully used to observe dynamics of the DNA four-way Holliday junction [22], polypeptide bio-sensor [33] and SSB protein diffusion [34].

In this study, a mononucleosome reconstituted with the 601 sequence DNA was anchored

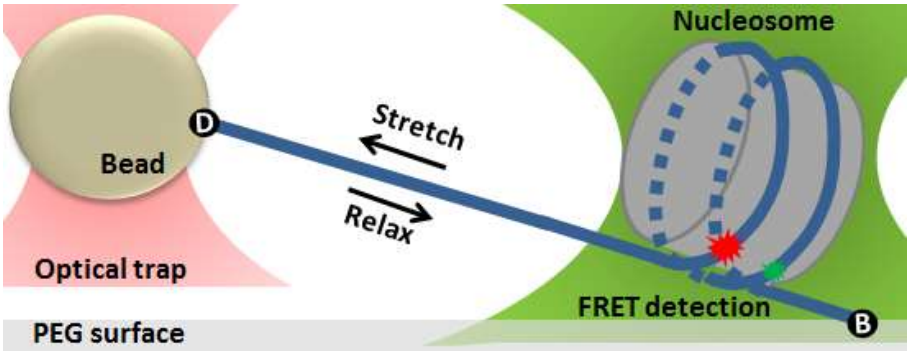

Figure 2.1: Experimental scheme

A nucleosome was immobilized on a microscope slide via a 14 bp dsDNA handle beyond the nucleosome core sequence. The other end was connected to a micron-diameter bead through a λ-DNA linker which was held in place by an optical trap which applies force. Local conformational changes were recorded by FRET between the donor (green) and the acceptor

to a PEG surface via biotin-neutravidin binding (Figure 2.1). The other end of the nucleosome was tethered to a micron bead via a lambda-DNA linker. The bead was then trapped by an optical trap. A pair of dyes attached to various positions on the nucleosome allows us monitor conformational changes of the nucleosome via measuring FRET efficiency of the dye pair. In order to apply force on the nucleosomal DNA, we moved the piezo stage at a constant velocity. At the same time, the confocal excitation laser followed the stage movement. For simplification, we chose to incorporate a dye pair on the nucleosomal DNA. Cy3 dye is the donor and Cy5 dye is the acceptor.

2.2. Outline of sample preparation protocol

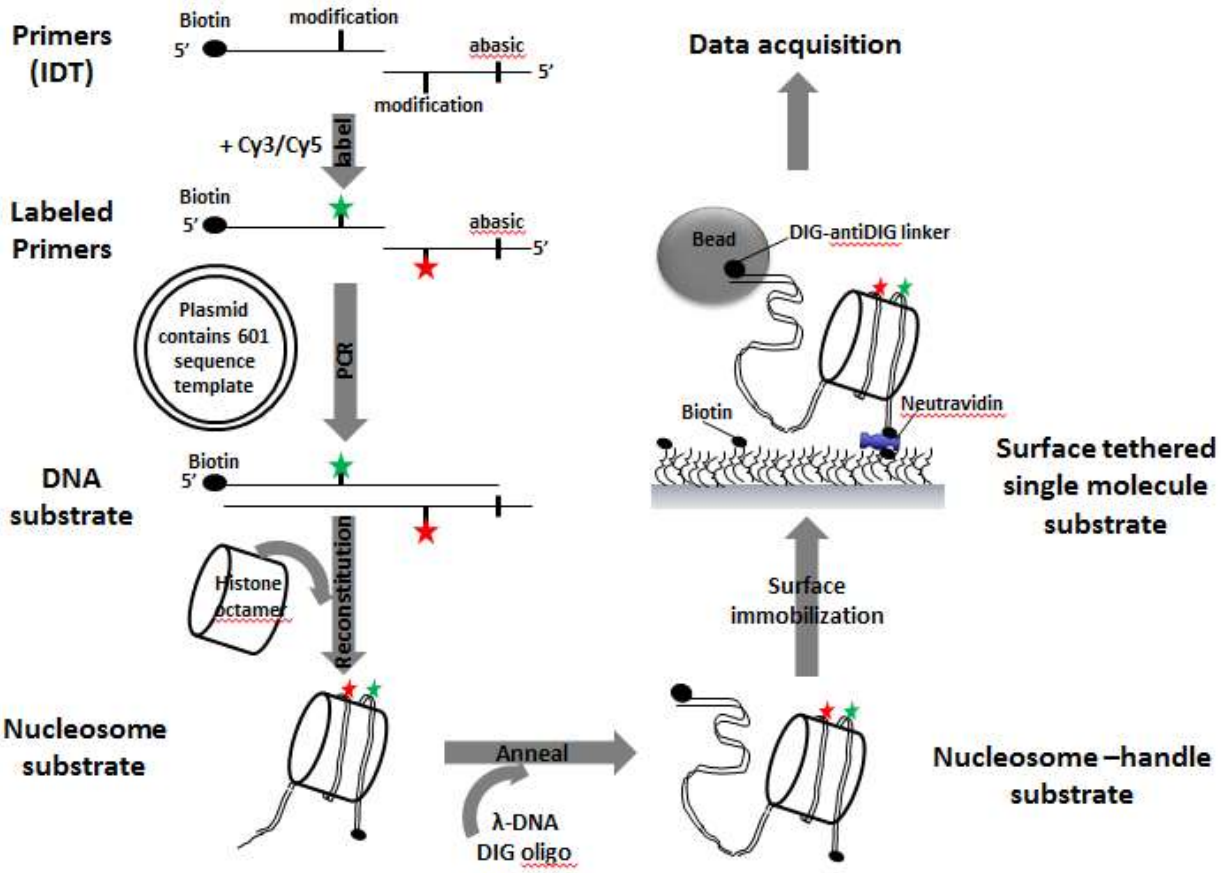

Figure 2.2: Illustration of sample preparation protocol

We used PCR to amplify 181 bp dsDNA which contains 147 bp 601 sequence from a plasmid template. The forward primer contains Biotin on the 5′ end and an amino modification (AmMC6T) and the reverse primer contains the same amino modification and an abasic site. The forward and reverse primers are then labeled with Cy3 and Cy5 dyes respectively before PCR. The PCR product is a 181 bp DNA with a COS overhang and is reconstituted with the histone octamer by stepwise dialysis method. The nucleosome is then annealed with λ DNA and an oligo containing digoxigenin. The sample now is ready for immobilization on a PEG surface via biotin-neutravidin binding and incubation with anti-digoxigenin beads.

The sample preparation protocol is schemed in figure 2.2. In summary it takes three major steps: (1) DNA template preparation, (2) nucleosome reconstitution, and (3) surface

immobilization. We used PCR to amplify 181 bp ds DNA which contains 147 bp of the 601 sequence, 14 bp linker to biotin and 20 bp spacer to a 12 nt COS overhang. Biotin is used to immobilize the complex to the surface and the COS overhang is used to anneal to lambda DNA. We designed primer oligos for such templates which were synthesized by IDT-DNA. The forward primer contains Biotin on the 5′ end and an amino modification (5AmMC6T) at a designated location. The reverse primer contains the same amino modification and an abasic site. The forward and reverse primers are then labeled with Cy3 and Cy5 dyes respectively before using in PCR. Double stranded DNA with an overhang obtained from PCR is reconstituted with the histone octamer by stepwise dialysis method [35]. The resultant nucleosome is then annealed with lambda DNA and an oligonucleotide containing digoxigenin. The sample now is ready for immobilization on a PEG surface via biotin-neutravidin binding and incubation with anti-digoxigenin beads. Finally, we collect data by the Fleezers assay.

2.3. List of DNA templates and oligos

DNA templates and labeling schemes (table 2.1):

A: The templates of the 601 sequence and derivatives used in this investigation. The 601 template is Addgene Plasmid 26656: pGEM-3z/601 plasmid. The top and bottom strands of the 601 sequence are denoted by I and J strand, respectively (pdb file: 3MVD). The 'left' and 'right' sides in our templates correspond to the 5′ and 3′ ends of the I strand shown in the table. The templates 601 RRH1-10 and 601 LL8-24 were synthesized by PCR, while 601MF and 601RTA were synthesized by IDT DNA. The 601 sequence is color coded: extra-chromosomal handles (black); left outer quarter (magenta); left inner quarter (orange); right inner quarter (green); right outer quarter (blue). The parts of the derivative sequences which are varied in comparison to the original 601 sequence are underlined and changed to the corresponding color portion of the 601 sequence.

B: Labeling schemes and names for all reconstituted nucleosomes using the original 601 sequence. The top and bottom strands of the 601 sequence are denoted by I and J strand, respectively. The I strand is shown in the table. The 601 sequence is color coded as described in panel A. Labeled positions are highlighted in red, and underlined. The sequence index starts from the 5′ end of the 601 on each strand. The specific primers (listed in table 2.2) used to generate each template are listed next to the template name.

Table 2.1. DNA templates and labeling schemes

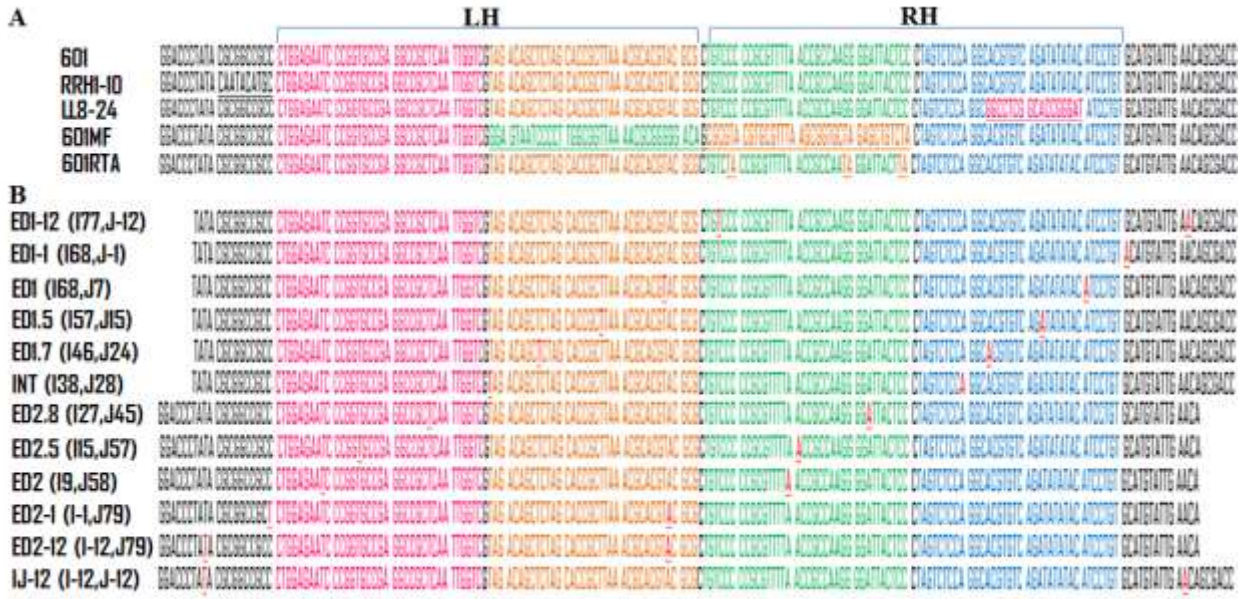

DNA sequences (table 2.2): Oligonucleotides (synthesized by IDT DNA) for PCR amplification of templates. The name of the oligonucleotide corresponds to the labeling strand and position. Biosg and ibio refer to biotin, idSp refers to abasic site, iAmMC6T refers to amino-modified C6 dT linker for labeling with Cy3 or C5, 5Cy5 and 5Cy3 refer to end-labeled positions generated through phosporamidite chemistry. Other abbreviations include: LH (left half), RH (right half), MF (middle fragment) RRH (right right handle), LL(left left), RTA (right TA (dinucleotide), A=(for immobilization scheme A), B= (for immobilization scheme B). The primer sequences are color-coded according

to the sections of the 601 template (see table 2.1): extra-chromosomal handles (black); left outer quarter (magenta); left inner quarter (orange); right inner quarter (green); right outer quarter (blue).

Table 2.2: DNA sequences

(1) I77	5'- /5Biosg/TATA CGCGG CCGCC CTGGAGAATC CCGGTGCCGA GGCCGCTCAA TTGGTCGTAG ACAGCTCTAG CACCGCTTAA ACGCACGTAC GCGCTG/iAmMC6T/CCC
(2) J-12	5'- GG GCGGCGACCT /idSp/GGTCGCTG/iAmMC6T/T CAATACATGC ACAGGAT GTATATATC
(3) I68	5′-/5Biosg/TATA CGCGG CCGCC CTGGAGAATC CCGGTGCCGA GGCCGCTCAA TTGGTCGTAG ACAGCTCTAG CACCGCTTAA ACGCACG/iAmMC6T/AC G
(4) J-1	5'- GG GCGGCGACCT /idSp/GGTCGCTGTT CAATACATG/iAmMC6T/ ACAGGAT GTATATA
(5) J7	5'- GG GCGGCGACCT /idSp/GGTCGCTGTT CAATACATGC ACAGGA/iAmMC6T/ GTATATA
(6) I57	5′-/5Biosg/TATA CGCGG CCGCC CTGGAGAATC CCGGTGCCGA GGCCGCTCAA TTGGTCGTAG ACAGCTCTAG CACCGC/iAmMC6T/TAA
(7) J15	5'- GG GCGGCGACCT /idSp/GGTCGCTGTT CAATACATGC ACAGGAT GTATATA/iAmMC6T/CT G

Table 2.2 (con't)	
(8) I46	5′-/5Biosg/TATA CGCGG CCGCC CTGGAGAATC CCGGTGCCGA GGCCGCTCAA TTGGTCGTAG ACAGC/iAmMC6T/CTA
(9) J24	5'- GG GCGGCGACCT /idSp/GGTCGCTGTT CAATACATGC ACAGGAT GTATATATCT GACACG/iAmMC6T/GCC TGGA
(10) I38	5′-/5Biosg/TATA CGCGG CCGCC CTGGAGAATC CCGGTGCCGA GGCCGCTCAA TTGGTCG/iAmMC6T/AG A
(11) J28	5'- /5Biosg/TGTT CAATACATGC ACAGGAT GTATATATCT GACACGTGCC /iAmMC6T/GGA
(12) I27	5′ GG GCGGCGACCT /idSp/GGA CCCTATA CGCGG CCGCC CTGGAGAATC CCGGTGCCGA GGCCGCTCAA TTGGTCG/iAmMC6T/AG A
(13) J45	5'- /5Biosg/TGTT CAATACATGC ACAGGAT GTATATATCT GACACGTGCC TGGAGACTAG GGAGTAA/iAmMC6T/CC C
(14) I15	5′- GG GCGGCGACCT /idSp/ GGA CCC TATA CGCGG CCGCC CTGGAGAATC CCGG/iAmMC6T/GCC
(15) J57	5'- /5Biosg/TGTT CAATACATGC ACAGGAT GTATATATCT GACACGTGCC TGGAGACTAG GGAGTAATCC CCTTGGCGG/iAmMC6T/ TAA
(16) I9-A	5′-/5Biosg/TATA CGCGG CCGCC CTGGAGAA/iAmMC6T/C CC

Table 2.2 (con't)	
(17) J58-A	5'- GG GCGGCGACCT /idSp/TGTT CAATACATGC ACAGGAT GTATATATCT GACACGTGCC TGGAGACTAG GGAGTAATCC CCTTGGCGGT /iAmMC6T/AAA
(18) I9	5′- GG GCGGCGACCT /idSp/ TATA CGCGG CCGCC CTGGAGAA/iAmMC6T/C CC
(19) J58	5'- /5Biosg/TGTT CAATACATGC ACAGGAT GTATATATCT GACACGTGCC TGGAGACTAG GGAGTAATCC CCTTGGCGGT /iAmMC6T/AAA
(20) I-1	5′-/5Biosg/TATA CGCGG CCGC/iAmMC6T/ CTGGAGAA/iAmMC6T/C CCGGT
(21) J79	5'- GG GCGGCGACCT /idSp/GGTCGCTGTT CAATACATGC ACAGGAT GTATATATCT GACACGTGCC TGGAGACTAG GGAGTAATCC CCTTGGCGGT TAAAACGCGG GGGACAGCGC G/iAmMC6T/AC G
(22) I-12	5′-/5Biosg/ GGACCCTA/iAmMC6T/A CGCGG CCGCC CTGGAGAA/iAmMC6T/C CCGGT
(23) I58-MF	5'- /5Biosg/TATA CGCGGCCGCC CTGGAGAATC CCGGTGCCGA GGCCGCTCAA TTGGTCGGGA GTAATCCCCT TGGCGGT/iAmMC6T/AA A

Table 2.2 (con't)	
(24) J58-MF	5'- /5Biosg/TGTT CAATACATGC ACAGGAT GTATATATCT GACACGTGCC TGGAGACTAG TAGACAGCTC TAGCACCGCT /iAmMC6T/AAA
(25) J58-RTA	5′- /5Biosg/TGTT CAATACATGC ACAGGAT GTATATATCT GACACGTGCC TGGAGACTAG **TA**AGTAATCC **TA**TTGGCGGT /iAmMC6T/AAA
(26) I9-RRH-1-10	5′- GG GCGGCGACCT /idSp/ TATA CAATACATGC CTGGAGAA/iAmMC6T/C CC
(27) J58-LL8-24	5′- /5Biosg/TGTT CAATACATGC ACAGGAT ATCCCGGTGC CGAGGCCGCC TGGAGACTAG GGAGTAATCC CCTTGGCGGT /iAmMC6T/AAA
(28) J7-LL8-24	5'- GG GCGGCGACCT /idSp/GGTCGCTGTT CAATACATGC ACAGGA/iAmMC6T/ ATCCCG
(29) DIG oligo	5′-AGGTCGCCGCCCT TT/digoxigenin/
(30) 601-LH top	/5Cy3/CAGAATCCGT CTGGAGAATC CCGGTGCCGA GGCCGCTCAA TTGGTCGTAG ACAGCTCTAG CACCGCTTAA ACGCACGTAC GCG
(31) 601-LH bottom	/5Cy5/ACGGATTCTG CGC GTACGTGCGT /iBiodT/TAAGCGGTG CTAGAGCTGT CTACGACCAA TTGAGCGGCC TCGGCACCGG GATTCTCCAG

Table 2.2 (con't)	
(32) 601-RH top	/5Cy5/ACGGATTCTG TGTCCC CCGCGTT/iBiodT/TA ACCGCCAAGG GGATTACTCC CTAGTCTCCA GGCACGTGTC AGATATATAC ATCCTGT
(33) 601-RH bottom	/5Cy3/CAGAATCCGT ACAGGAT GTATATATCT GACACGTGCC TGGAGACTAG GGAGTAATCC CCTTGGCGGT TAAAACGCGG GGGACA
(34) 601MF-LH top	/5Cy3/CAGAATCCGT CTGGAGAATC CCGGTGCCGA GGCCGCTCAA TTGGTCGGGA GTAATCCCCT TGGCGGTTAA AACGCGGGGG ACA
(35) 601MF-LH bottom	/5Cy5/ACGGATTCTG TGT CCCCCGCGTT /iBiodT/TAACCGCCA AGGGGATTAC TCCCGACCAA TTGAGCGGCC TCGGCACCGG GATTCTCCAG
(36) 601MF-RH top	/5Cy5/ACGGATTCTG CGCGTA CGTGCGT/iBiodT/TA AGCGGTGCTA GAGCTGTCTA CTAGTCTCCA GGCACGTGTC AGATATATAC ATCCTGT
(37) 601MF-RH bottom	/5Cy3/CAGAATCCGT ACAGGAT GTATATATCT GACACGTGCC TGGAGACTAG TAGACAGCTC TAGCACCGCT TAAACGCACG TACGCG
(38) 601RTA-RH top	/5Cy5/ACGGATTCTG TGTCTA CCGCGTT/iBiodT/TA ACCGCCAATA GGATTACTTA CTAGTCTCCA GGCACGTGTC AGATATATAC ATCCTGT

Table 2.2 (con't)	
(39) 601RTA-RH bottom	/5Cy3/CAGAATCCGT ACAGGAT GTATATATCT GACACGTGCC TGGAGACTAG TAAGTAATCC TATTGGCGGT TAAAACGCGG TAGACA
(40) LL8-24-RH top	/5Cy5/ACGGATTCTG TGTCCC CCGCGTT/iBiodT/TA ACCGCCAAGG GGATTACTCC CTAGTCTCCA GGCGGCCTCG GCACCGGGAT ATCCTGT
(41) LL8-24-RH bottom	/5Cy3/CAGAATCCGT ACAGGAT ATCCCGGTGC CGAGGCCGCC TGGAGACTAG GGAGTAATCC CCTTGGCGGT TAAAACGCGG GGGACA

2.4. Construct preparation

2.4.1. Preparation of DNA constructs

Prepare DNA constructs by PCR: We used PCR to amplify 181 bp ds DNA from templates which contain 147 bp 601 positioning sequence, flanked by a14 bp linker to biotin and 20 bp spacer connected to the 12 nt COS overhang. The construct was tethered to the surface via biotin and the COS overhang was used to anneal the template to λ DNA. PCR primer oligonucleotides were designed for various templates and synthesized by Integrated DNA Technologies. The forward primer contains an amino modification (5AmMC6T) at a designated location and a biotin at the 5′ end. The reverse primer contains the same amino modification and an abasic site to create the COS overhang. The forward and reverse primers were labeled with Cy3 and Cy5 dyes respectively according to [36], and HPLC-purified when necessary to bring the labeling efficiency to >90%.

Prepare DNA constructs by ligation: Each strand of DNA constructs for cyclization measurements were prepared by ligation of shorter DNA fragments containing labeled Cy3, Cy5 and biotin at the position according to each labeling scheme (table 1.1). After purification by a denaturing PAGE gel, the two complement strands were anneal by heating to 90°C followed by slow cooling over 3-4 hours.

2.4.2. Nucleosome reconstitution

The DNA templates were reconstituted with *X. laevis* recombinant histone octamer (purchased from Colorado State University) by salt- dialysis [13]. Reconstituted nucleosomes were stored at 4°C in the dark typically at concentrations of 100– 200 nM and used within 2 weeks. The efficiency of nucleosome reconstitution was measured by 5% native PAGE gel electrophoresis.

2.4.3. Annealing to lambda-DNA

The nucleosome was annealed to λ DNA and an oligonucleotide containing digoxigenin. First, λ DNA (NEB) at 16 nM was heated in the presence of 120 mM NaCl and 1.2 mM $MgCl_2$ at 80°C for 10 min, and then placed on ice for 5 min. Nucleosomes and BSA were added to the λ DNA at a final concentration of 8 nM and 0.1 mg/ml, respectively. The mixture was incubated with rotation in the dark at room temperature for 15 min and then for an additional 2-3 hrs.s at 4°C. DIG oligo was added to a final concentration of 200 nM and then incubated with rotation at 4°C for 1-2 hrs. Samples were stored at 4°C in the dark and could be used for data acquisition for up to 2 weeks.

2.4.4. Sample assembly

To eliminate nonspecific surface binding, a coverslip surface was coated with polyethyleneglycol (PEG) (mixture of mPEG-SVA and Biotin-PEG-SVA, Laysan Bio) according to [36]. After forming an imaging chamber using the PEG coated coverslip and

glass microscope slide, it was further incubated in blocking buffer (10 mM Tris-HCl pH 8.0, 50 mM NaCl, 1 mg/ml BSA (NEB), 1 mg/ml tRNA (Ambion)) for 1 hour. Thenucleosome sample was diluted to 10 pM in a nucleosome dilution buffer (10 mM Tris-HCl pH 8.0, 50 mM NaCl, 1 mM $MgCl_2$) and immobilized on the surface via biotin-neutravidin interaction. Next, 1 μm anti-digoxigenin-coated polystyrene beads (Polysciences) diluted in nucleosome dilution buffer were added to the imaging chamber for about 30 minutes for the attachment of beads to the free end of each tethers. Finally, imaging buffer (50 mM Tris-HCl pH 8, 50 mM NaCl, 1 mM $MgCl_2$, 0.5 mg/ml BSA (NEB), 0.5 mg/ml tRNA (Ambion), 0.1% v/v Tween-20 (Sigma), 0.5% w/v D-Glucose (Sigma), 165 U/ml glucose oxidase (Sigma), 2170 U/ml catalase (Roche) and 3 mM Trolox (Sigma)) was added for data acquisition.

2.5. Data acquisition

2.5.1. Single-molecule FRET experiment

A microscope quartz slide was coated with polyethyleneglycol (PEG) (mixture of mPEG-SVA and Biotin-PEG-SVA, Laysan Bio) according to [36]. The nucleosome sample was immobilized on the PEG coated slide at 50 pM in a nucleosome dilution buffer (10 mM Tris-HCl pH 8.0, 50 mM NaCl, 1 mM $MgCl_2$) through a biotin/neutravidin linker. Single-molecule FRET data was taken in the imaging buffer (50 mM Tris-HCl pH 8, 1 mM $MgCl_2$, 0.5 mg/ml BSA (NEB), 0.5 mg/ml tRNA (Ambion), 0.1% v/v Tween-20 (Sigma), 0.5% w/v D-Glucose (Sigma), 165 U/ml glucose oxidase (Sigma), 2170 U/ml catalase (Roche) and 3 mM Trolox (Sigma)) and a desired amount of NaCl using a home-build TIRF microscope (Roy et. al., 2008).

2.5.2. Single-molecule FRET data analysis

Single-molecule FRET data was analyzed using scripts written in IDL and Matlab. Briefly, time traces of individual molecule were extracted from movies recorded of 35 micron x

70 micron imaging area containing typically 500 molecules. We subtracted from the intensity time traces the background determined after photobleaching of both fluorophores. FRET value was calculated by ratio of intensity of the acceptor to the total intensity of the donor and acceptor after applying leakage and gamma factor correction (Roy et. al., Nature Method 2008). Mean dwell time of each FRET stage was calculated by dividing the total dwell time on each stage by the number of transitions from that stage. FRET histograms were constructed from collective of molecules averaging for ten frames of 50 ms each.

2.5.3. Single-molecule DNA cyclization assay

A single-molecule DNA cyclization assay was recently developed in our laboratory to quantify the flexibility of a short double stranded DNAs (< 100 bps) [26]. 601 DNA fragment regions listed in Table S2 are generated by slow annealing (90°C for 10 min) of appropriate oligonucleotides (Table S3) followed by slow cooling to room temperature

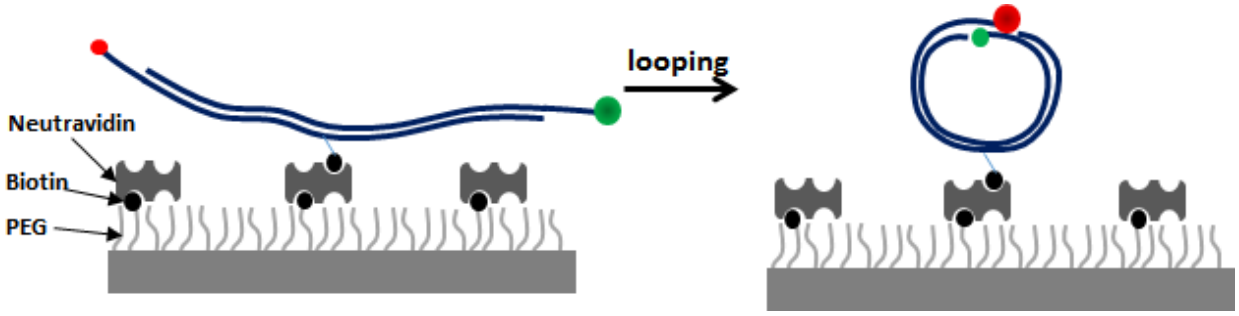

Figure 2.3: Single molecule cyclization assay
DNA fragments were immobilized on a microscope slide. A FRET pair is incorporate at the two sticky ends. High FRET population was monitored over time to quantify the fraction of looped DNA. If DNA is more flexible, it takes less time for loop formation.

over 4 hours. DNA fragments were immobilized on a PEG-coated microscope slide via biotin-neutravidin linkage. A FRET pair (Cy3 and Cy5) was incorporated at the two 10 nt

long 5′ overhangs that are complementary to each other so that loop formation via annealing of the two overhangs was detected as a FRET increase. Data acquisition was performed in a buffered solution (10 mM Tris-HCl pH 8.0, 1 M NaCl, 0.5% w/v D-Glucose (Sigma), 165 U/ml glucose oxidase (Sigma), 2170 U/ml catalase (Roche) and 3 mM Trolox (Sigma)). Time courses of generation of high FRET population allowed us to quantify the fraction of looped molecules versus time after the high salt buffer was introduced to the chamber that had low salt buffer (10 mM NaCl) of otherwise identical composition. Here, the rate of loop formation was used as a measure of DNA flexibility. The faster the looping occurs, the more flexible the sequence is.

2.5.4. Force-Fluorescence setup

We recently developed an instrument combining optical trap with fluorescence detection to monitor conformational changes of biomolecular systems under applied force [37]. The full details of this instrument can be found in our recent review [38]. Briefly, an optical trap was formed by an infrared laser (1064 nm, 800 mW, EXLSR-1064-800-CDRH, Spectra-Physics) through the back port of the microscope (Olympus) by expanding the laser beam 8-fold using two telescopes and focusing on the sample plane with a an 100x oil immersion objective (Olympus). Force was applied on the sample tethers by moving the microscope slide using a piezo stage (Physik Instrument).

Applied force was determined by position detection of the tethered beads using a QPD (UDT/SPOT/9DMI) and stiffness calibration as described [37]. The confocal excitation laser (532 nm, 30 mW, World StarTech) was coupled through the right port of the microscope. The excitation laser was scanned by a piezo-controled steering mirror (S-334K.2SL, Physik Instrument). The fluorescence emission was filtered from the infrared laser by a band pass filter (HQ580/60 m, Chroma) and separated from excitation by a dichroic mirror (HQ680/60 m, Chroma) before detection by two avalanche photodiodes.

2.5.5. Force-Fluorescence data collection

Single molecule data acquisition was performed according to [37]. In summary, after a bead was trapped, the origin of the tether was determined by stretching the tether in two opposite directions along both x and y axis. Then the confocal laser was scanned to locate the fluorescence spot on the tether after separating the trapped bead from its origin by 14 μm. Unless specified otherwise, the nucleosome unwrapping experiment was carried out by moving the stage between 14 μm and 16.8-17.2 μm at the speed of 455 nm/sec^{-1}. The confocal excitation was scanned concurrently with the stage movement. Fluorescence emission was detected for 20 ms after each step in stage movement. Force-fluorescence data was obtained in the imaging buffer (50 mM Tris-HCl pH 8, 50 mM NaCl, 1 mM $MgCl_2$, 0.5 mg/ml BSA (NEB), 0.5 mg/ml tRNA (Ambion), 0.1% v/v Tween-20 (Sigma), 0.5% w/v D-Glucose (Sigma), 165 U/ml glucose oxidase (Sigma), 2170 U/ml catalase (Roche) and 3 mM Trolox (Sigma)).

All single molecule measurements were performed at ~ 22^{o}C.

Chapter 3

Asymmetric Unwrapping of Nucleosomes under Tension Regulated by DNA Local Flexibility*

3.1. Probing local conformational dynamics of the nucleosome under tension

In order to obtain clearly interpretable data on local nucleosome dynamics we chose the nucleosome positioning sequence 601 [39], which has been used for previous high resolution single molecule studies [4, 14, 19-21, 31, 32, 40-47]. A nucleosome was anchored to a PEG-coated glass surface on one end of the DNA and pulled via a λ-DNA tethered to the other end by an optical trap. FRET (fluorescence resonance energy transfer) dye pairs, donor and acceptor, attached to various positions on the DNA enable the measurement of conformational changes of defined locality.

---

*This work was submitted for publication as:

Thuy T.M. Ngo, Qiucen Zhang, Ruobo Zhou, Jaya G. Yodh, Taekjip Ha. "Asymmetric Unwrapping of Nucleosomes under Tension Directed by DNA Local Flexibility"

To probe unwrapping of the outer DNA turn, we constructed the ED1 (Entry-Dyad 1) labeling scheme consisting of a donor close to the dyad and an acceptor close to an entry. ED1 nucleosomes displayed a single high FRET population due to close proximity of the probes (Figure 3.2A) as expected from the nucleosome crystal structure [48] (Figure 3.1A

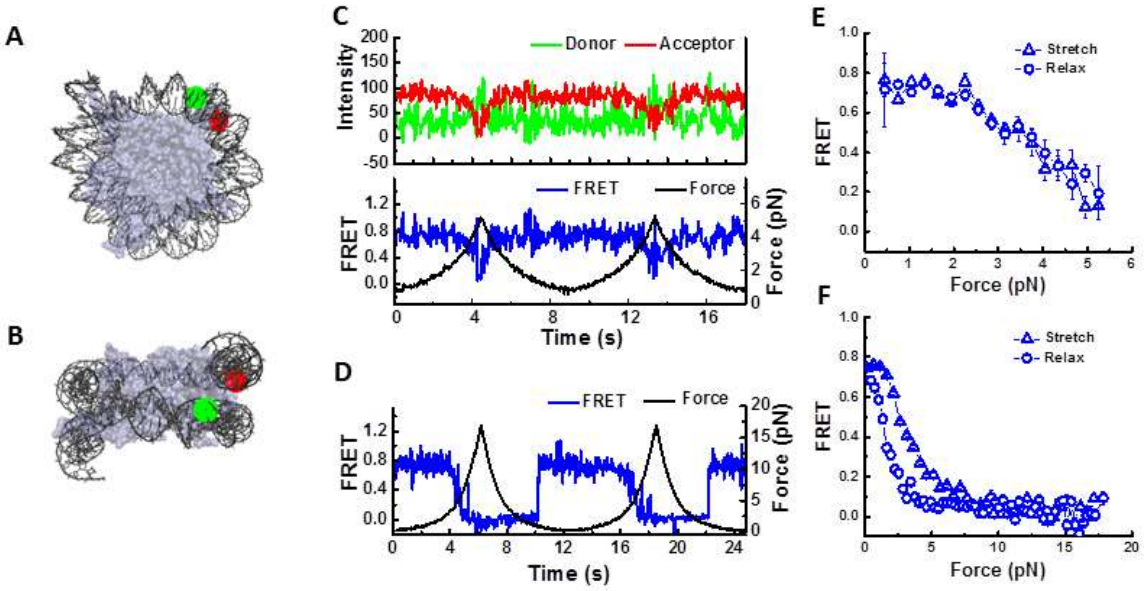

Figure 3.1: Observation of local conformational changes of nucleosome under tension
(**A, B**) Positions of donor and acceptor fluorophores in the ED1-labeling scheme superposed on two different views of the nucleosome structure (pdb file 3MVD).
(C, D). Single-molecule time traces of the ED1 construct recorded during stretching and relaxing at a stage speed of 455 nm/s at a set maximum force of ~ 6 pN (**C**) and ~20 pN (**D**): force (black), donor signal (green), acceptor signal (red) and FRET efficiency (blue).
(E, F) The average FRET vs. force when the maximum force was set to ~ 6 pN (**E**: average of 26 traces) and ~20 pN (**F**: average of 25 traces).

and 3.1B). In the absence of force, FRET time traces were stable within our temporal resolution of 30 ms (Figure 3.2B). The same DNA reconstituted with the $(H3/H4)_2$ tetramer produced a distinct low FRET population attributed to the tetrasome (Figure 3.2A).

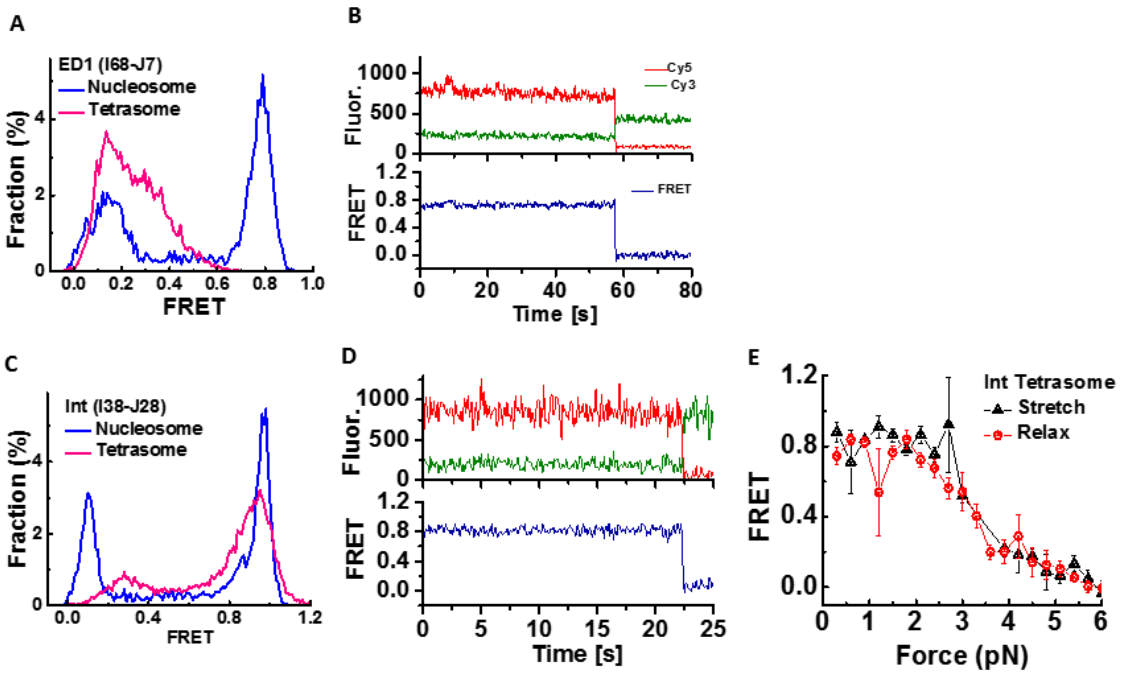

Figure 3.2: Single-molecule FRET histograms and time traces for reconstituted nucleosome and tetrasome for the 601- ED1 and INT scheme

(**A**) FRET histogram of Nucleosome (blue) and Tetrasome (magenta) reconstituted with the ED1 labeling scheme.The peak at ~0.1 corresponds to free DNA, the peak at ~ 0.75 corresponds to intact nucleosome. FRET peak of the tetrasome sample, which is broader and lower then nucleosome peak, corresponds to the mixture of free DNA and tetrasome.

(**B**) Representative single molecule time traces of the ED1 nucleosome at zero force show stable FRET over 1 min. (donor (Cy3, in green), acceptor (Cy5, in red) and corresponding FRET efficiency (blue)).

(**C**) FRET histogram of Nucleosome (blue) and Tetrasome (magenta) reconstituted from DNA construct in INT scheme. The FRET peak at ~0.1 corresponds to free DNA and the peak at ~ 0.95 corresponds to intact nucleosome (blue). The FRET peak of the tetrasome sample corresponds to the mixture of free DNA and tetrasome.

(**D**) Representative single molecule time traces under force free conditionat zero force of Cy3 donor (green), Cy5 acceptor (red) and corresponding FRET efficiency (blue) for the INT nucleosome.

(**E**) Averaged curves (23 traces) for FRET as a function of force during stretching and relaxation of INT tetrasomes

The force was increased from a low value (typically between 0.4 – 1.0 pN) to a predetermined higher value and then returned to the low value. FRET gradually decreased as the force increased followed by fast fluctuations and finally a sharp decrease in FRET (Figures 3.1C and 3.1D). Upon relaxation, the nucleosome reformed, retracing

the dynamics observed during stretching when the force was held below 6 pN to limit the extent of unwrapping (Figures3. 1C and 3.1E) or displaying hysteresis when we extended the force range to 20 pN (Figures 3.1D and 3.1F). The initial gradual FRET decrease indicates that DNA unwraps steadily without going through a major energy barrier at low tension. The FRET fluctuation that follows likely represents a bistable hopping behavior reported previously [21]. Subsequent stretching/relaxation cycles reproduced the same behavior, suggesting that each cycle brings the nucleosome back to the initial state. To probe inner turn unwrapping, we attached FRET probes to a region approximately 40 bp from the dyad (INT) (Figure 3.3G and 3.4 A). As with ED1, the INT nucleosome showed a single narrow FRET peak at zero force and was distinguishable from the tetrasome species which displayed a broad range of FRET (Figures 3.21C and 3.2D). At low forces, the INT nucleosome maintained a stable high FRET value with occasional hopping to an intermediate FRET state (Figure 3.3H). As the force increased to higher values (10-15 pN), FRET suddenly dropped to a final low value (Figure 3.3H). As an additional control, the INT–tetrasome showed a distinct FRET vs. force stretching pattern, unraveling at much lower force (3-5 pN), thus confirming that INT nucleosome contained the histone octamer (Figure 3.2E).

Taken together, our nucleosome stretching data probed at ED1 and INT positions are consistent with previous studies on the effect of force on global nucleosome dynamics [19, 21, 44, 45]; the outer turn unwraps at low force (3-5 pN) and the inner turn unwraps at higher force (12-15 pN). In addition, FRET detection of ED1 probe allows us to observe gradual unwrapping before an abrupt transition of the initial DNA end segment at the low force range (< 3 pN).

3.2. Nucleosome unwrapping is asymmetric

Previous investigations of nucleosome unwrapping [19, 21, 44] assumed that two nucleosomal DNA ends respond similarly to the applied force since unwrapping of the two DNA ends was not separately observable. Our assay, which is sensitive to local

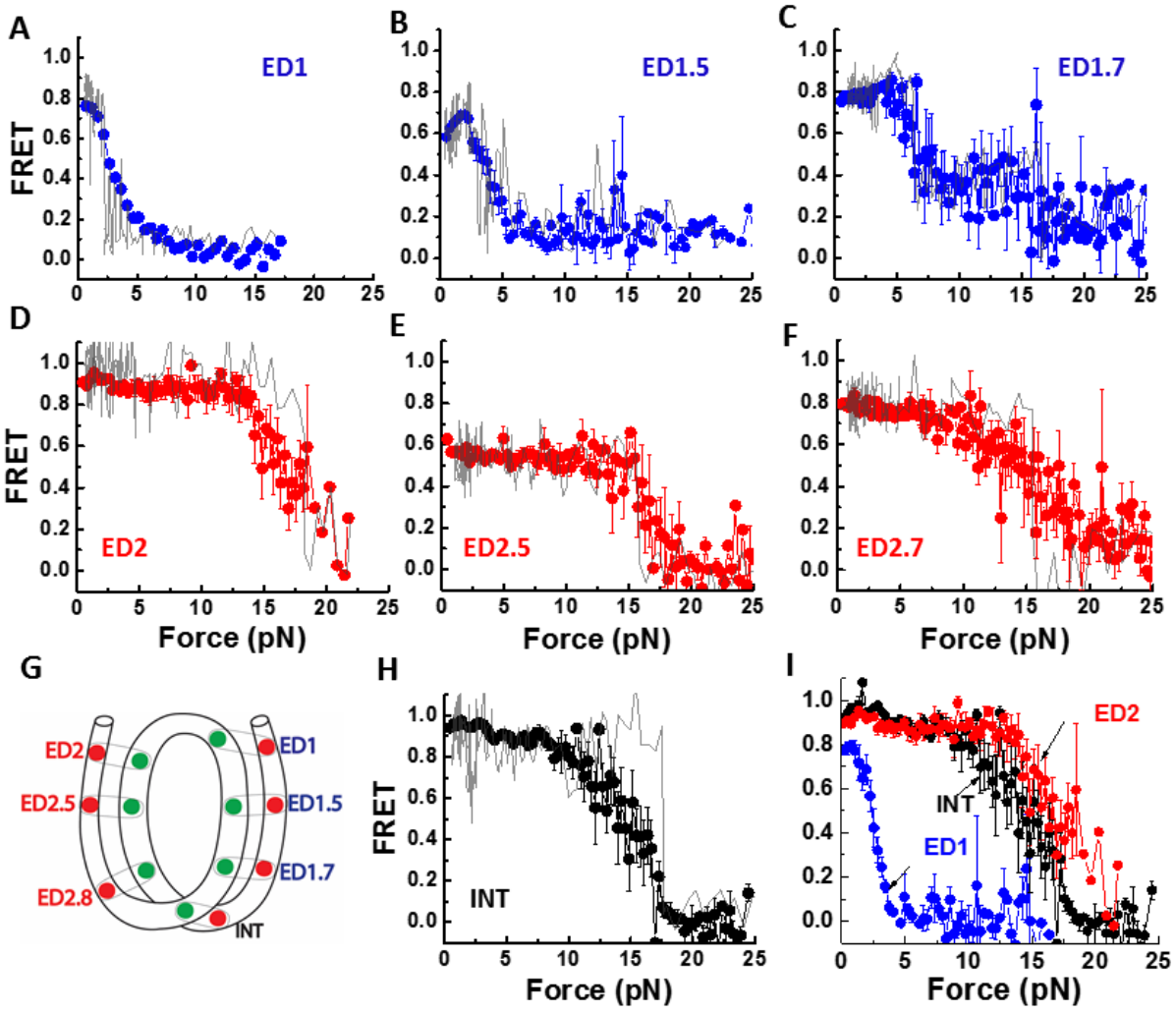

Figure 3.3: Nucleosome unwraps directionally under tension.
FRET vs. force during stretching for various FRET pairs spanning two sides of the nucleosome illustrated in **G** (See table 1.1 for labeling positions). Representative data for single cycles are shown in gray. The averaged curves are in blue for the weak side, in red for the strong side, and in black for the inner turn probes. Error bars are s.e.m. of 25 traces for ED1 (**A**), 15 traces for ED1.5 (**B**), 8 traces for ED1.7 (**C**), 20 traces for ED2 (**D**), 7 traces for ED2.5 (**E**), 40 traces for ED2.8 (**F**), and 22 traces for INT (**H**). **I**. Overlay of ED1, ED2, and INT stretching curves.

conformational changes, enables the examination of two sides separately by comparing the FRET-Force response on the two ends. We designed a construct termed ED2 with a FRET pair placed at the opposite entry/dyad region– the "left" end (Figure 3.3G). Surprisingly, the FRET-Force pattern of ED2 displayed a pattern very different from ED1 (Figure 2D). FRET remained stable at low forces and did not decrease until higher force (15 – 20 pN) was reached, in contrast to the decrease below 5 pN observed for ED1 on the "right" end. This result indicates that a significant asymmetry exists in the DNA unwrapping behavior.

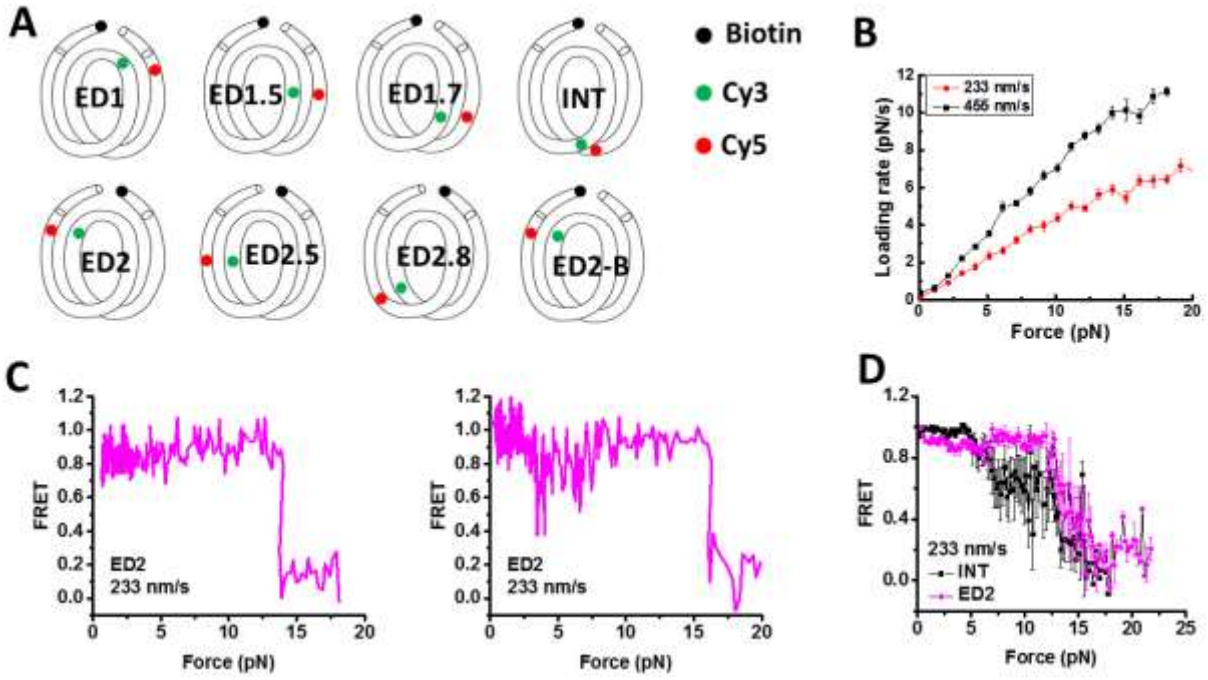

Figure 3.4: Effect of pulling speed (i.e. loading rate) on nucleosome unwrapping at higher force
(**A**) Illustration of Cy3, Cy5 and biotin position (see figure 3.3G also)
(**B**) The loading rate of pulling experiments at constant velocity of 233 nm/s (red, closed circle) and 455 nm/s (black, closed square). The loading rate increases monotonically as force increases. The maximum loading rate at high force is ~ 11 pN/s and 7 pN/s for two constant velocity experiments of 455 nm.s and 233 nm/s, respectively.
(**C**) Examples of single molecule stretching traces for ED2 construct at constant velocity of 233 nm/s.
(**D**) Averaging stretching curves for INT (I28, J28) (15 traces) and ED2 (I9, J58) (8 traces). ED2 unwraps at higher forces than INT, which was also the case at twice the pulling speed as discussed in the main text.

We performed various control experiments to confirm the unwrapping asymmetry result and to rule out alternative explanations. (1) High FRET of constructs with probes at symmetric locations on the DNA handles outside the core sequence confirmed that the nucleosome is not mis-positioned on the 601 sequence (Figure 3.6). (2) Switching the orientation of surface tethering and pulling for the ED2 construct verified that the

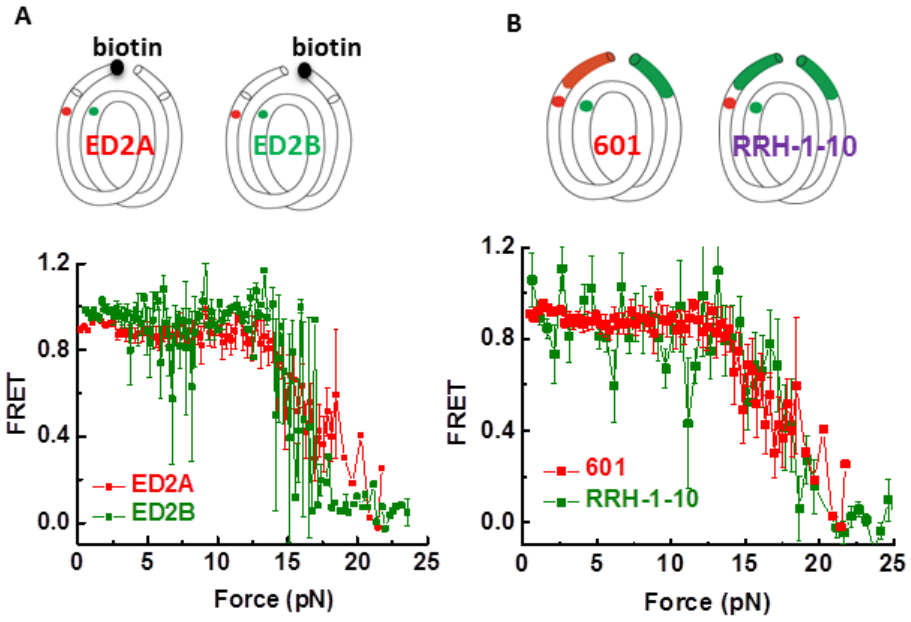

Figure 3.5: Unwrapping force is not affected by pulling configuration or extra-nucleosomal handle sequence

(**A**) Switched pulling configurations for the same labeling position ED2: In ED2A scheme, the 5′ end of the top I strand (the left end) is biotinylated. In the ED2B scheme, the 5′ end of the bottom J strand (the right side) is biotinylated. Averaged stretching traces for both ED2 pulling configurations show identical high force required for unwrapping (ED2A: average of 4 traces, ED2B: average of 20 traces).

(**B**) Changing the handle sequence on the left side does not alter the high force range required to open nucleosomal DNA on this side. Averaged stretching curves show identical high force required for unwrapping for 601-ED2 (average of 20 traces) and RRH-1-10-ED2 (average of 15 traces).

experimental configuration and the surface is not responsible for the observed asymmetry (Figure 3.5A). (3) Replacing the first 10 bp of the left handle with the corresponding region on the right handle showed that the sequence difference just outside the core region is not responsible for the asymmetry (Figure 3.5B).

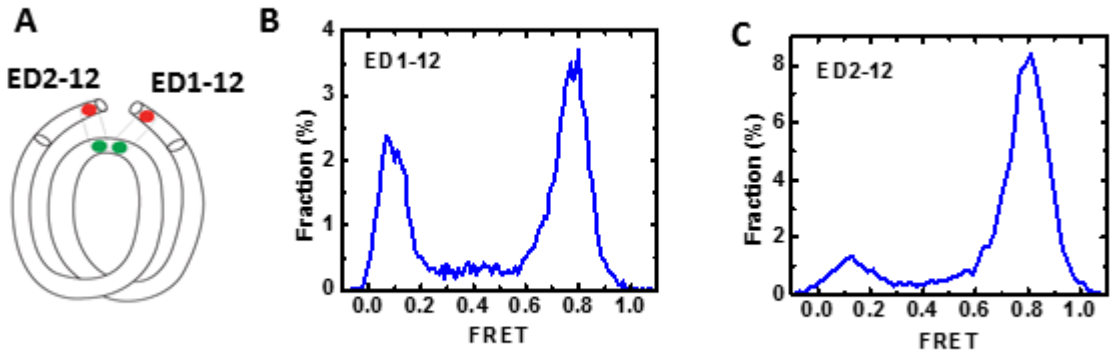

Figure 3.6: Ensuring the correct translational positioning of nucleosomes on the 601 sequence
(**A**) Illustration of labeling scheme ED1-12 and ED2-12. The acceptor dye at the -12 position on the extrachromosomal handle allows for probing for differences in translational positions of the nucleosome.
(**B, C**) Single-molecule FRET histograms for both ED1-12 and ED2-12 display similar high FRET peaks consistent with the correct translational frame for the nucleosome on the 601 sequence.

To examine if the observed asymmetry may be induced by position-specific perturbations caused by the fluorophores, we designed four additional constructs for comparison of the two sides: ED1 versus ED2, ED1.5 versus ED2.5, and ED1.7 versus ED2.8 (Figure 3.3G). Generally, the force required for a significant FRET decreases was lower for ED1 (Figure 2A), ED1.5 (Figure 3.3B) and ED1.7 (Figure 3.3C) than for those labeled at symmetrically related sites, ED2 (Figure 3.3D), ED2.5 (Figure 3.3E) and ED2.8 (Figure 3.3F), respectively, showing that the asymmetry is highly unlikely due to position-dependent perturbations by the fluorophores, and indicating that one side of the nucleosome is indeed weaker than the other when the DNA is under tension.

Strikingly, the force needed for a major unwrapping signal was larger for the ED2 end (16.8±1.5 pN) than the DNA inner turn (14.7 ±2.5 pN) (Figure 3.3D and 3.3F). This effect was even clearer when the pulling rate was halved to 233 nm/sec (14.2 ± 1.3 pN vs. 11.2±3.4 pN, Figure 3.4). Thus, the data suggest that DNA unwrapping occurs directionally, starting from the 'weak' end (ED1) at the lowest unwrapping force, followed by the inner turn, and then to the 'strong' end (ED2).

Such mechanical asymmetry may influence gene expression by affecting DNA exposure or transcriptional pausing. In fact, an *in vitro* transcription study [6] observed that nucleosomes can form a polar barrier to transcriptional elongation. Specifically, our "strong" side (ED2) corresponds to the transcription direction where polymerases face a higher outer turn barrier (the +15 barrier).

3.3. Unwrapping of the nucleosome on one end stabilizes the other end

In the low force range, FRET of the strong outer turn ED2 is stable and remains unchanged until the final drop at high force (16.8±1.5 pN) (Fig. 3.3D). When the pulling rate is lowered two-fold (Figure 3.4), we observed a signature of a minor reduction following by a recovery of FRET signal at the low force range for some stretching traces. Therefore, we probed the earliest unwrapping process of the strong (ED2) side by moving the probes to either one (ED2-1, Figure 3.7C) or twelve (ED2-12, Figure 3.8A) nucleotides beyond the nucleosome core sequence on the strong side. At low forces, ED2-1 and ED2-12 probes on the strong side showed the same stretching pattern as ED1 probe on the weak side: FRET decreased gradually at low force followed by fluctuations at 3-6 pN (Figures 3.7A and 3.8). However, on the weak side the FRET dropped entirely after 6 pN, while on the strong side, FRET recovered and did not fully drop until much higher force was reached. This may indicate that both extreme ends of the nucleosome are slightly

unwrapped at low forces but once the weak end significantly unwraps, the strong end

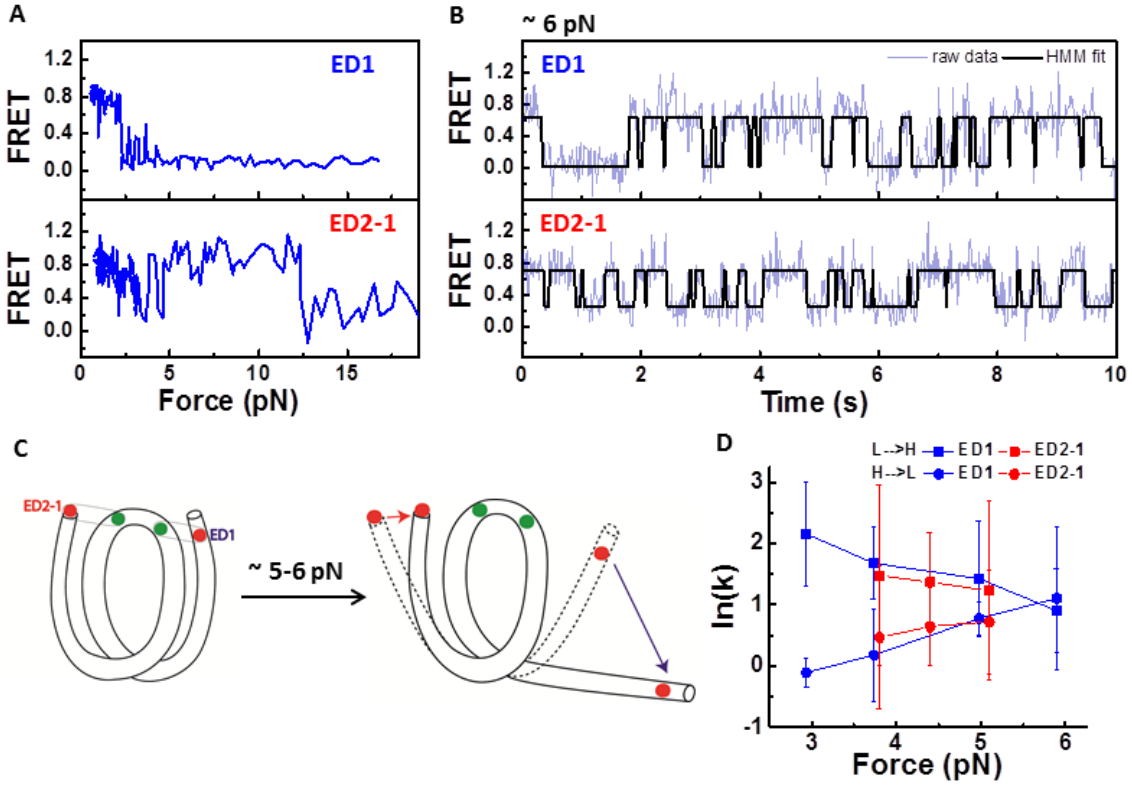

Figure 3.7: Coordinated dynamics of the two nucleosomal DNA ends
(**A**) Representative single-molecule stretching traces of ED1 and ED2-1 as indicated in **C**.
(**B**) Representative time traces of FRET efficiency at constant force of 6 pN, showing hopping between high and low FRET states. Fits from Hidden Mark modeling are overlaid.
(C) Illustration of how major unwrapping of one side of the nucleosome facilitates rewrapping on the other end. Initially, two extreme ends of the nucleosome synchronously unwrap and rewrap at forces below ~ 5pN (dashed shape). Once the ED1 side majorly unwraps (blue arrow), this facilitates the rewrapping of the ED2 side (red arrow).
(D) Rates of transition between high and low FRET states vs. force. Unwrapping rates (high to low FRET transitions) in circles and rewrapping rates (low to high FRET transitions) in squares.

rewraps and stays stable until much higher forces are applied. At constant forces, FRET time traces of the ED1 and ED2-1 constructs (Figure 3.7B) showed two-state hopping between wrapped and partially unwrapped state, respectively. Hidden Markov Modeling [49] was used to determine the transition rates between the two states (Figure 3.7D). As the force increased, the unwrapping rate increased and the wrapping rate decreased, consistent with a previous report [21], and the rates on the two DNA ends

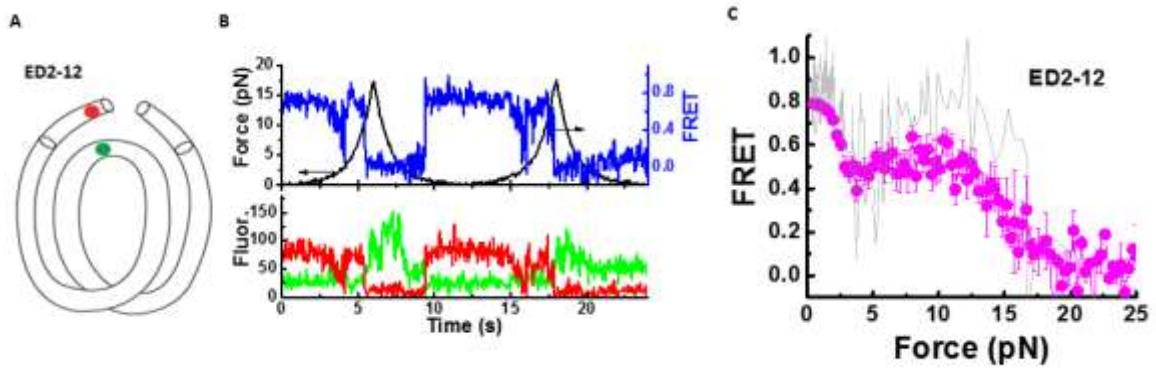

Figure 3.8: Probing the early unwrapping process on the 'strong' side
(A) Illustration of the ED2-12 construct which places Cy5 acceptor in the extra-nucleosomal handle of the strong side.
(**B**) Representative force-fluorescence single-molecule time traces for ED2-12 construct. At low force (≤5pN), FRET initially decreases, but then increases again and maintains a high FRET value (between approximately 5-15pN) until it fully drops at high force (16-20 pN)
(**C**) Representative FRET-force stretching for ED2-12 curve (light grey) with overlay by averaged (21 traces) curve (magenta).

were similar. Our observation that the two ends of the nucleosome are orchestrated such that the opening of one end helps stabilize the other end raises the possibility that even relatively small asymmetry between the two sides may result in one side winning reliably (cartoon in Figure 3.7C).

3.4. Asymmetry of nucleosome unwrapping is directed by DNA local flexibility

We propose that the observed asymmetry in mechanical stability originates from the DNA sequence differences between the two sides of the 601 sequence for the following reasons. (1) The protein core structure is symmetric around the dyad axis [3, 23] whereas the DNA sequence is nonpalindromic. (2) Unzipping of the nucleosomal DNA under certain experimental configurations shows a higher off-dyad barrier on one side

("strong" side in our study) than the other [43]. (3) Symmetrization of certain sequence features can affect the overall thermodynamic stability as measured by salt titration [23].

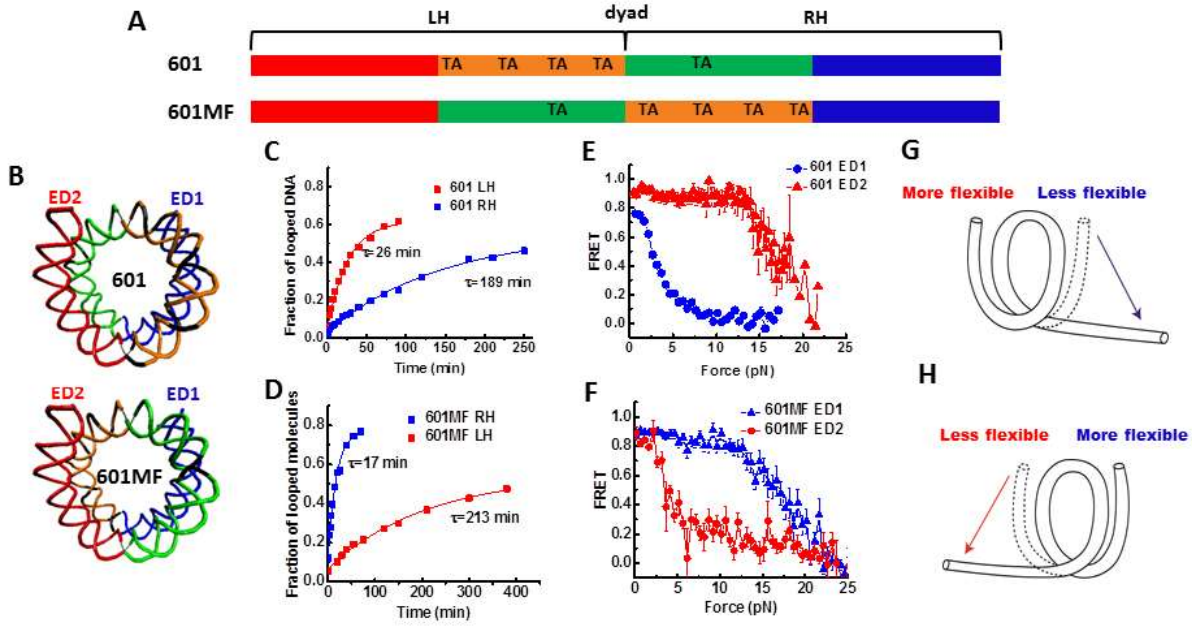

Figure 3.9: Asymmetric nucleosome unwrapping controlled by DNA local flexibility
(**A**) Variations of the 601 the sequence where the inner quarters are colored in orange and green and the outer quarters are colored in red and blue. TA steps are indicated.
(**B**) Nucleosomal DNA structures are shown in the same color scheme with corresponding scheme of the sequence.
(**C, D**) Single exponential fits to the looped DNA faction vs. time yield the average looping time τ measured using single DNA cyclization assay for the 73 bp left or right halves (LH and RH, respectively).
(**E, F**) Averaged stretching time traces of FRET efficiency vs. force for nucleosomes in ED1 and ED2 labeling schemes. Error bars denote s.e.m. of 25 traces for 601 ED1, 15 traces for 601 ED2, 29 traces for 601MF ED1, 19 traces for 601MF ED2.
(G, H) Illustrations of the relationship between the direction of nucleosome unwrapping and the DNA flexibility of the two halves of the nucleosomal DNA sequence. The nucleosome unwraps from the stiffer side (single-headed arrows) if the DNA flexibility differs significantly between the two sides.

Since the unwrapping asymmetry is observed for the outer turn, we first symmetrized DNA content at the entry regions by replacing the AT-rich region (nucleotide 8-24 from the right end) on the weak side with the corresponding GC-rich segment on the strong

side (Figure 3.10A). This construct, termed LL8-24, exhibited the same asymmetry as the 601 nucleosome (Figures 3.10C), ruling out the differences in AT/GC-content of the entry region as the source of asymmetry.

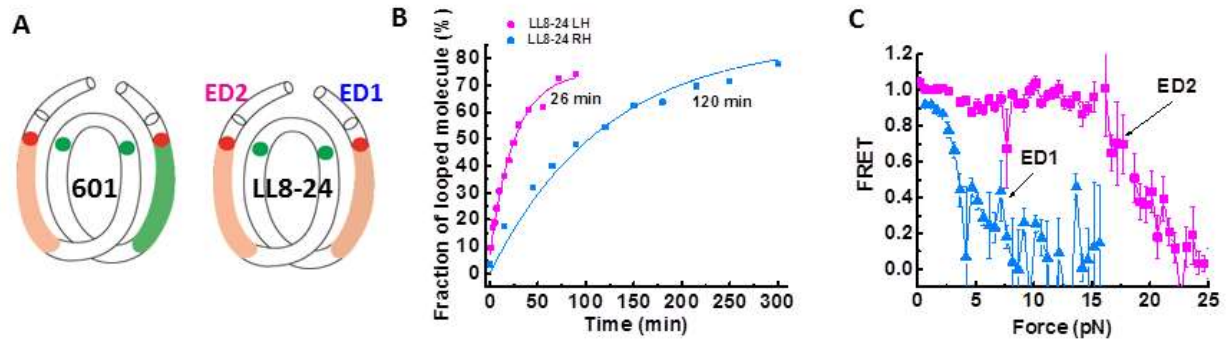

Figure 3.10: Stretching nucleosomes forming on 601 derivative sequences
A: The LL8-24 construct derived by replacing 17 nts from position 8-24 on the right (ED1) side by corresponding region on the left (ED2) side such that the sequence of the outer quarter from 8-24 nucleotides (orange) on the both sides becomes identical.
B: Looping time of the two halves of the LL8-24 construct.
C: Force-fluorescence stretching curves for LL8-24 nucleosome reconstituted with ED1 (7 traces) and ED2 (21 traces). The GC-richness of the outer regions does not affect pulling behavior of either side.

Because DNA has to be bent and deformed to wrap around the histone octamer, the intrinsic DNA flexibility may influence DNA-histone binding affinity [25, 39]. Therefore, we hypothesized that the more flexible sequences would unravel at higher forces by better tolerating the sharply bent DNA conformation. To test this hypothesis, we examined the relative flexibility of the two 73 bp DNA fragments flanking the dyad in the 601 sequence using a single molecule DNA cyclization assay [26]. The 'strong' side (LH for left half) yielded a cyclization time of 26 minutes while the 'weak' side (RH for right half) took 189 minutes to cyclize, indicating that the left side of the 601 is more flexible than the right side by a factor of 7 according to our measure (Figure 3.9C). Thus, the asymmetry in DNA flexibility appears to correlate with asymmetric unwrapping - the

more flexible DNA side unwraps at higher force and vice versa. Here, 'flexibility' is an operational definition equivalent to 'cyclizability' in our assay because we do not yet know whether a static bend or dynamic flexibility (represented by lower bending energy) determines the apparent flexibility.

In order to test the correlation further, we modified the 601 sequence so as to locally

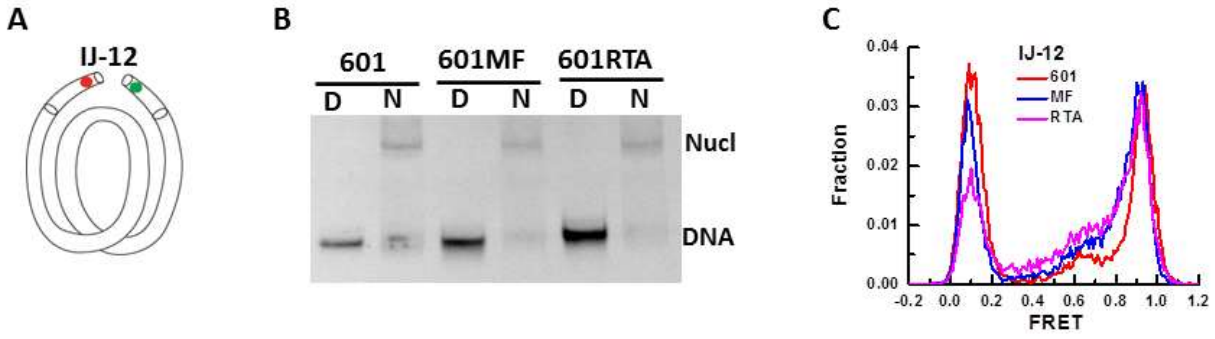

Figure 3.11: Nucleosome positioning on 601 derivative templates with reconstituted labeling scheme IJ-12

(**A**) Cartoon of labeling scheme IJ-12 in which donor and acceptor are placed at 12 nts upstream and downstream, respectively from the 601 nucleosome positioning frame.

(**B**) Nucleosomes with IJ-12 labeling scheme reconstituted on 601, 601-MF, and 601-RTA templates migrate at identical positions on 5% Native PAGE.

(**C**)Single-molecule FRET histogram for 601, 601MF and 601RTA (IJ-12) nucleosomes display the identical FRET peak at ~0.9, indicating positioning is maintained on all three sequences.

switch the DNA flexibility on the two sides by flipping the middle 73 bp (601MF) (Figures 3.9A and 3.9B). The single molecule cyclization showed that the right side of 601MF has now become more flexible (17 min. looping time) than the left side (213 min. looping time) by a factor of 12 (Figure 3.9D), reversing the relation found in the original 601 sequence, and correspondingly, the left side of the 601MF nucleosome (now containing stiffer DNA sequence) unwrapped at a lower force than the right side (Figure 3.9F). This implies that the direction of outer turn unwrapping can be controlled by the relative flexibility of

internal regions of DNA such that the nucleosome first unwraps from the DNA side connected to a less flexible inner turn DNA (Figures 3.9G and 3.9H).

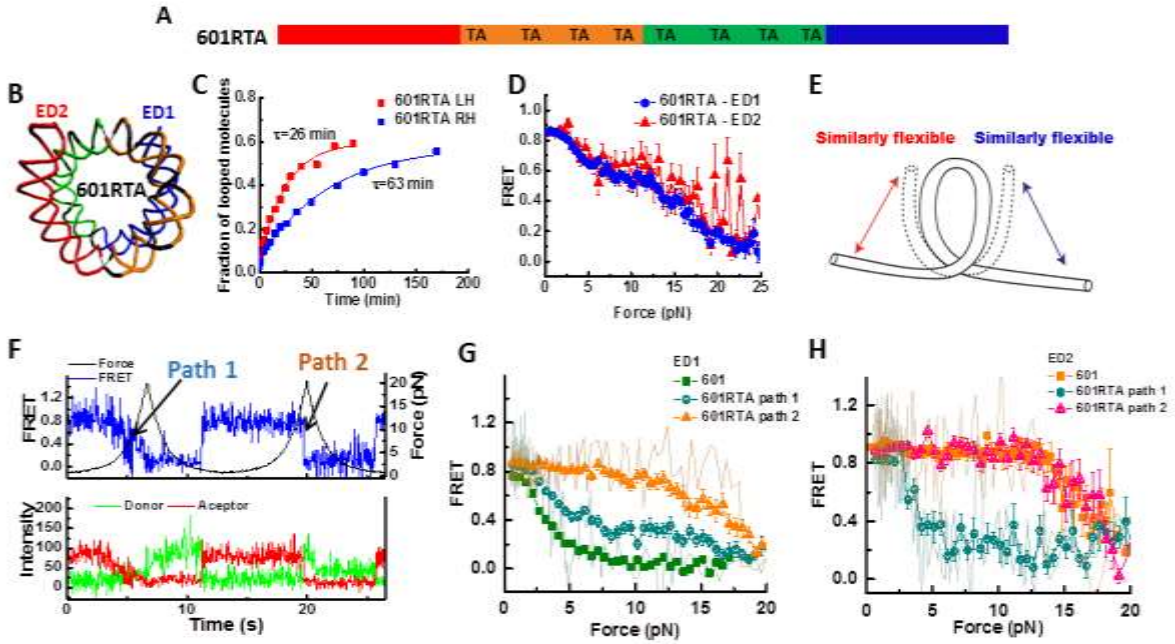

Figure 3.12: Stochastic unwrapping of nucleosome on the sequence with similar flexibility on two sides

(**A**): Scheme of the 601RTA sequence which is derived from the 601 the sequence by substitution of three dinucleotides on the right side by three TA steps.

(**B**): Nucleosomal DNA structures are shown in the same color scheme with the scheme of the sequence.

(**C**): Single exponential fits to the looped DNA faction vs. time yield the average looping time τ measured using single DNA cyclization assay for the 73 bp left or right halves (LH and RH, respectively) for the 601RTA sequence.

(**D**): Averaged stretching time traces of FRET efficiency vs. force for nucleosomes in ED1 (average of 57 traces) and ED2 (average of 7 traces) labeling schemes for the 601 RTA sequence. Error bars denote s.e.m.

(**E**): A cartoon illustrating stochastic unwrapping of nucleosome from the either side when the DNA flexibility on the two sides is made similar on the 601RTA sequence.

(**F**): Representative single-molecule fluorescence-force time trace for 601-RTA nucleosome reconstituted with the ED1 labeling scheme. Two unwrapping paths are shown – Path 1 is gradual FRET decrease at low force (similar to original weak side) while Path 2 is sudden FRET decrease at high force (similar to original strong side)

(**G, H**): Averaged FRET vs. force stretching curves for 601-RTA-ED1 (25 traces for path 1 and 32 traces for path 2) nucleosomes (**G**) and 601-RTA-ED2 (4 traces for path 1 and 3 traces for path 2) nucleosomes (**H**), comparing to that of ED1 and ED2 of the 601 sequence. Representative single-molecule stretching traces are shown in lighter color lines.

We further tested how nucleosome unwrapping is affected when the DNA sequence is similar in flexibility on both sides. We were guided by the 10 bp TA steps rule suggested by Widom [25, 39] to construct this DNA sequence. Chua *et al.* [23] confirmed by crystallography that TA dinucleotides accommodate the highest degree of distortion of the DNA structure within nucleosome. The 601 sequence is nonpalindromic with 10 bp TA steps situated only on the left side. Therefore, we pseudo-symmetrized the flexibility of the sequence by adding three copies of TA dinucleotides spaced 10 bp apart to the right (weak) side (601RTA) (Figures 6A and 6B). The resulting 601RTA right half (RH) became more flexible (cyclization time decreased from 189 to 63 min) (Figure 3.12C) and closer to the left half (26 min.). We ensured that the nucleosome positioning is maintained on all three sequences (601, 601MF and 601RTA), as nucleosomes reconstituted from all three sequences show the same electrophoretic mobility on a 5% native PAGE gel and displayed similar single-molecule FRET histograms (Figure 3.11). Strikingly, instead of one side winning the match every time, which side unwraps at low forces became stochastic (Figure 3.12F). The fraction of traces unwrapped at low force and high force was 37% and 67% for the left half (601RTA-ED2) and 44% and 56% for the right half (601RTA-ED1), respectively (Figures 3.12G and 3.12H). Averaging over all stretching traces produced almost identical FRET-force patterns for these two constructs (Figure 3.12D). These results imply that when the flexibility of DNA on the two sides of the nucleosome is similar, each side of the nucleosome unwraps stochastically at either low force or high force (Figure 3.12E).

3.5. Monte Carlo simulation of asymmetric unwrapping of Nucleosomal DNA

In order to model the asymmetric nucleosome dynamics under tension, we adopted a continuum model of symmetric nucleosomal DNA unwrapping developed by Sudhanshu et. al. [47] and extended it to a more general, asymmetric case where m and n base pairs can be unwrapped from the weak and strong side, respectively. In this model, the nucleosomal DNA is modeled as a left handed helix with a radius of 4.18 nm and height per turn of 2.39 nm. The total free energy change ΔF upon binding of DNA to the nucleosome spool (the histone core) relative to the unbound state is calculated at forces ranging from 0 pN to 12 pN as was done in Figure 3 of Sudhanshu *et. al.* . In a more general case of asymmetric unwrapping, m and n base pairs can be unwrapped from the weak and strong side, respectively, where m can be different from n. In the model of Sudhanshu et al, m=n. In our two-dimension model, in order to calculate the free energy change ΔF for (m, n) values, we assumed that the free energy change ΔF for (m, n) is equal to the (m + n) base pairs unwrapped case in the symmetric model. In

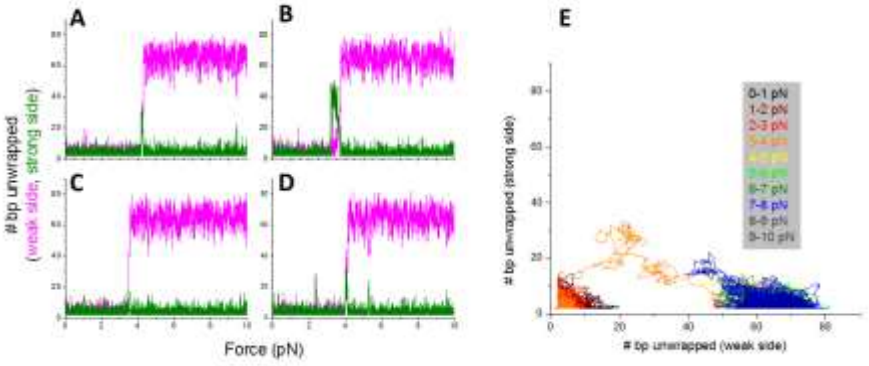

Figure 3.13: Monte Carlo simulation of nucleosome unwrapping
(**A,B,C,D**) Representative Monte Carlo simulation records show the number of base pairs unwrapped from the weak side (magenta) and the strong side (green) as the force increased from 0.1 pN to 10 pN.
(**E**) A two dimensional representation of unwrapping trajectory shown in (B). Different portions of the trajectory at difference forces are shown in different colors as indicated.

addition, we reduced the binding energy of the inner quarter of the weak side to 1.5 pN nm / bp while all other quarters (two outer quarters and the inner quarter of the strong side) are assumed to have the binding energy of 3.5 pN nm / bp so that the average binding energy is 3 pN nm / bp as was used by Sudhanshu et al. The only modification to the energy function used by Sudhanshu et al was a reduction in the binding energy of the inner quarter of the weak side (see Supplementary Information for details).

With this energy function, we performed Monte Carlo simulations starting from 0.1 pN and increasing the force in 0.1 pN increments every 2000 time steps until 10 pN of force was reached. Four representative trajectories of m and n values, the number of base pairs unwrapped from the weak and strong sides, respectively, are shown in Figure 3.13 (magenta for m and green for n). At around 3-5 pN of force, we observed major unwrapping of the weak side (m values reaching around 65 bp). In three cases (panels A, B and D), initial unwrapping of the strong side (transient increase in n, i.e. unwrapping of the strong side), precedes rewrapping of the strong side and major unwrapping of the weak side. Figure 3.13E shows an example trajectory in (m, n) space (corresponding to Figure 3.13B). A transient unwrapping of the strong side is seen in the force range 3-4 pN before the systems moves to the asymmetrically unwrapped state.

This simple model and simulation capture two important aspects of our data. First, asymmetric unwrapping can be obtained even when only the inner quarters are different in binding energy (presumably arising from differences in DNA flexibility where less flexible sequence has less binding energy). Second, a transient unwrapping of the strong side is often observed, and this is followed by rewrapping of the strong side and major unwrapping of the weak side in a coordinated fashion.

3.6. Discussion

Genetic information buried in nucleosome is made accessible for replication, transcription, repair and remodeling by partial unwrapping of nucleosomes [4, 8, 9, 24, 31, 50-52]. Our results provide the first demonstration of how the local flexibility of DNA governs the mechanical stability of the nucleosome and accessibility of nucleosomal DNA, and may be generalizable as a principal mechanism for regulation of DNA metabolism by nucleosomal DNA sequence and modifications.

The correlation that the more flexible the DNA sequence is, the more stable it stays bound to the histone core may aid the prediction of nucleosome positions imposed by DNA sequence. We found that this relation holds not only for DNA sequences but also for DNA modifications such as DNA mismatches, 5-methylcytosine and 5-formylcytosine (unpublished observations).

Stabilization of one nucleosomal DNA end upon the major opening of the other end may play a role in nucleosome integrity maintenance during transcription and nucleosome remodeling because both in vivo and in vitro studies suggest that a high fraction of nucleosomes survive after being transcribed [41, 53] and remodeled [46]. It is also possible that such orchestration between the two nucleosome ends may help stabilize one H2A/H2B dimer during the exchange or modification of the other dimer. For example, SWR-C/SWR-1 deposits H2A.Z into only one site at a time, not both [54].

Our Monte Carlo simulations could reproduce key features of asymmetric unwrapping and coordinated dynamics of two DNA ends (Figure 7). Nevertheless, this model ignores many structural details and represents DNA sequences with the resolution of 36 bp, a quarter of the nucleosomal DNA. Other properties of the nucleosome yet to be explored may make additional contributions to the coordination of DNA ends: (i) the proposed

electrostatic repulsion between two DNA turns [55] where upon force induced undocking of one end, the resulting loss of the electrostatic repulsion stabilizes the other end, (ii) DNA allostery [24] and (iii) the deformation of the histone octamer during unwrapping which may change charge distribution and/or contribute to the allosteric coupling. Histone deformation was suggested to govern salt induced nucleosome dissociation [14] and may also be involved in nucleosome remodeling by IWSI remodelers [42]. In our experiments at low tension, in addition to the early unwrapping of extreme DNA ends probed by ED1 and ED2-1, the FRET probes at ED1.5 (Figure 2B) and ED1.7 (Figure 2C) displayed an increase in FRET as a first response to applied force before a decrease, indicating possible partial DNA tightening mediated by twisting of the H_2A/H_2B dimer on the weak side.

We observed that nucleosomal DNA unwraps directionally under tension not only for the 601 sequence but also for the derivatives of the 601 sequence. Asymmetric unwrapping is likely to be generalizable to other sequences since the coordination of two ends would allow the system to amplify even a small difference in flexibility to cause a large asymmetry in mechanical stability.

Directionality of transcription can be ensured by the suppression of cryptic antisense [7] through epigenetic regulation and RNA degradation [56]. Our results linking sequence-dependent flexibility to mechanical stability of the nucleosome suggest another mechanism to maintain transcriptional direction– the possibility that nature selects for lower flexibility DNA sequences within the first half of nucleosomes in the direction of transcription. In this scenario, RNA polymerase would have greater initial access to the DNA template if it enters the nucleosomal DNA from the 'weak' side and would only pause when it reaches the nucleosomal dyad [4, 5]. We are currently investigating DNA flexibility on a genomic scale combining sequencing and single molecule cyclization to test this possibility.

3.7. Conclusion

Dynamics of the nucleosome and exposure of nucleosomal DNA play key roles in many nuclear processes but local dynamics of the nucleosome and its modulation by DNA sequence are poorly understood. Using single-molecule assays we observed that the nucleosome can unwrap asymmetrically and directionally under force and that the relative DNA flexibility of the inner quarters of nucleosomal DNA controls the unwrapping direction. The nucleosome unwraps from the stiffer side, and if the DNA flexibility is similar on two sides, it stochastically unwraps from either side. The two ends of the nucleosome are orchestrated such that the opening of one end helps stabilize the other end, providing a mechanism to amplify even small differences in flexibility to a large asymmetry in nucleosome stability. Our discovery of DNA flexibility as a critical factor for nucleosome dynamics and mechanical stability suggests a novel mechanism of gene regulation by DNA sequence and modifications.

Chapter 4

Effect of DNA Mismatches*

4.1. Introduction

Base-base DNA mismatches are generated by nucleotide misincorporation during DNA synthesis or chemical modification such as hydrolytic deamination of cytosine [57]. DNA mismatches, if unrepaired, are sources of genetic variation such as single nucleotide polymorphisms and point mutations which can alter cellular phenotype and cause dysfunction, diseases and cancer [57, 58]. DNA mismatches alter physical properties of the DNA such as local DNA flexibility and conformation heterogeneity [59-61].

It has been commonly observed that nucleosome pattern is correlated with oscillating pattern in the rate of genetic variation [62-65] such that substitution rate is higher while indel (insertion and deletion) rate is lower on nucleosomes. One possible explanation for this correlation is that mismatches may be generated randomly along the DNA but nucleosomes may block the repair machinery to remove the mismatch where nucleosomes occupy, and thus lead to substitutions. Therefore it is important to

---

*This work is in preparation for publication as:

Thuy T.M. Ngo, Qiucen Zhang, Taekjip Ha. "DNA Mismatches Enhance DNA Flexibility and Nucleosome Mechanical Stability".

understand how mismatches affect nucleosome stability and exposure which controls accessibility the nucleosome by the repair machinery.

In chapter 3, we demonstrated the correlation between DNA flexibility and nucleosome unwrapping. We showed that the nucleosome can unwrap asymmetrically under tension. One side of the outer DNA turn unwraps at lower force and the other side unwraps at higher force. The direction of unwrapping is controlled by the relative DNA flexibility of the two DNA halves flanking the dyad. The unwrapping force is lower for the nucleosomal DNA side with lower flexibility and vice versa. Here, we examined the effect of DNA mismatch on DNA flexibility and nucleosome unwrapping dynamics. We used a single molecule DNA cyclization assay to examine the flexibility of a DNA segment containing a mismatch and a force-fluorescence spectroscopy method to study the effect of a mismatch on nucleosome unwrapping dynamics. In addition, we used a mismatch as a flexible lesion placed at various positions on the nucleosome to investigate the effect of local flexibility on the nucleosome stability. With this design, protein surface – DNA interaction map is unchanged and only bending energy alters locally as a function of the mismatch position.

4.2. Results

4.2.1. DNA mismatches enhance DNA flexibility

A single DNA mismatch can cause the deviation of DNA conformation from B-form [60, 61] and increase DNA flexibility [59]. A previous study using DNA buckling assay suggested that C-C is the most flexible mismatch [59]. Therefore we chose C-C as a representative mismatch to investigate its effect on nucleosome. A single C-C mismatch was introduced at different positions on the 601 sequence, a nucleosome positioning sequence (Figure 4.1A). Previously, we showed that the right half of the 601 sequence has

a low relative flexibility than the left half (chapter 3) and a C-C mismatch will increase flexibility; therefore we placed the mismatch on the (less flexible) right half (Figure 4.1A).

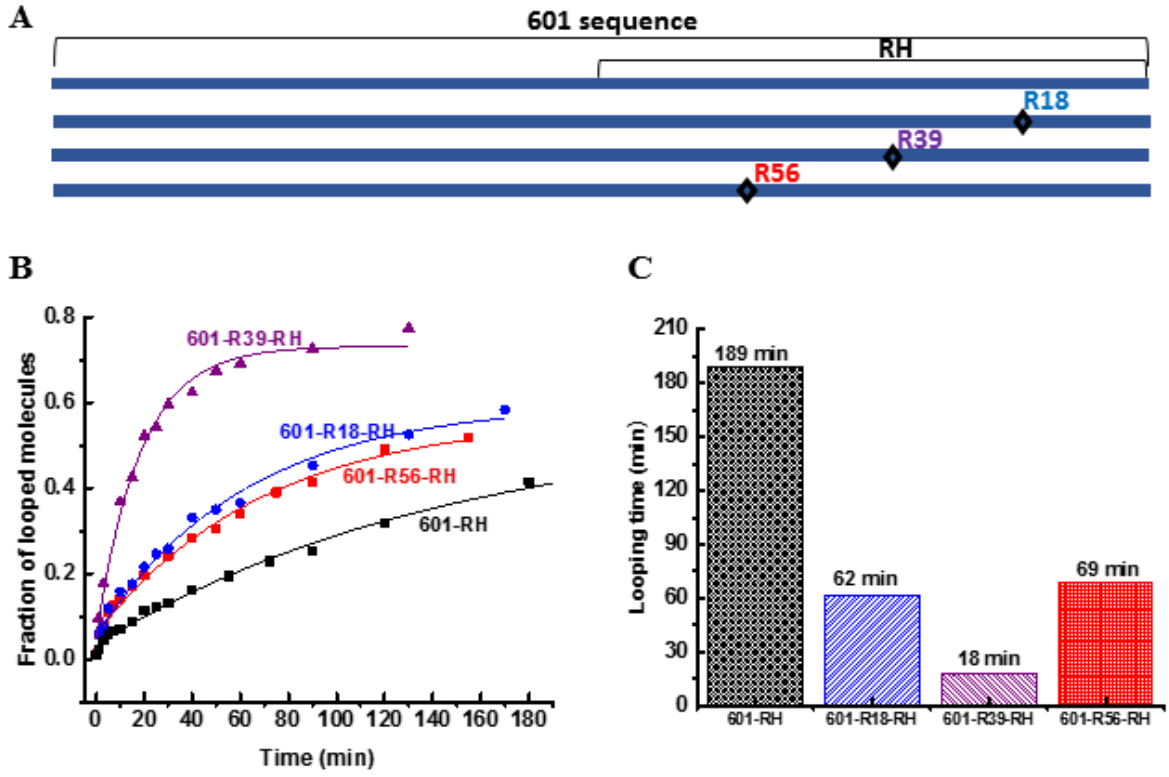

Figure 4.1: DNA mismatches enhance DNA flexibility
(A) Schematic of DNA constructs used in the looping measurement.
(B, C) Time course measurement of looped fraction for the right half of the 601 sequence without and with a mismatch.

We used a single molecule DNA cyclization assay to probe the change in apparent flexibility of that right half (RH) sequence upon introducing a mismatch. In this assay, DNA fragments with two 10 nt long 5′ overhangs were immobilized on a microscope slide. A FRET pair (Cy3 and Cy5) is incorporated at the 5′ end of the overhangs that are complementary to each other which allow the detection of high FRET when the two overhangs anneal with each other forming a closed circle. We used a time course of generation of high FRET population to quantify the fraction of looped molecules versus time after the high salt buffer is introduced to the chamber. The rate of loop formation was used as an operational measure of DNA flexibility. The faster the looping occurs, the

more flexible the sequence is. As expected, we observed a dramatic decrease in looping time on the construct containing a mismatch (Figures 4.1C and 4.1D). With adding a C-C mismatch at three different positions of the RH fragment (R18, R39 and R56), looping time reduces from 189 min to 62 min., 18 min., and 69 min. respectively. The reduction in apparent looping time is higher with the mismatch placing at the center (R39) than toward the side of the RH fragment (R18, R56) likely because the looping measurement is more sensitive to the change in flexibility at the center of the DNA fragment. The decrease in looping time indicates an increase of DNA flexibility.

4.2.2. Monitoring nucleosome unwrapping by force fluorescence spectroscopy

In chapter 3, we demonstrated that mechanical stability of nucleosome is controlled by DNA flexibility. Here we showed that a mismatch enhances DNA flexibility. Therefore, we sought to examine how a mismatch can change nucleosome mechanical stability. We measured conformational dynamics of the nucleosome in response to external force by a single-molecule assay which combines fluorescence with optical tweezers [37, 66, 67]. This assay allows us to simultaneously probe local conformational change of the nucleosome during unwrapping by tension.

Nucleosome were reconstituted from DNA constructs containing a DNA mismatch at the same location as in the looping measurement. The two strands of each DNA construct were created by ligation separately (Figure 4.2) to ensure the completion of ligation without nicks on the DNA. DNA constructs were then formed by slowly annealing of the two purified ligated strands. All four DNA constructs (with and without a mismatch) yielded nucleosomes with the same electro-mobility and FRET peak indicating the homogeneous positioning of the nucleosome on the four DNA constructs.

In the force fluorescence spectroscopy assay, a nucleosome was anchored to a PEG-coated glass surface via biotin-neutravidin on one end of the DNA and pulled via a λ-DNA tethered to the other end by an optical trap. As previously described, we attached a pair of donor and an acceptor fluorophore to the DNA to probe the unwrapping of nucleosomal DNA. To probe unwrapping of the outer DNA turn, we constructed DNA with a labeling scheme called ED1 in which the donor is incorporated to the nucleotide

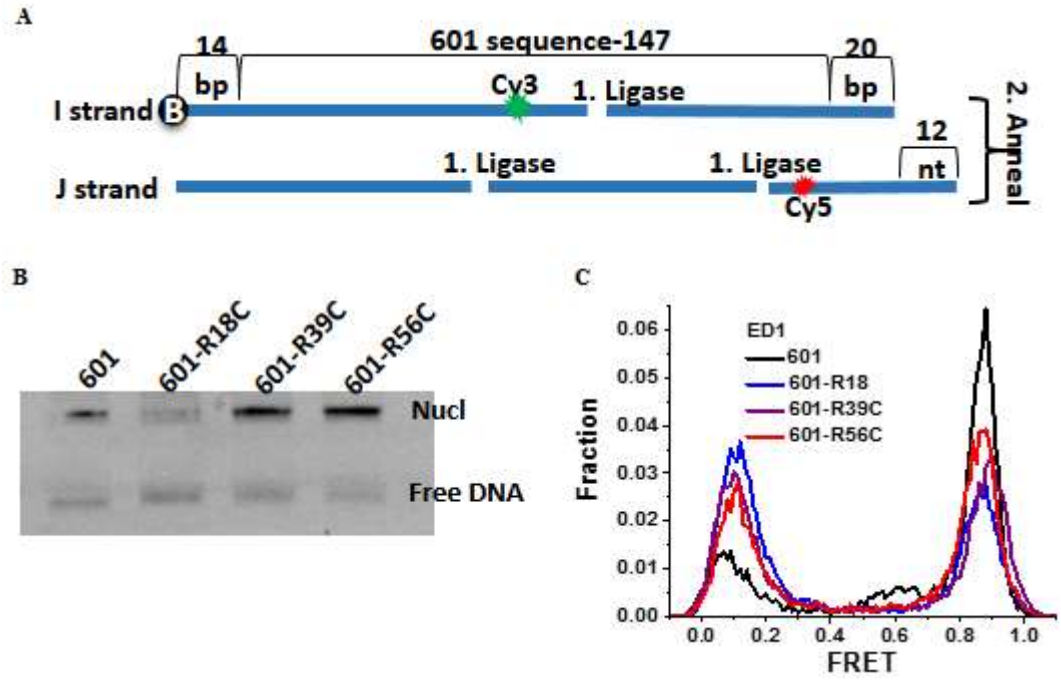

Figure 4.2: Nucleosome preparation
(A) Scheme of the DNA template prepared by ligation of short, labeled oligos
(B) Migration of the 601 nucleosome mismatch containing nucleosomes on 5% native PAGE
FRET histogram of the 601 nucleosome mismatch containing nucleosomes with ED1 labeling scheme.

68 from the 5′ end of the top strand (I68) and the acceptor is attached at nucleotide 7 from the 5′ end of the bottom strand (J7) (table 1.1). Upon formation of nucleosome, ED1 nucleosomes displayed high FRET due to close proximity (Figure 4.2). We applied tension to the nucleosomal DNA by moving the piezo stage at a constant speed of 455

nm/s while a focused laser (532 nm) follows the molecule to monitor fluorescence signals. Force is increased from a low value (typically between 0.4 – 1.0 pN) to a predetermined higher value and then returns to the low value. We observed a gradual decrease in FRET as the force increases followed by fast fluctuations in FRET, and finally a sharp decrease in FRET (Figure 4.3A). Upon relaxation, the nucleosome reformed with hysteresis.

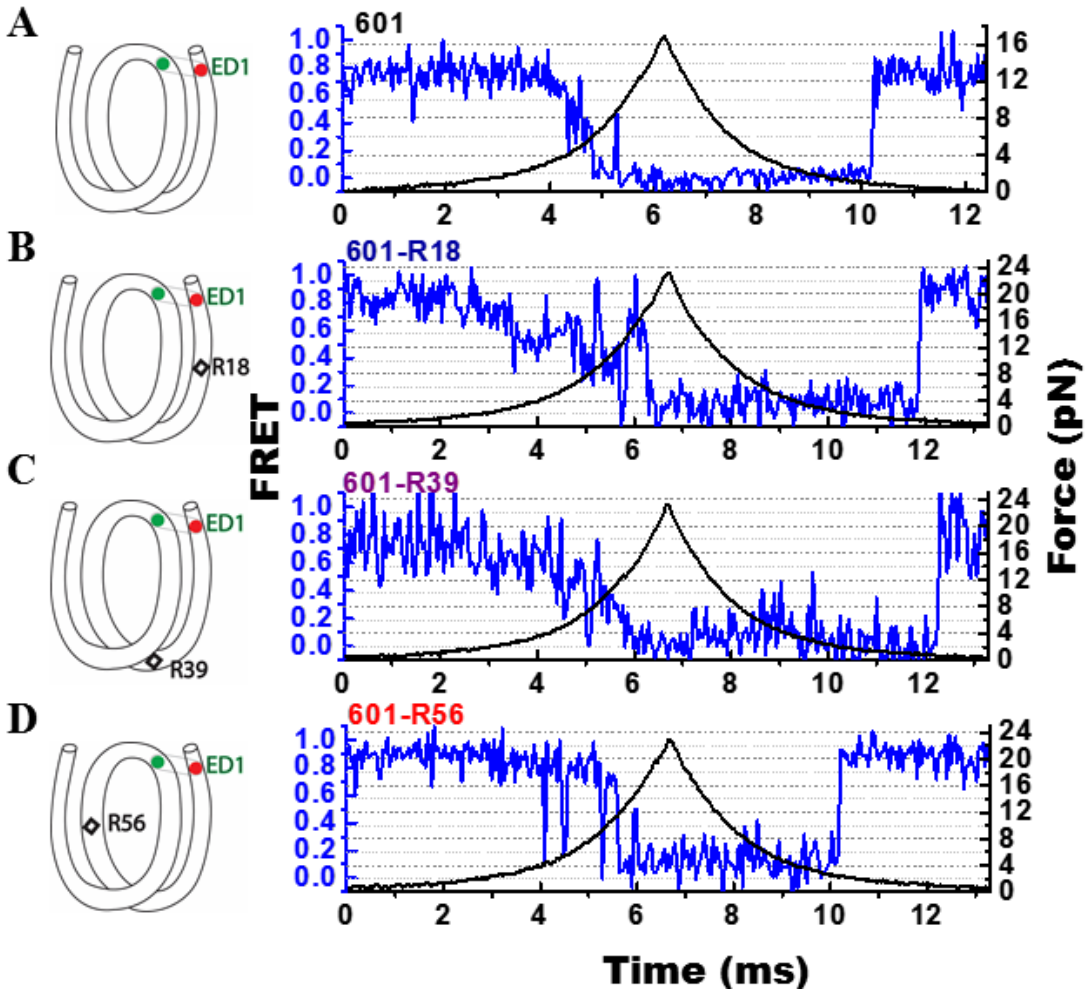

Figure 4.3: Nucleosome unwrapping measurement
Representative stretching traces of the outer turn (ED1) for nucleosomes reconstituted from the 601 sequence (**A**) and from the 601 sequence with containing a mismatch at different positions: on the outer turn (**B**), at the junction of the outer turn and inner turn (**C**) and at the inner turn (**D**).

4.2.3. Unwrapping force is higher for subsequent stretching cycles

Using electrophoretic mobility shift assay and FRET histogram at zero force, we did not observe a noticeable difference between normal nucleosomes and mismatch-containing nucleosomes (Figure 4.2). However, under perturbation by force all stretching traces showed the same behavior for the 601 nucleosome but different behaviors for mismatch-containing nucleosomes (Figure 4.4). For the mismatch constructs, unwrapping of the ED1 side was stochastic with a fraction of stretching cycles showed unwrapping at low force and a fraction of traces displayed unwrapping at high force (Figure 4.4). Interestingly, after relaxation, we observed a general trend of an increase in unwrapping force in the subsequence stretching cycles of mismatch-containing nucleosomes (Figure 4.4). This observation can be explained by re-positioning of nuclelosome such that the

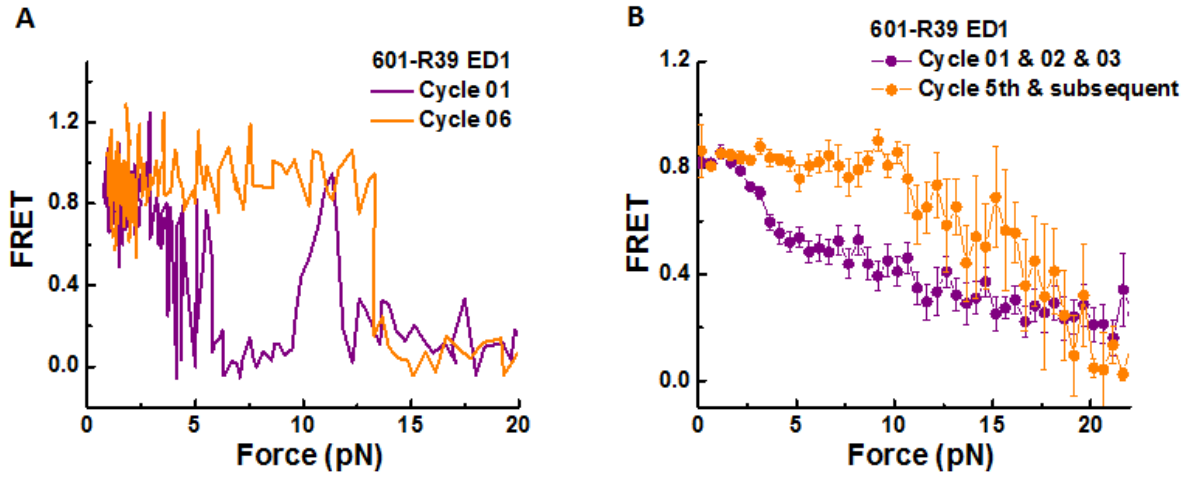

Figure 4.4: Unwrapping force of mismatch containing nucleosomes is higher for subsequent stretching cycles.
(A) Representative single-molecule stretching traces at two stretching cycles from the sample molecule, probe by the ED1 FRET pair.
(**B**) Averaging FRET vs. Force for many molecules at the first three stretching cycles (purple) and the subsequent stretching cycles (orange).

mismatch moves toward the dyad as predicted by a previous theoretical model [68]. According to this model, the position of nucleosome DNA containing flexible lesion is weakly affected, but under perturbation by other cellular components that either stiffen

the DNA overall or weaken histone binding, the lesion can be made to have a strong preference for the dyad. In our experiments, applied tension during stretching may act as the perturbation that weakens nucleosome binding.

4.2.4. DNA mismatch enhances nucleosome mechanical stability

In order to investigate the effect of single base pair mismatches, we compared the stretching patterns of nucleosomes containing mismatches (R18, R39, R56) with unmodified nucleosomes. We observed similar stretching patterns for the mismatch nucleosomes (R18, R39, R56) to that of the 601 nucleosome. However, the force range where FRET reduces gradually accompanied by fluctuation was wider and extended to higher force (Figures 4.3B-D). We used the averaging of FRET vs. force plot to compare unwrapping force. Because we observed the increase in unwrapping forces for subsequent stretching cycles in mismatch-containing nucleosome (Figure 4.4), we only used the first stretching cycle for this comparison (Figure 4.5). The averaged FRET vs. force pattern clearly showed an increase in unwrapping force for the mismatch containing nucleosomes (Figure 4.5A). This indicates the enhancement of mechanical stability of the mismatch nucleosome.

Next, we attempted to measure unwrapping of nucleosome on the side that does not contain the mismatch (ED2 side) for the construct containing a mismatch at the R39 position. In this configuration, the donor was placed on the inner DNA turn closed to the dyad (J58) which was similar to the ED1 construct, and the acceptor was incorporated to the opposite ends (I9) (Figure 4.5B). Stretching curves of nucleosome on this side yielded higher unwrapping force as compared to the ED1 side as previously recorded (chapter 3). The mismatch construct yielded the same unwrapping

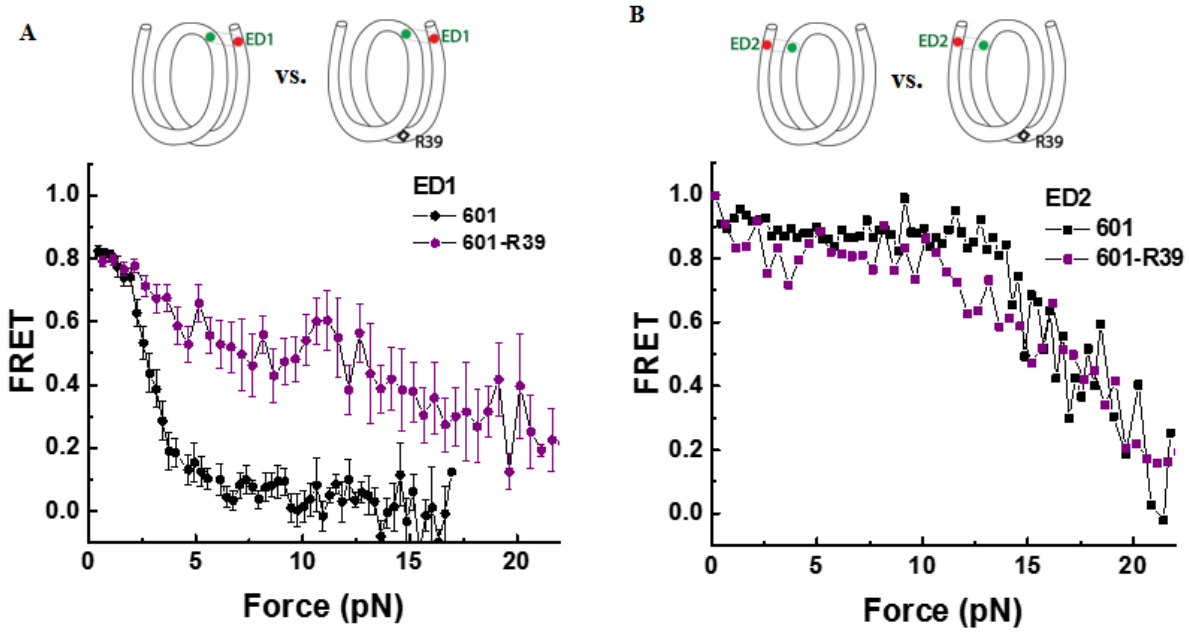

Figure 4.5: Enhancement of nucleosome mechanical stability by DNA mismatch Average of FRET vs. Force for ED1 probe (**A**) and ED2 probe (**B**) for the 601 nucleosome (black) and for the first stretching cycle of the mismatch containing nucleosome 601-R39 (purple).

pattern as the 601 nucleosome. This indicates that the change in local flexibility induced by the mismatch only has an effect on the side containing the mismatch (ED1 side) but does not have a global effect on the other side (ED2 side).

4.2.5. Effect of mismatch positions

Our previous finding demonstrated that local DNA flexibility of the inner turn control unwrapping of the outer turn (chapter 3). Here, we examined the effect of DNA flexibility at a defined locality of each quarter by changing the C-C mismatch at various position on the 601 sequence. Alternative placing the mismatch at various positions allows us to examine the effect of only local DNA flexibility of different portions of DNA on nucleosome unwrapping since DNA-protein contacts remain the same for all cases and

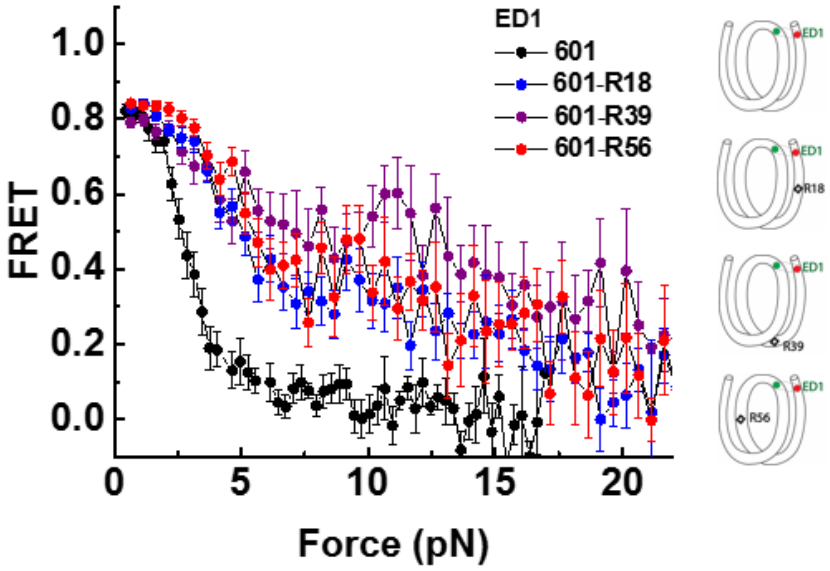

Figure 4.6: Mismatch position dependence of nucleosome unwrapping
Average of FRET vs. Force for ED1 probe for the 601 nucleosome (black) and the mismatch containing nucleosome 601-R39 (purple), 601 R18 (blue) and 601-R56 (red).

only DNA bending is altered. We designed three DNA constructs 601-R18, 601-R39 and 601-R56 with the mismatch situated in the middle of the outer turn, at the junction region between DNA outer turn and inner turn and in the middle of the inner turn, respectively. For all three cases, unwrapping force increased indicating that local flexibility of either the inner turn or the outer turn would affect unwrapping force of the nucleosome (Figure 4.6). The effect was largest for the mismatch placing at the junction of the inner turn and outer turn (R39).

4.3. Discussion

Using the looping time of single molecule DNA cyclization as a measurement of DNA flexibility, we showed that a DNA mismatch increases DNA flexibility. Our results are consistent with previous studies on the effect of a mismatch to DNA conformational dynamics using other methods such as NMR [60] and the DNA Euler buckling assay [59].

Possible explanation for the enhancement of DNA flexibility is the existence of a kink at the mismatch position on the DNA.

We observed the enhancement of mechanical stability of nucleosome reconstituted from a mismatch DNA construct. This result is consistent with our previous study on the correlation of DNA flexibility with unwrapping force (chapter 3). We reported that nucleosome unwraps at low force from the side with lower flexibility and unwraps at a higher force from the side with higher DNA flexibility. This observation suggests that apparent flexibility of DNA induced by either a mismatch or flexible elements results in a similar enhancement effect on nucleosome mechanical stability. However, here we only observed stochastic unwrapping of the nucleosome on the side containing the mismatch (ED1 side) but not the other side (ED2 side), in contrast to stochastic unwrapping of both sides in our previous observation when we changed DNA sequence such that DNA on both sides of the nucleosome are flexible. This discrepancy suggests that though apparent flexibility of DNA containing a mismatch and containing a flexible elements are the same, the mismatch uncouple the coordination unwrapping of the two DNA ends. Uncoupling in coordination of the two DNA ends in the mismatch containing nucleosome can be explained by attenuation of DNA allostery [24] by mismatched bases.

Our observation of the enhancement of DNA mechanical stability predicts that a mismatch reduces nucleosome accessibility, providing mechanism to explain the accumulation of substitutions in the nucleosomes that may be the source for genetic variation during evolution and cancer progression. The reduction in nucleosomal DNA accessibility would enhance the blockage of the DNA mismatch repair machinery on the nucleosome. An unrepaired mismatch leads to point mutation on DNA. In fact, previous observations show the higher frequency of single nucleotide polymorphism on the nucleosome. The higher frequency of substitutions in the nucleosomes DNA may be

attributed to the difficulty of accessing the extra stable nucleosomes. More experiment approaches are needed to confirm our prediction.

We observed an increase in unwrapping force induced by the mismatch placing at all three positions at the inner, outer quarter or the junction. This implies that DNA flexibility of both the inner and outer quarter determines the unwrapping force of the DNA outer turn. In addition, the mismatch situated at the junction of the inner turn and outer turn shows the highest unwrapping force. This suggests that dimer may undock during unwrapping. If histone core does not deform during unwrapping, the unwrapping of the outer turn of DNA which in contact with the H2A/H2B dimers should be influenced only by the sequence of the outer turn. However, we observed that changing the DNA flexibility at either the inner or outer turn affects unwrapping. If the dimer undocking is involved in the DNA unwrapping process, both inner and outer DNA turn should affect unwrapping. Moreover, the specific location at the junction of the inner turn and outer turn which is also the transition between H2A/H2B dimer and $(H3/H4)_2$ contacts should have a major impact on the conformation transition as what we observed. More experiments with cross-linked histone octamer and/or labelled on both tetramer and dimer are needed to provide further evidence to support our hypothesis of dimer undocking.

4.4. Conclusion

In eukaryotes, DNA is organized by regular arrangement of the basic units, nucleosomes, as beads on string. Nucleosomes pattern is correlated with oscillation pattern of genetic variations which is originated from mismatches during replication and chemical modification of DNA. However, how DNA mismatches affect the stability and exposure of nucleosome is unknown. Here, we used single molecule DNA cyclization assay and optical trap combining with FRET detection to investigate the effect of DNA mismatches

on DNA flexibility and force induced nucleosome dynamics. We found that DNA mismatches enhance DNA flexibility nucleosome mechanical stability. The increase in unwrapping force is induced by the mismatch placing at all three positions: at the inner turn, at the outer turn or the junction of the inner and outer turn of the nucleosome. The mismatch placed at the junction displayed the most profound effect on unwrapping force of the DNA outer turn. Interestingly, under perturbation by force, after relaxation unwrapping force is higher for subsequent stretching cycles, suggesting possible force induced sliding of the mismatch containing nucleosome. Our results predict the reduction of nucleosome accessibility by mismatches, suggesting a mechanism to explain the accumulation of nucleotide substitutions in the nucleosomes which may be the source for genetic variation during evolution and cancer progression.

Chapter 5

Effect of Cytosine Modifications*

5.1. Introduction

DNA comprises of four genetic nucleobases: adenine (A), thymine (T), cytosine (C) and guanine (G). It has long been recognized that nonmutagenic cytosine can undergo chemical modifications at the fifth carbon of its pyrimidine ring (5-C) that plays important regulation roles [69-71]. In mammals, new DNA methylation (5-mC) is established by transferring the methyl group from S-adenosylmethionine to cytosine on CpG islands by DNA methyltransferases DNMT3A and DNMT3B [69]. DNA methylation is stable in somatic cells but gets lost in specific developmental stages such as preimplantation embryos and developing primordial germ cells [72-74]. Loss of DNA methylation is required to set up pluripotent states in embryos and to erase parental methylation imprints in developing germ cells. In addition to passive loss of methylation due to DNA replication, cytosine methylation marks can be erased through active demethylation pathway involving stepwise oxidation by TETs enzymes of 5-

---

*This work is in preparation for publication as:

Thuy T.M. Ngo, Jejoong Yoo, Qing Dai, Qiucen Zhang, Aleksei Aksimentiev, Chuan He, Taekjip Ha. "Effect of Cytosine Modifications on DNA Flexibility and Tension Induced Nucleosome Dynamics".

methylcytosine to 5-hydroxymethylcytosine (5-hmC), 5-formylcytosine (5-fC) and 5-carboxylcytosine (caC) and base excision of 5-fC or 5-caC by DNA glycosylase TDG followed by base excision repair to convert an abasic site to cytosine [75-77].

Methylation cytosine (5-mC) is found in most plants, animals and fungi and has a profound effect on genome stability, gene expression, and development [69, 78]. Recently, there is emerging evidence suggesting the association of oxidation products of cytosine including 5-hmC, 5-fC and 5-caC with gene regulation [75]. For instance, 5-hmC is preferentially enriched at the promoters of genes that are expressed at medium-to-low levels in mouse and human ESCs [79-82] and 5fC/5caC tend to accumulate at transcriptionally inactive or poised promoters [83]. Possible mechanisms for regulatory role of cytosine modifications may include: (1) affecting DNA physical properties, (2) altering chromatin accessibility and (3) mediating binding of proteins such as modifying enzymes that recognize cytosine modifications as their substrates and transcriptional activators/repressors which will translate modifications to downstream signaling of transcription machinery [78, 84].

DNA flexibility was shown to affect binding of proteins to methylated DNA and DNA containing lesions [85-88]. For instance, DNA mismatch increases DNA flexibility leading to facilitation of the recognition of mismatch by repair proteins such as DNA glycosylases, CPD and MutS [88]. CpG methylation reduces DNA flexibility and thus affects binding of some proteins to their cognitive sequences such as EcoRI restriction site and cAMP DNA responsive element [85, 86]. However, how 5-hmC, 5-fC and 5-caC affect DNA flexibility is unknown.

Stable packing of DNA in nucleosomes imposes a barrier for replication, transcription and repair [5-7, 89]. The nucleosomal DNA can be made accessible by partial unwrapping of DNA from the histone core [4, 9, 52]. Cytosine modifications may affect gene regulation

by changing nucleosome stability and unwrapping. For example, 5-mC has been reported to affect nucleosome structure [16, 90, 91]. However, how cytosine modifications including 5-mC and its oxidation products (5-hmC, 5-fC and 5-caC) affect nucleosome unwrapping is unknown.

Previously, we suggested a new mechanism that DNA sequence and modifications may affect gene expression by altering nucleosome unwrapping which can be controlled by DNA flexibility (chapter 3). We demonstrated the correlation that the more flexible the DNA sequence is, the more stable it stays bound to the histone core. Here we reported a comprehensive survey on the effect of cytosine modifications on DNA flexibility using single molecule cyclization assay and examined the correlation between DNA flexibility and nucleosome unwrapping using combination of optical tweezers with smFRET detection.

5.2. Results

5.2.1. Effect of cytosine modifications on DNA flexibility

We synthesized DNA oligos with various cytosine modifications at different locations as indicated in the figure 5.1A. Two strands of the DNA construct were ligated from the modified oligos and biotin/fluorophores labeled oligos and purified separately in order to ensure completed ligation of the two strands. Then we annealed the two strands by heating up to 90^{o}C followed by slow cooling.

We used a single molecule DNA cyclization assay to quantify the effect of cytosine modifications on DNA flexibility. In this assay, DNA fragments with two complement 5' overhangs of 10 nts were immobilized on a PEG-coated quartz slide using biotin-neutravidin interaction. A FRET pair at the 5' ends enabled the detection of loop formation of single DNA molecules via FRET increase. High FRET population was monitored over time to quantify the fraction of looped DNA (Figure 5.1B). Here, we used

the rate of loop formation as our operational measure of DNA flexibility. If DNA is more flexible, it takes less time to form a loop and vice versa.

We observed that 5-methylcytosine resulted in slower looping while 5-formylcytosine and 5-hydroxylcytosine accelerate looping of the DNA construct and 5-carboxymcytosine

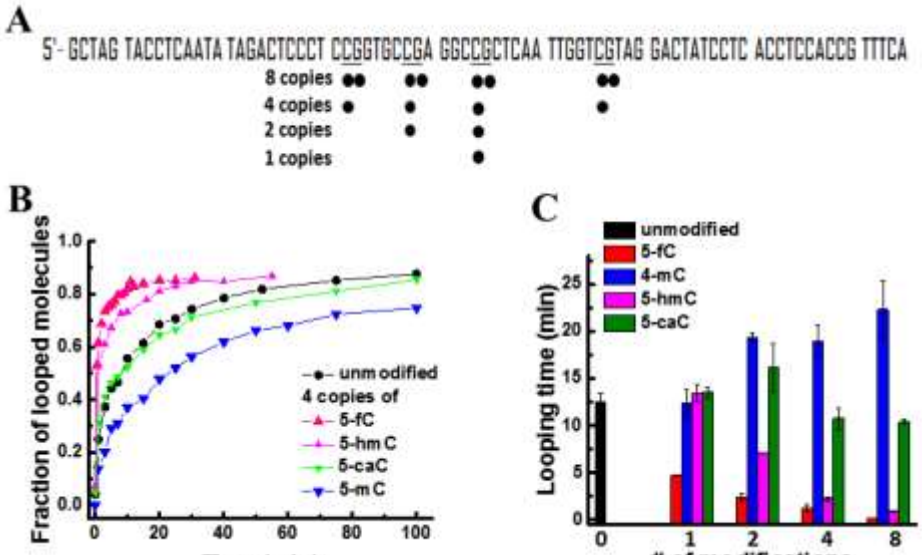

Figure 5.1: Effect of cytosine modifications on DNA flexibility
(A) DNA sequence with modified CpG sites in underscore used for DNA cyclization experiments. Positions and number of copy of cytosine modifications were indicated in black dots.
(B) Fraction of looped molecule as a function of time for unmodified DNA and DNA with 4 copies of cytosine modifications 5-formylcytosine (5-fC), 5-hydroxymmethylcytosine (5-hmC), 5-carboxylcytosine (5-caC) and 5-methylcytosine (5-mC).
(C) Looping time for different number of modifications for all four cytosine modifications.

did not show a detectable effect on DNA flexibility (Figure 5.1B). With single copy of modification, 5-methylcytosine had almost no effect while 5-formylcytosine displayed remarkable effect on looping time (a 3-fold reduction) (Figure 5.1C). More copies of each modification magnified their effect. We obtained a similar reduction in DNA flexibility of enzymatically methylated DNA using methyltransferase M.SssI (Figure 5.2). This indicates that 5-methylcytosine decreases DNA flexibility while 5-formylcytosine and 5-hydroxylcytosine increases DNA flexibility.

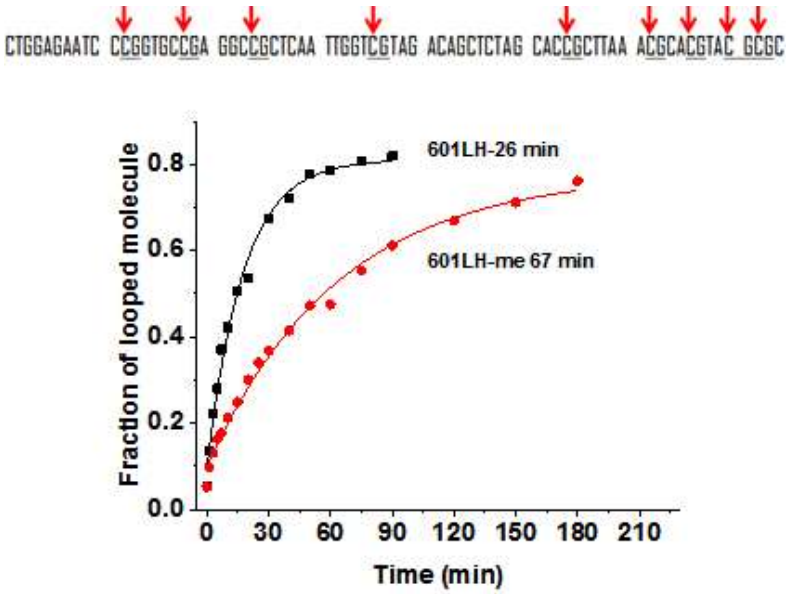

Figure 5.2: Cyclization measurement of the unmodified and enzymatically methylated DNA

CpG sites on left half of the 601 sequence which were methylated using M.SssI enzyme are shown in underlie and marked by red arrows.

5.2.2. 5- methylcytosine loosens packing of nucleosomal DNA ends

5-methylcytosine has been demonstrated to change nucleosome structure and dynamics [16, 87, 90, 91]. Using single molecule FRET, Choy *et. al.* showed that DNA methylation induces tighter wrapping of DNA around the histone core [91]. The more packing effect of nucleosomal DNA outer turn was deduced from the dynamics excursion to a more compaction state. However the authors were not able to rule out alternative explanations because a nucleosome formed on the 5S sequence in their study allows multiple translational frames for nucleosome positioning. Later, Jimenez-Useche *et. al.* used bulk FRET and SAXS to demonstrate that DNA methylation decreases the packaging of nucleosomal DNA ends at various degrees depending on positions of CpG with respect to histone core [90]. Therefore, we attempted to use single-molecule FRET to examine the effect of DNA methylation on the packing of nucleosomal DNA ends (Figure 5.4). In order to have a clear interpretation using FRET, we chose to use the 601 sequence (Figure

5.4A). We attached a pair of dye at the first nucleotides just outside of the 601 core sequence (Figure 5.4B). DNA was constructed by PCR amplification using labeled primers. DNA methylation was introduced enzymatically by *Spiroplasma* methyltransferase M.SssI [90, 91]. The methylation level was completed on all CpG sites, confirmed by digestion of restriction enzyme which does not function on 5-methylcytosine (Figure 5.3A). Nucleosomes were reconstituted from the unmodified or methylated DNA constructs with *Xenopus laveis* histone octamer (Figure 5.3B).

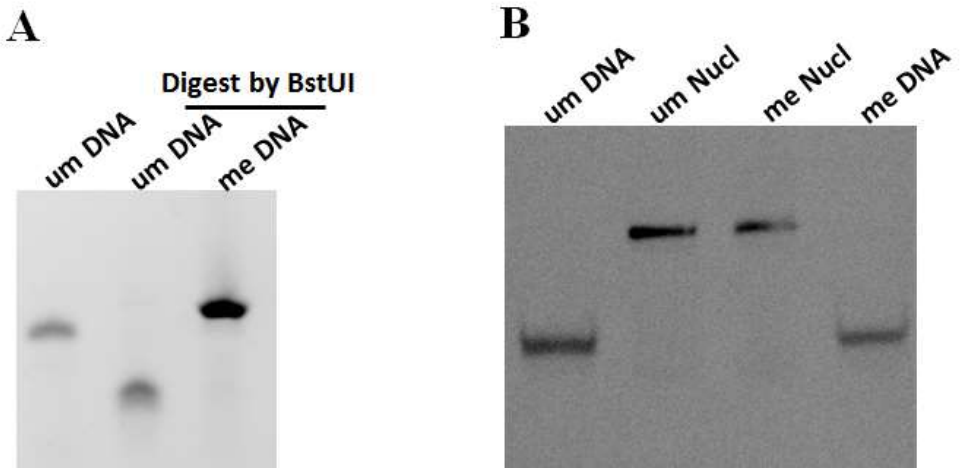

Figure 5.3: Formation of nuclesosome on methylated DNA

Checking methylation efficiency (**A**) and formation of nuclesosome on methylated DNA (**B**) by 5% native PAGE gel.

In single-molecule FRET measurement, nucleosomes were immobilized a PEG-coated quartz slide. In agreement with well-defined positioning of the nucleosome indicated by electrophoretic mobility shift assay (Figure 5.3B), FRET histogram of nucleosome showed a single peaked distribution (Figure 5.4C). Methylated nucleosomes showed lower FRET efficiency (0.69 ± 0.006) than unmodified nucleosomes (0.73 ± 0.008). The reduction in

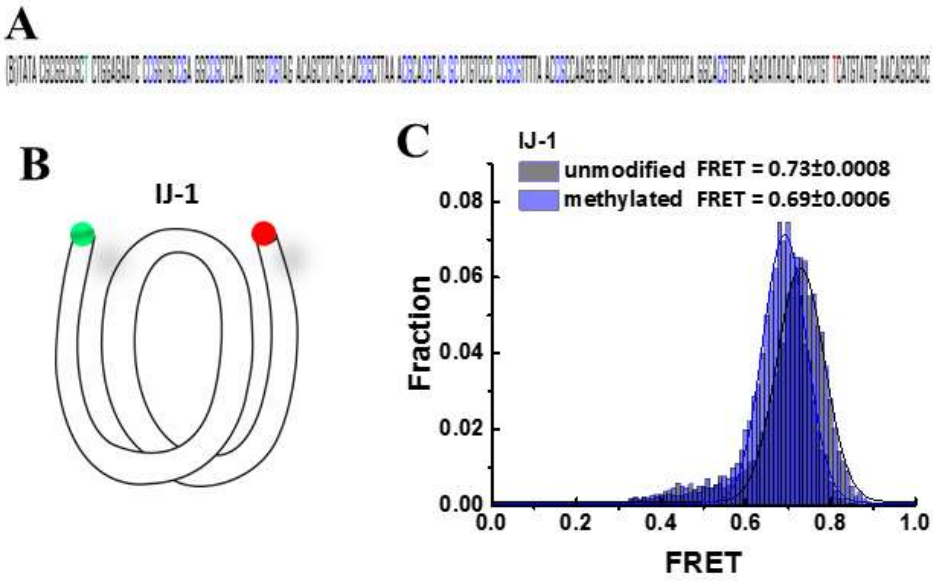

Figure 5.4: 5-mC loosens packing of nucleosomal DNA ends
(A) The DNA construct containing the 601 sequence used to reconstitute nucleosome. CpG sites which were methylated using M.SssI enzyme is in blue. The nucleotides incorporated to Cy3 and Cy5 is in green and red.
(B) Scheme of nucleosomal DNA with IJ-1 labeling position.
(C) FRET histogram of IJ-1 nucleosome with and without methylation on DNA.

FRET indicates that DNA methylation causes loosening of the nucleosomal DNA end packing, supporting the study by Jimenez-Useche *et. al.* [90] but contradicting the study by Choy *et. al.* [92]. We further examined this discrepancy with a previous smFRET study and found that having the presence methyltransferase during the measurement induces FRET increases, likely due to the binding of the enzyme to the nucleosome, and after 90 minutes waiting, the FRET value returns to the original lower level (data not shown).

5.2.3. Investigate effect of cytosine modification on nucleosome mechanical stability by force fluorescence spectroscopy

In an earlier work, we demonstrated that mechanical stability of nucleosome is controlled by DNA flexibility (chapter 3). From which we established that DNA flexibility can be used as an epoxy of nucleosome stability. Here we showed that 5-methylcytosine

decreases DNA flexibility while 5-formylcytosine increases DNA flexibility. Therefore, we sought to examine how 5-methylcytosine and 5-formylcytosine change the nucleosome's mechanical stability. We measured conformational dynamics of the nucleosome in responding to external force by a single-molecule assay that combines fluorescence detection with optical tweezers [37, 66]. This assay allows us to simultaneously probe local conformational change of the nucleosome during unwrapping by tension.

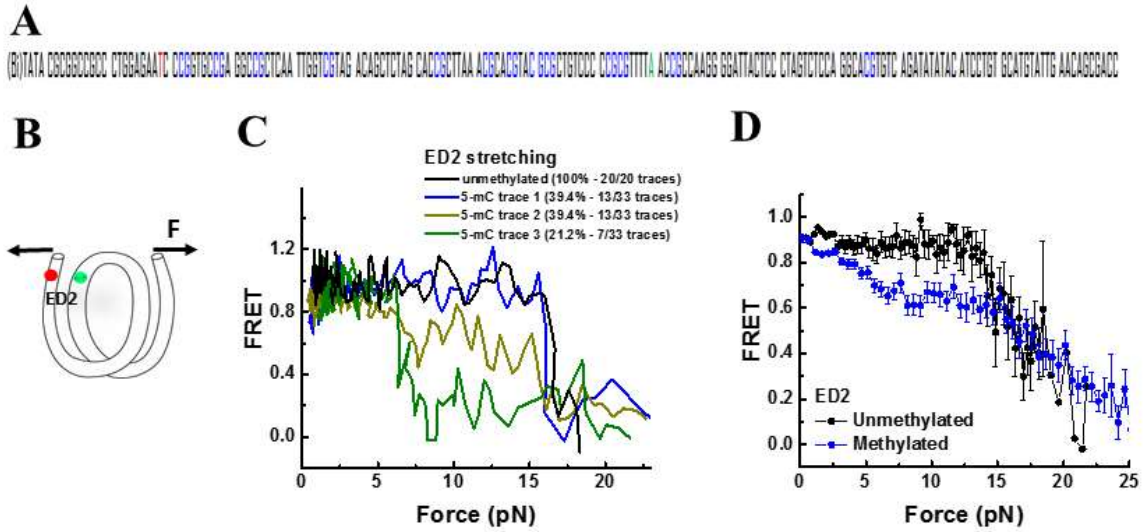

Figure 5.5: 5-mC reduces initial unwrapping force of nucleosome on the strong side
(A) The DNA construct containing the 601 sequence used to reconstitute nucleosome. CpG sites which were methylated using M.SssI enzyme are show in blue. The nucleotides incorporated to Cy3 and Cy5 is in green and red.
(B) Scheme of nucleosomal DNA with ED2 labeling scheme for unwrapping experiments.
(C) Representative stretching traces of ED2 nucleosome with unmodified and methylated DNA.
(D) Averaging of stretching traces for ED2 nucleosome with unmodified (20 traces) and methylated DNA (33 traces).

In the force fluorescence spectroscopy assay, a nucleosome was anchored to a PEG-coated glass surface via biotin-neutravidin on one end of the DNA and pulled via a λ-DNA tethered to the other end by an optical trap. As previous described, we attached a pair of donor and acceptor fluorophores to the DNA to probe unwrapping of nucleosomal DNA.

We applied tension to the nucleosomal DNA by moving the piezo stage at a constant speed of 455 nm/s while a focused laser (532 nm) follows the molecule to monitor fluorescence signals. The force is increased from a low value (typically between 0.4 – 1.0 pN) to a predetermined higher value and then returned to the low value. As the force increases, we observe a reduction in FRET indicating opening of nucleosomal DNA (Figures 5.5C and 5.5D). We compared the force range where a signification FRET signal drops for different locations of FRET probes to determine the order of unwrapping of different parts of DNA and for different DNA constructs with modifications to evaluate the effect of modification on nucleosome mechanical stability.

5.2.4. 5- methylcytosine destabilizes nucleosome mechanical stability

In chapter 3, we presented that two DNA ends of the nucleosome unwraps asymmetrically – one end unwraps at lower force (~ 3 pN) and one end opens at higher force (~ 15 pN). To probe the effect of DNA methylation, we attached the FRET probe on the strong side (ED2) because of the following reasons. (1) Based on our previous demonstration that DNA flexibility determined the direction of the unwrapping such that the stiffer DNA would result in the lower unwrapping force, we hypothesized a reduction in unwrapping force upon DNA methylation. (2) The strong side contains 9 methylation sites while the weak side contains 4 methylation sites (Figure 5.5A).

For the unmodified construct, all stretching traces of the ED2 probe showed the same pattern with stable FRET at low force and a drop at high force (~ 15 pN) (Figure 5.5C). Subsequent pulls displayed the same pattern, i.e. no irreversible change. Upon methylation, though staring from the same value of FRET at zero force, 39.4% of trace (13 of 33) showed the same behavior as the unmodified one, 39.4% of traces (13 of 33) showed an additional gradual decrease before the final drop at ~15 pN and 21.2% of traces (7 of 33) showed a major drop in FRET at low force range (~ 5 pN) (Figure 5.5C). Averaging of

FRET as a function of force for all traces exhibited pronounced unwrapping at low force range of the DNA methylated nucleosome compared to stable FRET of the unmethylated nucleosome in the low force range. However, the slope at higher than 15 pN resulting from the final drop remained unchanged. This result indicates that DNA methylation does not alter the force range of the major structural transition but destabilizes and assists the early unwrapping of the DNA end.

5.2.5. 5- formylcytosine enhances nucleosome mechanical stability

Next, we investigated the effect of 5-formylcytosine on the mechanical stability of the nucleosome. Because 5-formylcytosine enhances DNA flexibility, we predicted that it will promote stronger binding of DNA to the histone core. Therefore, we introduced two copies of 5-formylcytosine modifications on the weak side at the 22 (J22) and 54 (J54) nucleotides from the right end of the 601 sequence (Figure 5.7A). These two modifications resided in the middle of the outer turn and inner turn, respectively, on the weak side of the nucleosome (Figure 5.7B). To probe unwrapping on the weak side which contains the

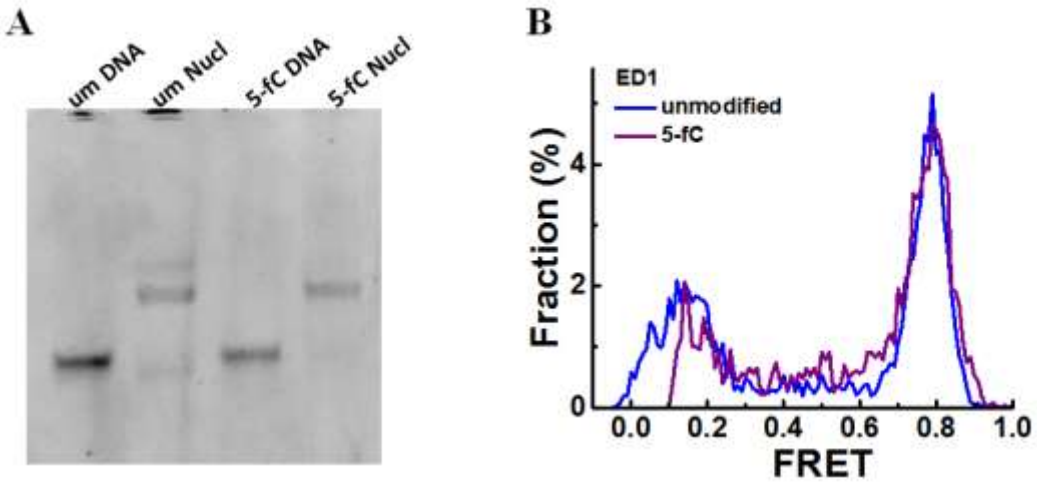

Figure 5.6: Checking formation of nucleosome on unmodified DNA and DNA containing two copies of 5-fC
(A) 5% native PAGE gel
(B) FRET histogram (ED1 labeling scheme

5-formyl modifications, a donor was incorporated to the nucleotide 68 from the 5′ end of the top strand (I68) and an acceptor was attached at nucleotide 7 from the 5′ end of the bottom strand (J7) (ED1 labeling scheme – Figure 5.7B). The two strands of the DNA construct were created by ligation separately to ensure the completion of ligation without nicks on the DNA. The DNA construct was then formed by slowly annealing of the two purified ligated strands. The unmodified and the 5-formylcytosine DNA constructs yielded nucleosomes with the same electro-mobility indicating the homogeneous positioning of the nucleosome on the two DNA constructs (Figure 5.6).

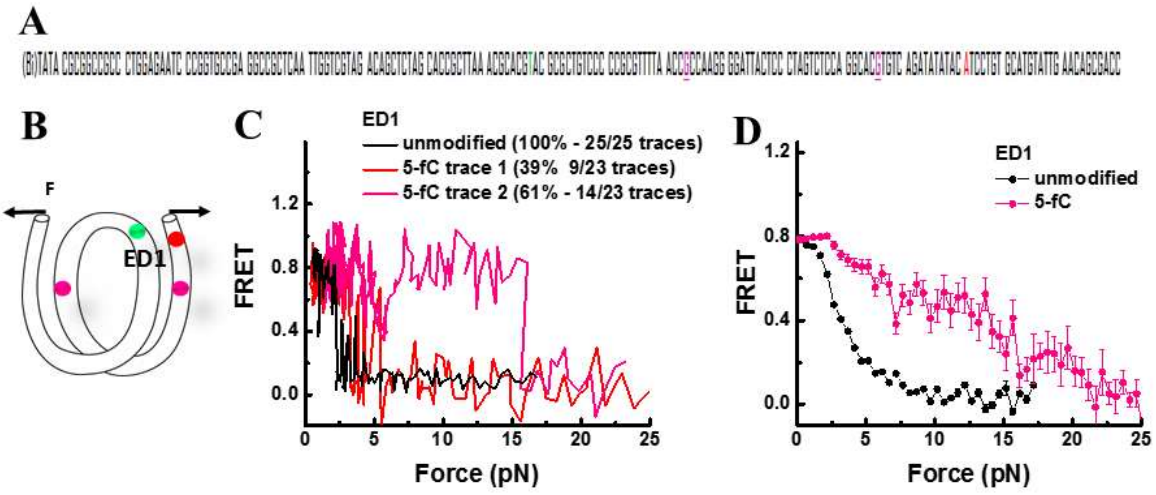

Figure 5.7: 5-fC enhances nucleosome unwrapping force

(A) The DNA construct containing the 601 sequence used to reconstitute nucleosome. CpG sites with 5-fC modifications are shown in magenta and underlie. The nucleotides incorporated to Cy3 and Cy5 are shown in green and red.

(B) Scheme of nucleosomal DNA with ED1 labeling scheme containing two copies of 5-fC at nucleotide 22 (J22) and 54 (J54) of the bottom strand of the 601 sequence for unwrapping experiments.

(C) Representative stretching traces of ED1 nucleosome with unmodified DNA and DNA containing two copies of 5-fC.

Averaging of stretching traces for ED2 nucleosome with unmodified (25 traces) and DNA containing two copies of 5-fC (23 traces).

As previously reported for the unmodified DNA, 100% of stretching traces of the weak side probed by ED1 displayed a gradual decrease in FRET as the force increases followed by fast fluctuations, and finally a sharp decrease at ~ 3-5 pN (Figure 5.7C). For the 5-formylcytosine construct, 39% of traces exhibited similar stretching patterns to that of the 601 nucleosome. However, 61% of traces showed the final drop in FRET at higher force. The averaged FRET vs. force pattern clearly showed an increase in unwrapping force for the 5-formylcytosine containing nucleosomes (Figure 5.7D). This indicates the enhancement of mechanical stability by the 5-formylcytosine nucleosome.

5.3. Discussion

Here we performed a comprehensive survey on the effect of cytosine modifications on DNA flexibility. With a single copy of each modification, 5-fomylcytosine (5-fC) displayed a remarkable increase in DNA flexibility (3 folds increase in looping rate) while 5-methylcytosine (5-mC), 5-hydroxmethylcytosine (5-hmC) and 5-carboxylcytosine (5-caC) exhibited a modest effect. Higher copy numbers of 5-mC induced a decrease in DNA flexibility; 5-hmC accelerated DNA flexibility and caC did not exhibit detectable effect of DNA flexibility. Our observation of the effect of mC is consistent with previous reports on reduction of DNA flexibility by mC using other methods such as NMR spectroscopy [85, 92], DNA cyclization assay [86] and DNA transportation through a synthetic nanopore [30]. Methylation induced increase in DNA stiffness arises from the restriction in conformational space by the bulky methyl groups and a folding of DNA around the hydrophobic methyls [85, 87].

Though *in vivo* 5-fC level is low [83], a single copy of fC within 90 bp of DNA induced 3 folds change in DNA cyclization rate. The significant enhancement of DNA flexibility induced by 5-fC may indicate a mechanism to explain their substrate specificity role for recognition of TDG, a base excision enzyme that works on fC and caC substrate in the

demethylation pathway. Active demethylation pathway includes sequential oxidation by TETs enzymes of 5-mC (5-mC to 5-hmC, 5-fC and 5-caC) and base excision by TDG (5-fC or 5-caC to an abasic) followed by base excision repair (abasic --> C) [75, 76]. TDG is a member of glycosylases (a BER repair protein) and use the same base-flipping mechanism to remove the base which requires disruption of base stacking and formation of a sharp kink [88]. Interestingly, TDG only works on 5-fC or 5-caC substrates and more efficiently on 5-fC but not on mC and hmC [75]. As what we observed, fC remarkably increases DNA flexibility explaining that 5-fC should be a favored substrate for TDG since an increase in DNA flexibility reduces the energy required for DNA bending and unstacking during base-flipping by TDG, similar to recognition mechanism of repair proteins [88].

We found that methylated cytosine loosens packaging of nucleosomal DNA ends and assists the unwrapping of DNA ends which is consistent with previous reports [90, 93] and opposite to [91]. The discrepancy between our results and Choy *et. al.* may originate from the difference in experiment protocol. Choy *et. al.* used enzyme to methylated nucleosomal DNAs which are immobilized on the slide. We followed the same protocol and found that a temporary increase in FRET for both samples with and without SAM during enzymatic reaction but after a long period of waiting time, the same with SAM showed the final reduction in FRET consistent with our result using nucleosome reconstituted from methylated DNA (data not shown).

In vivo, methylated cytosine correlated with gene inactivation. Three possible mechanisms for the suppression role of methylated cytosine are: (1) stabilizes nucleosome, (2) facilitates packaging of chromatin at higher order structure and (3) methylated CpGs prevents the binding of transcriptional activators and facilitates the binding of transcriptional repressors. We found that methylated cytosine loosens packaging of nucleosomal DNA ends. We also found that nucleosome is less stable

mechanically, which by itself would not make it more difficult to gain access to the nucleosomal DNA. We suggest that transcription suppression role of DNA methylation may be mediated mainly through stabilization of inner DNA turn [16] and the latter two mechanism. For example, the loosening of DNA end may allow histone tails bind to the adjacent nucleosomes and mediate inter nucleosomes interaction which facilitate packaging of chromatin at higher order structure.

Introducing 2 copies of 5-fC in 147 bps of DNA of the 601 sequence results in a remarkable enhancement of nucleosome mechanical stability. This observation supports our previous proposed correlation between DNA flexibility and nucleosome stability such that the more flexible DNA is more stably bound to histone octamer core since it tolerates the sharp bending configuration of DNA around the rigid body of histone octamer (chapter 3). The increase in nucleosome stability induced by 5-fC provide a mechanism to explain the enrichment of 5fC at poised enhancers and the TSSs of gene with low expression [83] since the enhancement of nucleosome stability limits exposure of nucleosomal DNA for the accessibility of transcription machinery at enhancers and TSSs.

5.4. Conclusion

In addition to four genetic nucleotides (A, T, C, G), cytosine can undergo chemical modifications at the fifth carbon of its pyrimidine ring, such as 5-methylcytosine and its oxidized products 5-hydroxylmethylcytosine, 5-formylcytosine and 5-carboxylcytosine. These modifications are crucial epigenetic marks and play important roles in cellular processes. Here we report a comprehensive survey on the effect of cytosine modifications on DNA flexibility using single molecule cyclization assay. We found that even a single copy of 5-fC accelerates DNA flexibility by three folds while multiple copies of 5-mC reduces DNA flexibility; 5-hmC increases DNA flexibility but with lower magnitude than the effect of 5-fC and 5-caC has modest effect on DNA flexibility. We chose 5-mC and 5-

fC which have opposite effects on DNA flexibility to test its correlation with nucleosome stability under tension using combination of optical tweezers with smFRET detection. We observed that 5-mC assisted unwrapping of nuclesomal DNA ends while 5-fC enhanced nucleosome stability, further supporting the model that DNA flexibility is a major determinant of the mechanical stability of the nucleosome.

Chapter 6

Slow Spontaneous Nucleosome Gaping*

6.1. Introduction

Nucleosome structures are diverse due to histone variants, histone modifications [2] and dynamic variation in its composition [17]. Histone variants CenH3, H2A.Bdb and H2ALap1 form nucleosomes with loosely organized DNA termini [2]. During transcription, replication and remodeling, parts of nucleosome such as H2A/H2B dimer dissociate creating additional structural intermediates and diversity [17, 41, 45, 94]. Even intact nucleosomes are highly dynamic and can deviate from the canonical crystal structure by DNA breathing [8-10, 18, 95] and H2A/H2B dimer splitting [2, 14, 95, 96]. In DNA breathing, nucleosomal DNA ends partially and reversibly unwrap from the histone core on a rapid time scale (10-250 ms) [8]. Spontaneous unwrapping of nucleosomal DNA ends allows the accessibility to DNA binding factors to chromatin [4, 9]. Dimer splitting is partially disruption of H2A/H2B dimer from contact with histone $(H3/H4)_2$ tetramer while dimers stay intact with DNA. Dimer splitting was proposed

*This work is in preparation for publication as:
Thuy T.M. Ngo and Taekjip Ha. "Slow Spontaneous Gaping of Nucleosomes".

theoretically as gaping to accommodate tightly package of chromatin higher order structure, the 30 nm fiber [97]. Nucleosome unwrapping was identified to happen spontaneously in solution at physiological condition [8, 10, 18]. However, nucleosome gaping/dimer splitting was only observed during elevated salt condition [14] or on a highly charged surface in an AFM measurement [95]. Whether nucleosome gaping exists spontaneously in solution under physiological condition is still unknown.

Here we sought to look for possible spontaneous local conformational dynamics of nucleosome using the single-molecule FRET technique. We found that nucleosomes under physiological condition can undergo a slow spontaneous local switching motion around the off-dyad position. This structural switching is along the direction perpendicular to the DNA plane, which we called gaping, a type of motion very different from the canonical in-plane motion previously observed. The structure variation between gaping modes is subtle of about 5 Angstrom. Kinetic of gaping happens at minute time scale.

6.2. Results

6.2.1. Nucleosome undergoes spontaneous conformational switching

To get clearly interpretable single molecule FRET signals, we chose to use the 601 sequence which positions nucleosome at a defined translation frame [39]. A donor was attached to the DNA inner turn that primarily contacts the histone tetramer, at the 45 nucleotide from the 5′ end of the bottom strand and an acceptor was attached to the DNA outer turn that primarily contacts the histone dimer, at the 27 nucleotide from the 5′ end of the top strand on the 601 sequence (Figure 6.2A). We named this labeling scheme as ED2.8 (I27 – J45). The DNA construct was generated by PCR amplification form Cy3 (donor) and Cy5 (acceptor) labeled primers. One primer contains biotin at the 5′ end for

surface immobilization. Reconstituted nucleosomes display a single broad high FRET peak accompanied by a low FRET peak attributed to the free DNA from histone dissociation population in a histogram plot (Figure 6.1).

Surprisingly, smFRET traces revealed spontaneous transition between three FRET sub-states (Figure 1B). Nucleosome resided dominantly at the middle FRET state (84.71 percent of total observed time) and transiently stayed at higher (11.83 percent of total observed time) and lower (3.46 percent total observed time) FRET states. Kinetic of the transition was quantified by mean dwell time on each state with average of 7.98 minutes, 1.67 minutes and 0.7 minutes spending on the middle, higher and lower FRET states, respectively (Table 6.1). This result implies that the nucleosome can undergo slow local conformational switching.

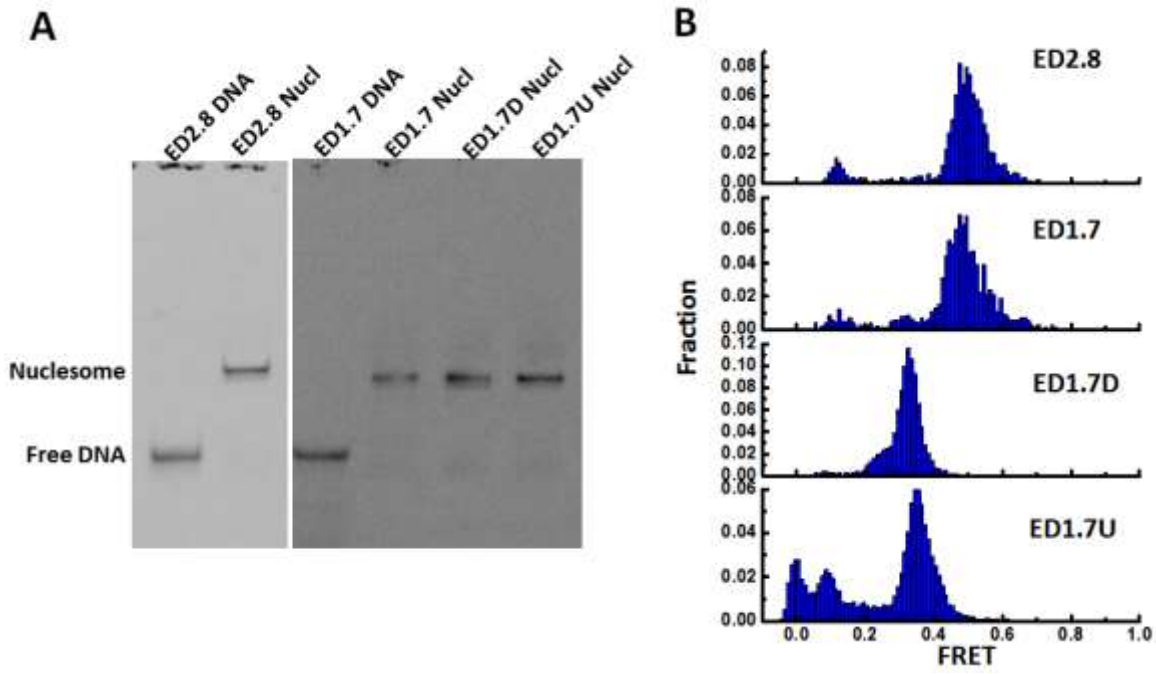

Figure 6.1: Formation of nucleosomes with ED2.8, ED1.7. ED1.7D. ED1.7U labeling schemes
(**A**) Nucleosomes with ED2.8, ED1.7. ED1.7D. ED1.7U labeling schemes migrate at identical positions on 5% Native PAGE.
(**B**): FRET histogram of these 4 nucleosomes

Next, we tested if the similar conformation dynamics can be observed at an equivalent site on the other side of the nucleosome. We designed a new DNA construct ED1.7 with the FRET pair attached on the site opposite to ED2.8. The donor was attached to the 46th nucleotide of the top strand and the acceptor was attached to the 24th nucleotide of the bottom strand of the 601 sequence (I46 – J24). The ED1.7 FRET probe at the new location

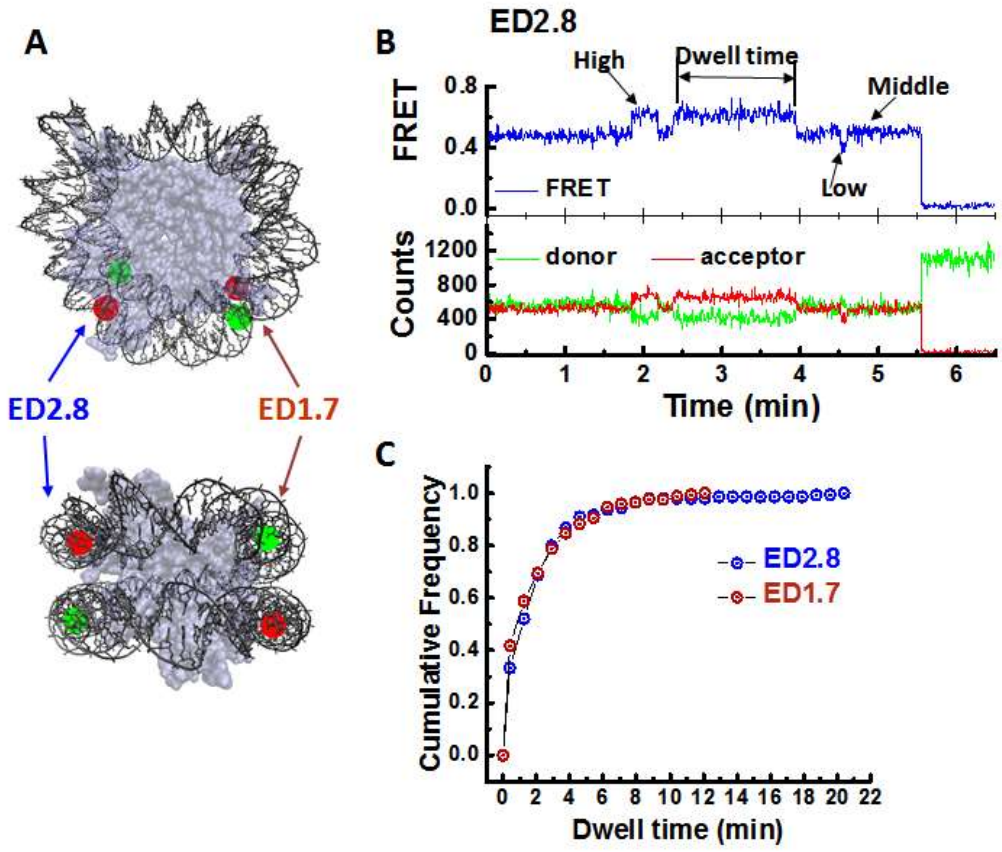

Figure 6.2: Slow spontaneous conformational switching of Nucleosome
A: Labeling scheme of the FRET pair (front view and side view): Cy3 and Cy5 are attached on the two turns of the nucleosomal DNA (Crystal structure: 3MVD).
B: Single molecule time traces of donor intensity (green), acceptor intensity (red) and calculated FRET (blue) show spontaneous switching between three FRET levels indicating the coexistence of multiple states of the nucleosome.

Table 6.1: Distribution of three states		
	Mean dwell time (min)	Distribution
High FRET	1.67	11.83%
Mid FRET	7.98	84.71%
Low FRET	0.7	3.46%

reported a similar transition between three FRET states as exhibited by the ED2.8 FRET probe (Figure 6.3). To quantify the similarity between the two probes, we attempted to compare the kinetic of dwell time of each equivalent state. Since the resident time of the nucleosome at the middle FRET state is long (7.98 minutes) whose dwell time kinetic

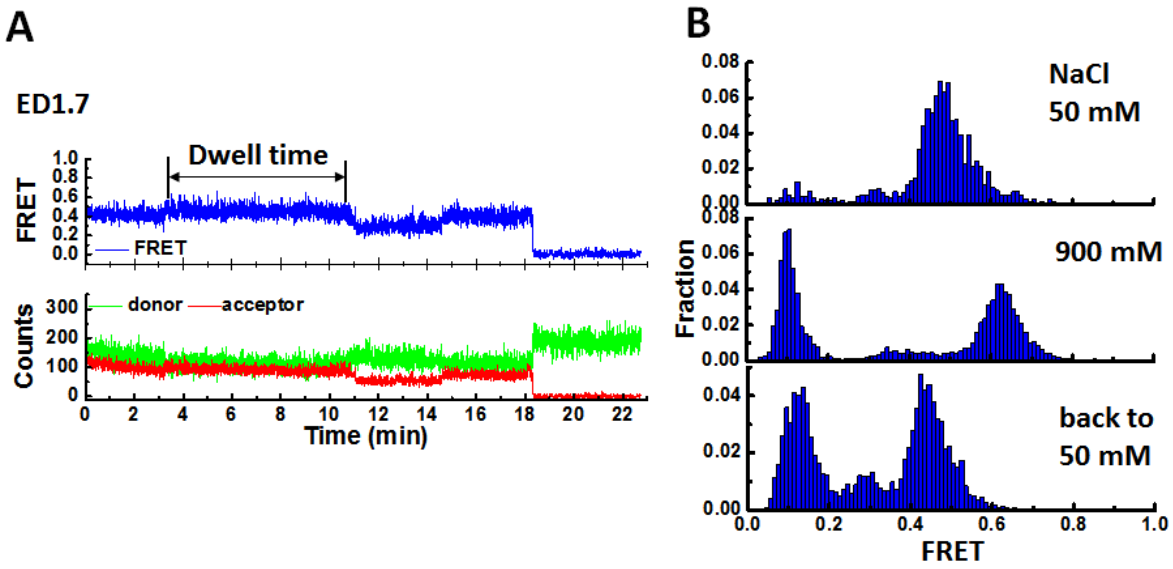

Figure 6.3. FRET of the ED1.7 nucleosome
(**A**) Single molecule time traces of donor intensity (green), acceptor intensity (red) and calculated FRET (blue) show spontaneous switching between three FRET levels indicating the coexistence of multiple states of the ED1.7 nucleosome.
(**B**) Histogram of ED1.7 at 50 mM NaCl, 900 mM NaCl then back to 50 mM NaCl after incubation in 900 mM NaCl.

analysis requires a collection dwell time beyond the limit of lifetime of fluorophores due to photobleaching, we chose to analyse the distribution of dwell time of the higher FRET state only. Cumulative distributions of dwell time of the higher FRET state were identical for the two FRET probes (Figure 6.2C). The comparison between the two probes confirmed that the spontaneous conformation switching of nucleosome is located on both sides of the nucleosome and around the junction between the DNA inner turn and DNA outer turn which are in contact with the histone $(H3/H4)_2$ tetramer and the two H2A/H2B dimers, respectively.

6.2.2. Salt dependent kinetics

Since nucleosome stability is salt dependent, we attempted to examine the kinetics of the switching at different ionic conditions. FRET histograms of the ED1.7 nucleosome were recorded at a wide range of NaCl concentrations from 50 mM to 1 M. As the salt increased, we observed an increase of the FRET value of the nucleosomal peak (Figure 6.4A). A fraction of nucleosomes dissociated and converted to free DNA at high salt concentration, resulting in a low FRET peak which is unchanged in FRET value. In

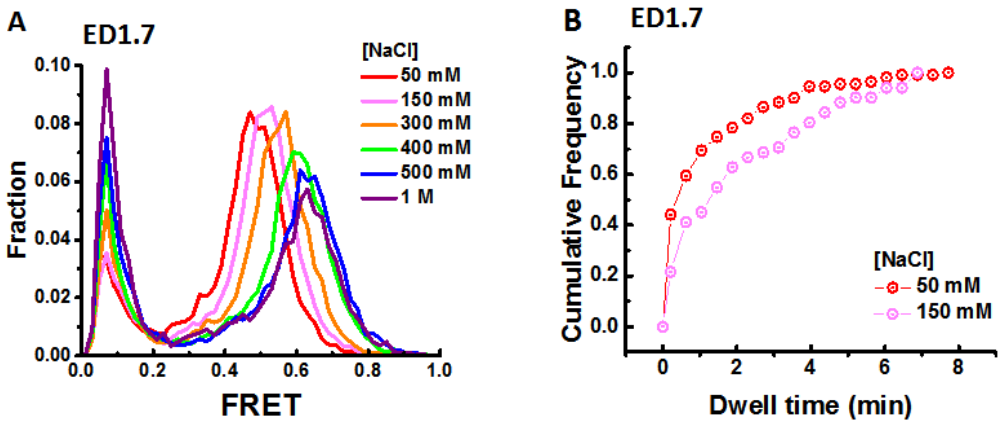

Figure 6.4: Salt dependent kinetics
A: FRET histogram of ED1.7 at different salt condition
B: Cumulative distribution function of the dwell time of the high FRET state at 50 mM (N=170) and 150 mM (N = 140) NaCl.

addition, FRET histogram of a FRET pair attached to the end of nucleosomal DNA displayed a decrease in FRET as salt increase as we would expect of increased unraveling from the ends (Figure 6.5), ruling out the possibility that the increase in FRET of the ED1.7 probe stems from a change in photophysical properties of the donor and acceptor caused by changing salt conditions. These results confirmed that the increase in FRET of nucleosome population results from a structure change. The nucleosome population with elevated FRET at high salt returned to the same FRET value after exchanging back to low salt condition (Figure 6.3B), indicating that the molecular compositions of nucleosome at the different FRET stages are the same, that is no dimer ejection.

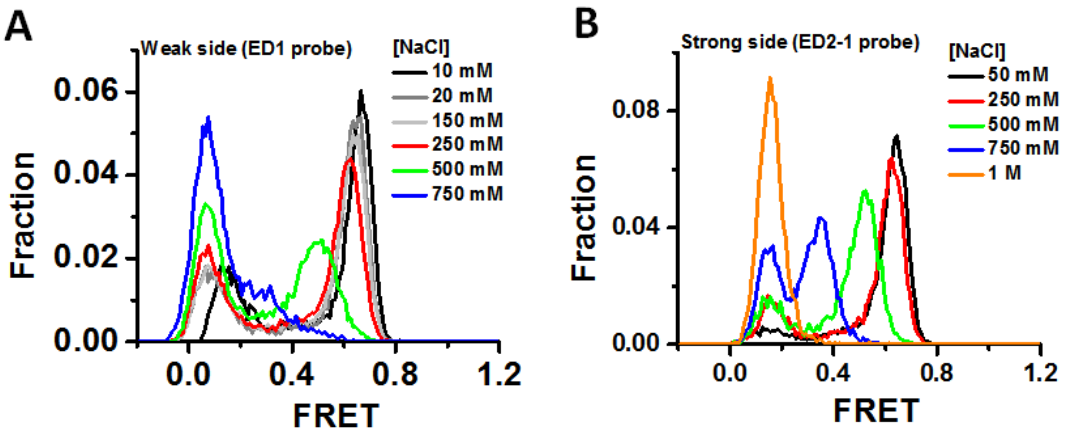

Figure 6.5: Salt dependent FRET histogram of nucleosome exit probes: FRET histogram of ED1 (**A**) nucleosome and ED2-1 (**B**) nucleosome at different NaCl concentration showing a reduction in FRET as NaCl concentration increases.

The increase in FRET of the ED1.7 probe could come from the shift of all three FRET sub-states or the change in the distribution of from the middle FRET state to the higher FRET state. To distinguish between these two possibilities, we quantified the distribution of dwell time of the higher FRET state at the two different salt concentrations (Figure 6.4B). As the salt increased, the cumulative distribution of dwell time of the higher FRET state shifted to a long dwell time. This observation indicates that the change in distribution of resident time of nucleosome shifts to the higher FRET state.

6.2.3. Nucleosome gaping

Next, we investigated the molecular origin of the conformational switching. We considered four possible structural modes of conformational dynamics that could in principle result in the observed switching in FRET: DNA breathing, DNA tightening/loosening, nucleosome sliding and nucleosome gaping. In a DNA breathing mode (Figure 6.6A), the nuclesomal DNA ends transiently dissociate from the histone surface resulting in a relative change in distance between two DNA turns [8-10]. In a tightening/loosening mode (Figure 6.6B), DNA overwraps or underwraps around the histone octamer surface [16]. In a sliding mode, the number of bp of bound DNA on histone core is unchanged but the frame of DNA in contact with the octamer surface shifts

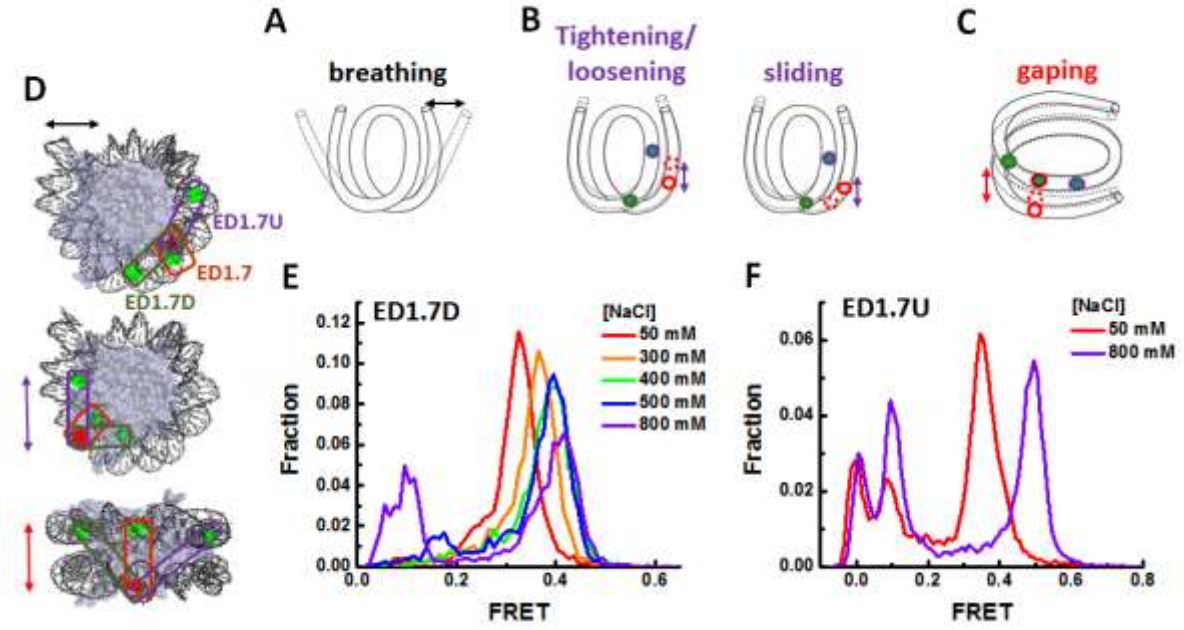

Figure 6.6: Nucleosome gaping
A, B, C: Possible structure modes of nucleosome conformational dynamics: breathing (A), tightening/loosening and sliding (B), and gaping (C).
D: Illustration of three labeling schemes ED1.7, ED1.7U and ED1.7D overlay on the nucleosome crystal structure. All three labeling schemes share the acceptor position at 24 nucleotide from the right end of the 601 sequence on the bottom strand and the donors at labeled at 45, 57 and 38 nucleotides from the left end on the top strand, respectively.
E, F: FRET histogram of ED1.7D and ED1.7U at different salt conditions.

up or down stream of DNA. In gaping mode, two turns of nucleosomal DNA move relative to each other in the direction perpendicular to two DNA planes [97]. With both tightening/loosening and slide modes, the relative change in the two DNA turns is along the wrapping direction while in the nucleosome gapping mode (Figure 6.6C) the switching happened in the normal direction to the DNA planes.

Using stopped-flow FRET measurement of nucleosomes in the presence of transcription factor LexA [8] and a direct measurement by single-molecule FRET [10], the rate of spontaneous of nucleosome unwrapping in the breathing mode was determined to be at millisecond time scales which is two orders of magnitude faster than the rate of switching that we observed here. Moreover, in the breathing mode, dissociation of nucleosomal DNA ends from the histone core is facilitated by high salt [14] resulting in a decrease in FRET as salt increases (Figure 6.5). Here the observed switching results in an increase in FRET as increasing NaCl concentration. Combining the difference in transition rate and the trend of FRET change upon salt titration, we ruled out DNA breathing as the source of observed FRET switching.

To distinguish between tightening/loosening/sliding and gaping, we designed two additional labeling schemes ED1.7U and ED1.7D that share the acceptor on the outer DNA with the ED1.7 scheme (Figure 6.6D). The two donors of ED1.7U and ED1.7D were located at the two opposite positions comparing to the donor of ED1.7 FRET pair. In tightening/loosing or sliding, the outer DNA turn will move relatively to the inner DNA turn such that if the acceptor on the outer turn gets closer to the donor of ED1.7D on the inner turn, it will be further away from the donor of ED1.7U on the opposite direction, and vice versa. Therefore, trend of change in FRET of ED1.7U should be opposite to that of ED1.7D. However, both FRET histograms of ED1.7D and ED1.7U nucleosomes gave a rise in FRET value as increasing NaCl concentration as the same as FRET of ED1.7 nucleosomes (Figure 6.6E and 6.6F). This ruled out that tightening/loosening or sliding is

not the source of switching motion we are investigating. In contrast, it supported the gaping mode since the gaping mode allows an increase in FRET of all three pair ED1.7. ED1.7U and ED1.7D since the two DNA planes get close to each other in their normal direction.

6.3. Discussion

Nucleosomes are diverse by histone variants and histone modifications which accommodate specific tasks in gene regulation. Nucleosomes constituted of the same DNA and protein components are also dynamic in conformation such as breathing and opening of tetramer/dimer interface. The spontaneous breathing of nucleosomal DNA ends allows accessibility on nucleosome substrates for protein acting on DNA such as transcription factors, polymerases and chromatin remodelers.

Here, we discovered that nucleosomes can undergo a local switching motion which is along the direction perpendicular to the DNA plane, a type of motion very different from the canonical in-plane motion previously observed. We call this switching as gaping similar to the direction of molecular conformation change proposed theoretically by Mozziconacci and Victor [97]. They proposed that conformational transition of nucleosome participates co-operatively to the compaction and decompaction of the chromatin fiber. Our results indicate that a free nucleosome in solution can adopt and switch between multiple configurations which may dictate the heterogeneous enzymatic reactions on chromatin substrates and the formation of multiple compression forms of chromatin fibers [97, 98].

Single molecule FRET with resolution of sub-nanometer allowed us to discover a new conformation switching of free nucleosome in physiological condition. To minimize the effect of labeling, we incorporate fluorophores to DNA through a C6 linker. The configuration of the C6 liker is unknown; therefore, we are limited by a poor conversion

of FRET to distance. As a result, we reported here the relative change in conformational switching only without actual linking to the crystal structure of nucleosome. Moreover, since single molecule FRET can report dimensional change in the coordinate of FRET pair only, within scope of this study, we have no information about any possible conformation motion of histone proteins. Further studies with better approaches such as precision FRET [15] or femtosecond crystallography by free-electron lasers are needed to resolve detail structure of nucleosome gaping [99, 100].

6.4. Conclusion

In eukaryotes, DNA is packaged into a basic unit, the nucleosome, which consists of 147 bp of DNA wrapped around histone octamer composed of two copies each of the histones H2A, H2B, H3 and H4. Nucleosome structures are not only diverse by histone variants, histone modifications, histone composition but also accommodate different stages such as DNA breathing and dimer splitting. The variation in nucleosome structures allows it to perform a variety of cellular functions. Here, we identified a slow spontaneous local gaping of nucleosomes under physiological conditions using single-molecule FRET. Gaping modes switch along the direction normal to the DNA plane at minutes (1-10 minutes) time scale. The existence of nucleosome in different gaping modes may underlie the heterogeneous enzymatic reactions on chromatin substrates and the formation of multiple compression forms of chromatin fibers.

Bibliography

1. Kornberg, R.D., *Chromatin Structure - Repeating Unit of Histones and DNA.* Science, 1974. **184**(4139): p. 868-871.
2. Luger, K., M.L. Dechassa, and D.J. Tremethick, *New insights into nucleosome and chromatin structure: an ordered state or a disordered affair?* Nature Reviews Molecular Cell Biology, 2012. **13**(7): p. 436-447.
3. Luger, K., et al., *Crystal structure of the nucleosome core particle at 2.8 angstrom resolution.* Nature, 1997. **389**(6648): p. 251-260.
4. Hodges, C., et al., *Nucleosomal Fluctuations Govern the Transcription Dynamics of RNA Polymerase II.* Science, 2009. **325**(5940): p. 626-628.
5. Churchman, L.S. and J.S. Weissman, *Nascent transcript sequencing visualizes transcription at nucleotide resolution.* Nature, 2011. **469**(7330): p. 368-+.
6. Bondarenko, V.A., et al., *Nucleosomes can form a polar barrier to transcript elongation by RNA polymerase II.* Molecular Cell, 2006. **24**(3): p. 469-479.
7. Gorman, J., et al., *Visualizing one-dimensional diffusion of eukaryotic DNA repair factors along a chromatin lattice.* Nature Structural & Molecular Biology, 2010. **17**(8): p. 932-U37.
8. Li, G., et al., *Rapid spontaneous accessibility of nucleosomal DNA.* Nature Structural & Molecular Biology, 2005. **12**(1): p. 46-53.
9. Li, G. and J. Widom, *Nucleosomes facilitate their own invasion.* Nature Structural & Molecular Biology, 2004. **11**(8): p. 763-769.
10. Koopmans, W.J.A., et al., *Single-pair FRET microscopy reveals mononucleosome dynamics.* Journal of Fluorescence, 2007. **17**(6): p. 785-795.
11. Yin, H., et al., *TRANSCRIPTION AGAINST AN APPLIED FORCE.* Science, 1995. **270**(5242): p. 1653-1657.
12. Sirinakis, G., et al., *The RSC chromatin remodelling ATPase translocates DNA with high force and small step size.* Embo Journal, 2011. **30**(12): p. 2364-2372.
13. Ha, T., et al., *Probing the interaction between two single molecules: Fluorescence resonance energy transfer between a single donor and a single acceptor.* Proceedings of the National Academy of Sciences of the United States of America, 1996. **93**(13): p. 6264-6268.
14. Boehm, V., et al., *Nucleosome accessibility governed by the dimer/tetramer interface.* Nucleic Acids Research, 2011. **39**(8): p. 3093-3102.
15. Kalinin, S., et al., *A toolkit and benchmark study for FRET-restrained high-precision structural modeling.* Nature Methods, 2012. **9**(12): p. 1218-U129.
16. Lee, J.Y. and T.-H. Lee, *Effects of DNA Methylation on the Structure of Nucleosomes.* Journal of the American Chemical Society, 2012. **134**(1): p. 173-175.
17. Gansen, A., et al., *Nucleosome disassembly intermediates characterized by single-molecule FRET.* Proceedings of the National Academy of Sciences of the United States of America, 2009. **106**(36): p. 15308-15313.
18. Poirier, M.G., et al., *Spontaneous access to DNA target sites in folded chromatin fibers.* Journal of Molecular Biology, 2008. **379**(4): p. 772-786.
19. Brower-Toland, B.D., et al., *Mechanical disruption of individual nucleosomes reveals a reversible multistage release of DNA.* Proceedings of the National Academy of Sciences of the United States of America, 2002. **99**(4): p. 1960-1965.
20. Mack, A.H., et al., *Kinetics and Thermodynamics of Phenotype: Unwinding and Rewinding the Nucleosome.* Journal of Molecular Biology, 2012. **423**(5): p. 687-701.

21. Mihardja, S., et al., *Effect of force on mononucleosomal dynamics.* Proceedings of the National Academy of Sciences of the United States of America, 2006. **103**(43): p. 15871-15876.
22. Hohng, S., et al., *Fluorescence-force spectroscopy maps two-dimensional reaction landscape of the Holliday junction.* Science, 2007. **318**(5848): p. 279-283.
23. Chua, E.Y.D., et al., *The mechanics behind DNA sequence-dependent properties of the nucleosome.* Nucleic Acids Research, 2012. **40**(13): p. 6338-6352.
24. Kim, S., et al., *Probing Allostery Through DNA.* Science, 2013. **339**(6121): p. 816-819.
25. Widom, J., *Role of DNA sequence in nucleosome stability and dynamics.* Quarterly Reviews of Biophysics, 2001. **34**(3): p. 269-324.
26. Vafabakhsh, R. and T. Ha, *Extreme Bendability of DNA Less than 100 Base Pairs Long Revealed by Single-Molecule Cyclization.* Science, 2012. **337**(6098): p. 1097-1101.
27. Hagerman, P.J., *Flexibility of DNA.* Annual Review of Biophysics and Biophysical Chemistry, 1988. **17**: p. 265-286.
28. Rief, M., H. Clausen-Schaumann, and H.E. Gaub, *Sequence-dependent mechanics of single DNA molecules.* Nature Structural Biology, 1999. **6**(4): p. 346-349.
29. Severin, P.M.D., et al., *Cytosine methylation alters DNA mechanical properties.* Nucleic Acids Research, 2011. **39**(20): p. 8740-8751.
30. Mirsaidov, U., et al., *Nanoelectromechanics of Methylated DNA in a Synthetic Nanopore.* Biophysical Journal, 2009. **96**(4): p. L32-L34.
31. North, J.A., et al., *Regulation of the nucleosome unwrapping rate controls DNA accessibility.* Nucleic Acids Research, 2012. **40**(20): p. 10215-10227.
32. Toth, K., et al., *Histone- and DNA sequence-dependent stability of nucleosomes studied by single-pair FRET.* Cytometry Part A, 2013. **83**(9): p. 839-846.
33. Zhou, R.B., et al., *SSB Functions as a Sliding Platform that Migrates on DNA via Reptation.* Cell, 2011. **146**(2): p. 222-232.
34. Grashoff, C., et al., *Measuring mechanical tension across vinculin reveals regulation of focal adhesion dynamics.* Nature, 2010. **466**(7303): p. 263-U143.
35. Dyer, P.N., et al., *Reconstitution of nucleosome core particles from recombinant histones and DNA.* Chromatin and Chromatin Remodeling Enzymes, Pt A, 2004. **375**: p. 23-44.
36. Roy, R., S. Hohng, and T. Ha, *A practical guide to single-molecule FRET.* Nature Methods, 2008. **5**(6): p. 507-516.
37. Hohng, S., et al., *Fluorescence-force spectroscopy maps two-dimensional reaction landscape of the Holliday junction.* Science, 2007. **318**(5848): p. 279-283.
38. Zhou, R.B., M. Schlierf, and T. Ha, *FORCE FLUORESCENCE SPECTROSCOPY AT THE SINGLE-MOLECULE LEVEL*, in *Methods in Enzymology, Vol 475: Single Molecule Tools, Pt B: Super-Resolution, Particle Tracking, Multiparameter, and Force Based Methods*, N.G. Walter, Editor. 2010, Elsevier Academic Press Inc: San Diego. p. 405-426.
39. Lowary, P.T. and J. Widom, *New DNA sequence rules for high affinity binding to histone octamer and sequence-directed nucleosome positioning.* Journal of Molecular Biology, 1998. **276**(1): p. 19-42.
40. Bintu, L., et al., *Nucleosomal Elements that Control the Topography of the Barrier to Transcription.* Cell, 2012. **151**(4): p. 738-749.
41. Bintu, L., et al., *The elongation rate of RNA polymerase determines the fate of transcribed nucleosomes.* Nature Structural & Molecular Biology, 2011. **18**(12): p. 1394-1399.
42. Deindl, S., et al., *ISWI Remodelers Slide Nucleosomes with Coordinated Multi-Base-Pair Entry Steps and Single-Base-Pair Exit Steps.* Cell, 2013. **152**(3): p. 442-452.
43. Hall, M.A., et al., *High-resolution dynamic mapping of histone-DNA interactions in a nucleosome.* Nature Structural & Molecular Biology, 2009. **16**(2): p. 124-129.

44. Kruithof, M. and J. van Noort, *Hidden Markov Analysis of Nucleosome Unwrapping Under Force.* Biophysical Journal, 2009. **96**(9): p. 3708-3715.
45. Sheinin, M.Y., et al., *Torque modulates nucleosome stability and facilitates H2A/H2B dimer loss.* Nature Communications, 2013. **4**.
46. Shundrovsky, A., et al., *Probing SWI/SNF remodeling of the nucleosome by unzipping single DNA molecules.* Nature Structural & Molecular Biology, 2006. **13**(6): p. 549-554.
47. Sudhanshu, B., et al., *Tension-dependent structural deformation alters single-molecule transition kinetics.* Proceedings of the National Academy of Sciences of the United States of America, 2011. **108**(5): p. 1885-1890.
48. Makde, R.D., et al., *Structure of RCC1 chromatin factor bound to the nucleosome core particle.* Nature, 2010. **467**(7315): p. 562-U81.
49. McKinney, S.A., C. Joo, and T. Ha, *Analysis of single-molecule FRET trajectories using hidden Markov modeling.* Biophysical Journal, 2006. **91**(5): p. 1941-1951.
50. Kulaeva, O.I., et al., *Molecular mechanisms of transcription through a nucleosome by RNA polymerase II.* Molecular Biology, 2013. **47**(5): p. 655-667.
51. Maffeo, C., et al., *A Coarse-Grained Model of Unstructured Single-Stranded DNA Derived from Atomistic Simulation and Single-Molecule Experiment.* Journal of Chemical Theory and Computation, 2014. **10**(8): p. 2891-2896.
52. Bowman, G.D., *Mechanisms of ATP-dependent nucleosome sliding.* Current Opinion in Structural Biology, 2010. **20**(1): p. 73-81.
53. Workman, J.L., *Nucleosome displacement in transcription.* Genes & Development, 2006. **20**(15): p. 2009-2017.
54. Yen, K., V. Vinayachandran, and B.F. Pugh, *SWR-C and INO80 Chromatin Remodelers Recognize Nucleosome-free Regions Near+1 Nucleosomes.* Cell, 2013. **154**(6): p. 1246-1256.
55. Mollazadeh-Beidokhti, L., F. Mohammad-Rafiee, and H. Schiessel, *Nucleosome Dynamics between Tension-Induced States.* Biophysical Journal, 2012. **102**(10): p. 2235-2240.
56. Richard, P. and J.L. Manley, *How bidirectional becomes unidirectional.* Nature Structural & Molecular Biology, 2013. **20**(9): p. 1022-1024.
57. Li, G.M., *Mechanisms and functions of DNA mismatch repair.* Cell Research, 2008. **18**(1): p. 85-98.
58. Hanahan, D. and R.A. Weinberg, *Hallmarks of Cancer: The Next Generation.* Cell, 2011. **144**(5): p. 646-674.
59. Fields, A.P., E.A. Meyer, and A.E. Cohen, *Euler buckling and nonlinear kinking of double-stranded DNA.* Nucleic Acids Research, 2013. **41**(21): p. 9881-9890.
60. Isaacs, R.J. and H.P. Spielmann, *A model for initial DNA lesion recognition by NER and MMR based on local conformational flexibility.* DNA Repair, 2004. **3**(5): p. 455-464.
61. Wang, H., et al., *DNA bending and unbending by MutS govern mismatch recognition and specificity.* Proceedings of the National Academy of Sciences of the United States of America, 2003. **100**(25): p. 14822-14827.
62. Semple, C.A.M. and M.S. Taylor, *MOLECULAR BIOLOGY The Structure of Change.* Science, 2009. **323**(5912): p. 347-348.
63. Sasaki, S., et al., *Chromatin-Associated Periodicity in Genetic Variation Downstream of Transcriptional Start Sites.* Science, 2009. **323**(5912): p. 401-404.
64. Warnecke, T., N.N. Batada, and L.D. Hurst, *The Impact of the Nucleosome Code on Protein-Coding Sequence Evolution in Yeast.* Plos Genetics, 2008. **4**(11): p. 12.
65. Washietl, S., R. Machne, and N. Goldman, *Evolutionary footprints of nucleosome positions in yeast.* Trends in Genetics, 2008. **24**(12): p. 583-587.

66. Zhou, R., et al., *SSB Functions as a Sliding Platform that Migrates on DNA via Reptation.* Cell, 2011. **146**(2): p. 222-232.
67. Maffeo, C.N., Thuy T. M.; Ha, Taekjip; Aksimentiev, Aleksei, *A Coarse-Grained Model of Unstructured Single-Stranded DNA Derived from Atomistic Simulation and Single-Molecule Experiment.* Journal of Chemical Theory and Compuation, 2014.
68. LeGresley, S.E., J. Wilt, and M. Antonik, *DNA damage may drive nucleosomal reorganization to facilitate damage detection.* Physical Review E, 2014. **89**(3): p. 8.
69. Law, J.A. and S.E. Jacobsen, *Establishing, maintaining and modifying DNA methylation patterns in plants and animals.* Nature Reviews Genetics, 2010. **11**(3): p. 204-220.
70. Jaenisch, R. and A. Bird, *Epigenetic regulation of gene expression: how the genome integrates intrinsic and environmental signals.* Nature Genetics, 2003. **33**: p. 245-254.
71. Smith, Z.D. and A. Meissner, *DNA methylation: roles in mammalian development.* Nature Reviews Genetics, 2013. **14**(3): p. 204-220.
72. Hajkova, P., et al., *Genome-Wide Reprogramming in the Mouse Germ Line Entails the Base Excision Repair Pathway.* Science, 2010. **329**(5987): p. 78-82.
73. Hajkova, P., et al., *Epigenetic reprogramming in mouse primordial germ cells.* Mechanisms of Development, 2002. **117**(1-2): p. 15-23.
74. Mayer, W., et al., *Embryogenesis - Demethylation of the zygotic paternal genome.* Nature, 2000. **403**(6769): p. 501-502.
75. Wu, H. and Y. Zhang, *Reversing DNA Methylation: Mechanisms, Genomics, and Biological Functions.* Cell, 2014. **156**(1-2): p. 45-68.
76. Kohli, R.M. and Y. Zhang, *TET enzymes, TDG and the dynamics of DNA demethylation.* Nature, 2013. **502**(7472): p. 472-479.
77. Pastor, W.A., L. Aravind, and A. Rao, *TETonic shift: biological roles of TET proteins in DNA demethylation and transcription.* Nature Reviews Molecular Cell Biology, 2013. **14**(6): p. 341-356.
78. Leonhardt, H., H.P. Rahn, and M.C. Cardoso, *Functional links between nuclear structure, gene expression, DNA replication, and methylation.* Critical Reviews in Eukaryotic Gene Expression, 1999. **9**(3-4): p. 345-351.
79. Pastor, W.A., et al., *Genome-wide mapping of 5-hydroxymethylcytosine in embryonic stem cells.* Nature, 2011. **473**(7347): p. 394-397.
80. Szulwach, K.E., et al., *Integrating 5-Hydroxymethylcytosine into the Epigenomic Landscape of Human Embryonic Stem Cells.* Plos Genetics, 2011. **7**(6).
81. Wu, H., et al., *Genome-wide analysis of 5-hydroxymethylcytosine distribution reveals its dual function in transcriptional regulation in mouse embryonic stem cells.* Genes & Development, 2011. **25**(7): p. 679-684.
82. Xu, Y., et al., *Genome-wide Regulation of 5hmC, 5mC, and Gene Expression by Tet1 Hydroxylase in Mouse Embryonic Stem Cells.* Molecular Cell, 2011. **42**(4): p. 451-464.
83. Song, C.-X., et al., *Genome-wide Profiling of 5-Formylcytosine Reveals Its Roles in Epigenetic Priming.* Cell, 2013. **153**(3): p. 678-691.
84. Tate, P.H. and A.P. Bird, *Effects of DNA methylation on DNA-binding proteins and gene expression.* Current opinion in genetics & development, 1993. **3**(2): p. 226-31.
85. Derreumaux, S., et al., *Impact of CpG methylation on structure, dynamics and solvation of cAMP DNA responsive element.* Nucleic Acids Research, 2001. **29**(11): p. 2314-2326.
86. Nathan, D. and D.M. Crothers, *Bending and flexibility of methylated and unmethylated EcoRI DNA.* Journal of Molecular Biology, 2002. **316**(1): p. 7-17.
87. Perez, A., et al., *Impact of Methylation on the Physical Properties of DNA.* Biophysical Journal, 2012. **102**(9): p. 2140-2148.

88. Yang, W., *Structure and mechanism for DNA lesion recognition.* Cell Research, 2008. **18**(1): p. 184-197.
89. Petesch, S.J. and J.T. Lis, *Overcoming the nucleosome barrier during transcript elongation.* Trends in Genetics, 2012. **28**(6): p. 285-294.
90. Jimenez-Useche, I., et al., *DNA Methylation Regulated Nucleosome Dynamics.* Scientific Reports, 2013. **3**.
91. Choy, J.S., et al., *DNA Methylation Increases Nucleosome Compaction and Rigidity.* Journal of the American Chemical Society, 2010. **132**(6): p. 1782-+.
92. Geahigan, K.B., et al., *The dynamic impact of CpG methylation in DNA.* Biochemistry, 2000. **39**(16): p. 4939-4946.
93. Portella, G., F. Battistini, and M. Orozco, *Understanding the Connection between Epigenetic DNA Methylation and Nucleosome Positioning from Computer Simulations.* Plos Computational Biology, 2013. **9**(11).
94. Ma, J., L. Bai, and M.D. Wang, *Transcription Under Torsion.* Science, 2013. **340**(6140): p. 1580-1583.
95. Miyagi, A., T. Ando, and Y.L. Lyubchenko, *Dynamics of Nucleosomes Assessed with Time-Lapse High-Speed Atomic Force Microscopy.* Biochemistry, 2011. **50**(37): p. 7901-7908.
96. Tims, H.S., et al., *Dynamics of Nucleosome Invasion by DNA Binding Proteins.* Journal of Molecular Biology, 2011. **411**(2): p. 430-448.
97. Mozziconacci, J. and J.M. Victor, *Nucleosome gaping supports a functional structure for the 30nm chromatin fiber.* Journal of Structural Biology, 2003. **143**(1): p. 72-76.
98. Belmont, A.S., J.W. Sedat, and D.A. Agard, *A 3-DIMENSIONAL APPROACH TO MITOTIC CHROMOSOME STRUCTURE - EVIDENCE FOR A COMPLEX HIERARCHICAL ORGANIZATION.* Journal of Cell Biology, 1987. **105**(1): p. 77-92.
99. Chapman, H.N., et al., *Femtosecond X-ray protein nanocrystallography.* Nature, 2011. **470**(7332): p. 73-U81.
100. Boutet, S., et al., *High-Resolution Protein Structure Determination by Serial Femtosecond Crystallography.* Science, 2012. **337**(6092): p. 362-364.